AD_____

Award Number: W81XWH-04-1-0876

TITLE: Diversity, replication, pathogenicity and cell biology of Crimean Congo hemorrhagic fever virus

PRINCIPAL INVESTIGATOR: Adolfo Garcia-Sastre, Ph.D.

CONTRACTING ORGANIZATION: Mount Sinai School of Medicine
New York, NY 10029

REPORT DATE: October 2010

TYPE OF REPORT: Final Addendum

PREPARED FOR: U.S. Army Medical Research and Materiel Command
Fort Detrick, Maryland 21702-5012

REPORT DOCUMENTATION PAGE

Form Approved
OMB No. 0704-0188

1. REPORT DATE *(DD-MM-YYYY)*	**2. REPORT TYPE**	**3. DATES COVERED** *(From - To)*
01-10-2010	Final Addendum	16 Sep 2009 - 30 sep 2010

4. TITLE AND SUBTITLE
Diversity, replication, pathogenicity and cell biology of Crimean Congo hemorrhagic fever virus

5a. CONTRACT NUMBER

5b. GRANT NUMBER
W81XWH-04-1-0876

5c. PROGRAM ELEMENT NUMBER

6. AUTHOR(S)
Adolfo Garcia-Sastre, Ph.D.

E-Mail: adolfo.garcia-sastre@mssm.edu

5d. PROJECT NUMBER

5e. TASK NUMBER

5f. WORK UNIT NUMBER

7. PERFORMING ORGANIZATION NAME(S) AND ADDRESS(ES)
Mount Sinai School of Medicine
New York, NY 10029

8. PERFORMING ORGANIZATION REPORT NUMBER

9. SPONSORING / MONITORING AGENCY NAME(S) AND ADDRESS(ES)
U.S. Army Medical Research and Materiel Command
Fort Detrick, Maryland 21702-5012

10. SPONSOR/MONITOR'S ACRONYM(S)

11. SPONSOR/MONITOR'S REPORT NUMBER(S)

12. DISTRIBUTION / AVAILABILITY STATEMENT
Approved for Public Release; Distribution Unlimited

13. SUPPLEMENTARY NOTES

14. ABSTRACT

This research project was a result of a collaboration between three research groups aimed at elucidating basic replication processes of CCHFV with the expected outcome of providing basic research reagents and establishing the foundation of knowledge necessary for discovery of vaccines and antiviral therapeutics for Crimean Congo hemorrhagic fever. Our major findings during the total period of support were the following: We have cloned and expressed all proteins of CCHFV. We found that the protease activity associated with the N-terminal of the L protein is responsible for overcoming innate immune responses mediated by ubiquitin and by the ubiquitin-like molecule ISG15. We have identified inhibitors of this protease, and solved its structure. We have characterized in detail the processing of the G protein and the expression of the NSm protein of CCHFV, and developed constructs with fusogenic activity based on expression of the G ORF. We have successfully passaged CCHFV 18 times in SCID mice and conducted preliminary studies in macaques. We have confirmed that infection of STAT1 -/- mice with CCHFV results in lethal disease, opening the possibility of using a mouse model of this virus. Our results have provided novel insights on the molecular biology of this highly pathogenic human virus and opened new avenues for the discovery of CCHFV antivirals.

15. SUBJECT TERMS
CCHFV, bunyavirus, virus receptor, virus-host interaction, animal model, arbovirus, antiviral

16. SECURITY CLASSIFICATION OF:			**17. LIMITATION OF ABSTRACT**	**18. NUMBER OF PAGES**	**19a. NAME OF RESPONSIBLE PERSON**
a. REPORT	**b. ABSTRACT**	**c. THIS PAGE**			USAMRMC
U	U	U	UU	73	**19b. TELEPHONE NUMBER** *(include area code)*

Table of Contents

1. Introduction.

This investigator-initiated project represents a collaborative team approach to the study of a highly pathogenic emerging virus of military importance, Crimean Congo hemorrhagic fever virus (CCHFV). CCHFV causes disease characterized by abrupt onset fever and can progress to hemorrhage, renal failure and shock. Mortality 13-50% is common. This severe disease is endemic in sub-Saharan Africa, the Middle East, and central Asia, all areas of current significant military operations. The extremely pathogenic nature of CCHFV has led to the fear that it might be used as an agent of bioterrorism or biowarfare. This proposal, originally comprised of three interrelated subprojects, has been under no cost extension for continuation of research in two subprojects (1 and 3), aimed at elucidating basic replication processes of CCHFV with the expected outcome of providing basic research reagents and establishing the foundation of knowledge necessary for discovery of vaccines and antiviral therapeutics for CCHF. The body of the final report for each sub-project covering the time from Sept 15, 2004 to Sept 30, 2010 is outlined in the following pages. As this is the final report, it repeats information provided in previous year's reports (though more briefly) and also contains information about progress made in the past year.

2. Body.

Subproject #1: Reverse genetics of CCHFV

Subproject #1, directed by Adolfo García-Sastre, focuses on understanding the molecular interactions between the components of the RNA replication machinery of CCHFV: the N and L proteins and the viral RNAs, with the final goal of establishing reverse genetics techniques for the rescue of CCHFV from plasmid DNA. These techniques will be used to generate attenuated strains of CCHFV. During the first years of support, our studies on task 1 led to the identification of a protease activity associated with the CCHVF L protein. Based on these results we requested a modification of the SOW to allow the inclusion of item d under Task 1, entitled "Characterization of the enzymatic properties of the protease domain of L of CCHFV and development of screening assays for small molecule inhibitors as potential antivirals".

Task 1. Characterization of cis- and trans-acting signals involved in RNA replication and transcription of CCHFV.
This task included the development of expression plasmids encoding the N and L proteins of CCHFV and model vRNAs encoding reporter genes supporting the replication and transcription of this viral RNA when transfected into cells (Item a). These plasmids were to be used also under this task to perform mutational analysis to identify sequence/structure regulatory motifs involved in viral RNA replication and transcription(Item b), as well as to identify domains involved in protein-protein interactions and protein-RNA interactions (Item c). The SOW was latyer on modified to include the characterization of the enzymatic properties of the protease domain of L of CCHFV and the development of screening assays for small molecule inhibitors as potential antivirals (Item d).

During the first year, we sequenced and cloned the L (large polymerase) and N (nucleoprotein) open reading frames of CCHFV, strain 10200 into expression plasmids, as well as generated different reporter genes (GFP and luciferase) flanked by the 3' and 5' noncoding regions of the S segment of CCHFV. For instance, we completed the genome sequencing of the large RNA segment of CCHFV, strain 10200. The gene contains 12,160 nucleotides, with a 76 nucleotide long 3' UTR and a 246 long 5' UTR. A single ORF was identified, encoding for a

3,945 amino acid protein. After obtaining the sequence, two other groups also reported sequences from the L gene of CCHFV. Our sequence is identical to that of the other two groups except for a few amino acid changes. T The protein sequence showed the core polymerase motifs characteristic of the RNA-dependent RNA polymerases of segmented negative-stranded viruses and in the amino terminal portion, an ovarian tumor (OTU) –like protease motif was identified (Fig.1)

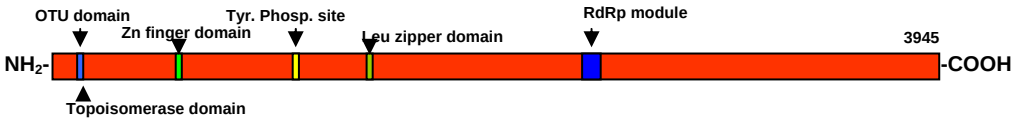

Figure1: Predicted domains present in CCHFV L protein

During the second year, we mapped domains in N involved in the interaction of this protein with RNA, with itself and with the L protein. In order to identify domains in the N protein interacting with RNA we made truncations in the N protein, expressed as GST fusion proteins in bacteria, and determined the ability of these truncations to bind to ssRNA in the same dot blot assay. The results are represented in Fig. 2 and indicate that the N protein has a strong RNA-binding domain in the C-terminal half of the protein (amino acids 240 to 482) and a second weaker RNA-binding domain at the N-terminus (amino acids 1 to 160).

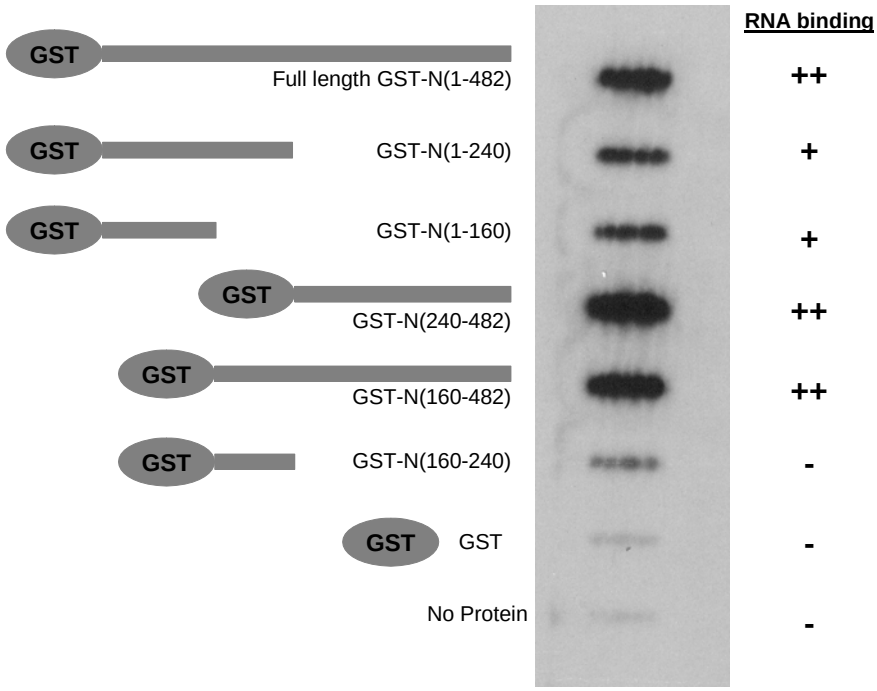

Fig. 2. RNA binding domains of the N protein of CCHFV. The depicted GST-fusion proteins were expressed in E. coli and purified using a gluthation-agarose column. Equal amount of GST-fusion proteins were GST-N or GST recombinant proteins at the indicated concentration were incubated with 12ng of radiolabeled in vitro transcribed RNA in binding buffer for 30min at 37°C and then slot-blotted onto nitrocellulose filters.

In order to characterize domains involved in N-N interactions, we performed co-immunoprecipitations using Flag-tagged and HA-tagged N constructs expressed in 293 cells. Truncations of N similar to those shown in Fig. 2 were made to characterize the domains involved in N-N interactions. The results shown in Fig. 3 demonstrate that N oligomerizes, and that the first 160 amino acids are dispensable for N-N interaction.

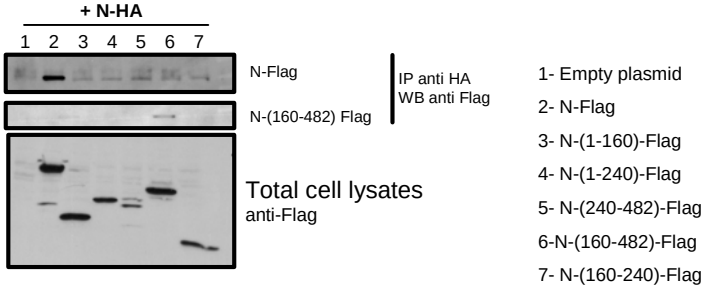

Fig. 3. N-N interactions. A plasmid expressing HA tagged N (N-HA) was cotransfected with empty plasmid or with plasmids expressing Flag tagged full length N or truncated N mutants. Two days after transfection, cell extracts were made, immunoprecipitated with anti-HA antibody, subjected to SDS-PAGE, and western blotted with anti-flag antibodies.

We also investigated the ability of the N protein to interact with the L protein. For this purpose, we divided the L protein in three fragments of approximately 3 kbases each, and expressed as HA-tagged constructs together with N-Flag. Co-immunoprecipitations revealed a strong interaction of N with the N-terminal fragment of L, and a weak interaction with the C-terminal fragment. No interaction was observed with the middle portion of L (Fig. 4).

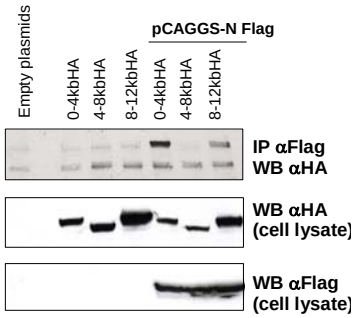

Fig. 4. N-L interactions. A plasmid expressing Flag tagged N (N-Flag) was cotransfected with plasmids expressing HA tagged L fragments. Two days after transfection, cell extracts were made, immunoprecipitated with anti-Flag antibody, subjected to SDS-PAGE, and western blotted with anti-HA antibodies.

During the third and fourth year of this project, we concentrated in studying the unusual protease activity that we identified associated with the N-terminal OTU domain of L (see Fig. 1 in appended manuscript 4, Frias-Staheli et al., Cell Host Microbe 2:404-16). The ovarian tumor (OTU) domain represents a superfamily of predicted proteases found in eukaryotic, bacterial, and viral proteins, some of which have Ub-deconjugating activity. We found that the OTU domain-containing proteases from CCHFV and from arteriviruses, two unrelated groups of RNA viruses, hydrolyze ubiquitin (Ub) and the Ub-like molecule ISG15 from cellular target proteins (see Figs. 2, 3 and 4A, in appended manuscript 4, Frias-Staheli et al., Cell Host Microbe 2:404-16). This broad activity was in contrast with the target specificity of known mammalian OTU domain-containing proteins (see Fig. 4B, in appended manuscript 4, Frias-Staheli et al., Cell Host Microbe 2:404-16). Expression of the CCHFV OTU domain antagonized the antiviral effects of ISG15 (see Fig. 6, in appended manuscript 4, Frias-Staheli et al., Cell Host Microbe 2:404-16) and enhanced susceptibility to Sindbis virus infection *in vivo* (see Fig. 5, in appended manuscript 4, Frias-Staheli et al., Cell Host Microbe 2:404-16). We also showed that the CCHFV OTU domain inhibited NF-kappaB-dependent signaling (see Fig. 7, in appended manuscript 4, Frias-Staheli et al., Cell Host Microbe 2:404-16). Thus, the deconjugating activity of viral OTU proteases, including the CCHFV OTU domain, represents a unique viral strategy to inhibit Ub- and ISG15-dependent antiviral pathways.

In the last years we also focused in developing an enzymatic assay for the CCHFV OTU domain that we have optimized for high-throughput screening of specific inhibitors. For this purpose, we expressed and purified CCHFV-L OTU in bacteria, and we performed kinetic analysis of its enzymatic activity using ubiquitin or ISG15 fused in its carboxy-terminus to the

fluorogenic substrate 7-amido-4-methylcoumarin (AMC). Ub-AMC (Fig. 5) and ISG15-AMC (data not shown) were efficiently hydrolyzed by CCHFV-L OTU enzyme with liberation of highly fluorescent AMC. Hydrolysis of Ub-AMC or ISG15-AMC substrates was determined spectrofluorometrically in a final volume of 200 µl. The assays contained Ub-AMC (or ISG15-AMC) at different concentrations, 50 mM Tris HCl pH 7.6, 2mM DTT, 50µg/ml BSA. The excitation wavelength was 380 nm, and emission was monitored at 440 nm. Absolute concentrations were determined by reference to a standard curve of fluorescence versus concentration of AMC. These substrates proved to be highly sensitive and allowed monitoring continuous enzymatic activity.

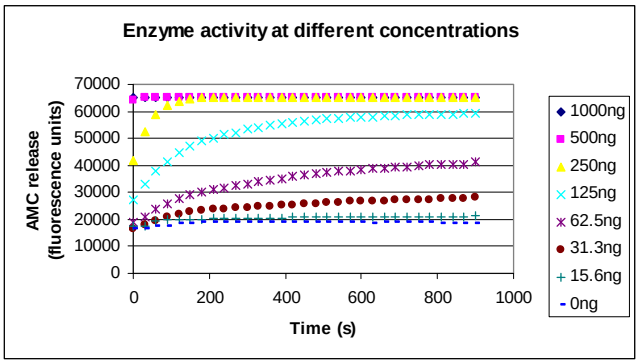

Fig. 5. Representative determination of CCHFV OTU enzymatic activity over Ub-AMC substrate. CCHFV-L OTU activity was established by adding increasing amounts of enzyme (indicated in the box at the right) and measuring fluorescence every 30 seconds for 10 minutes.

We are now seeking to conduct a high throughput screening (HTS) against the CCHFV-L OTU. In order to develop a robust and suitable high throughput assay to be used to screen for inhibitors of the CCHFV-L OTU, we took advantage of the commercially available substrate peptide, RLRGG-AMC, which contains the cleavage motif that is recognized by ubiquitin and ISG15 deconjugating enzymes. The assay was easily adapted to be used with this substrate in a 386 well plate format. We thus conducted kinetic analysis, evaluated substrate stability at room temperature, determined reproducibility and calculated the Z' score (of 0.75) to evaluate the robustness for the assay (Fig. 6 A-E).

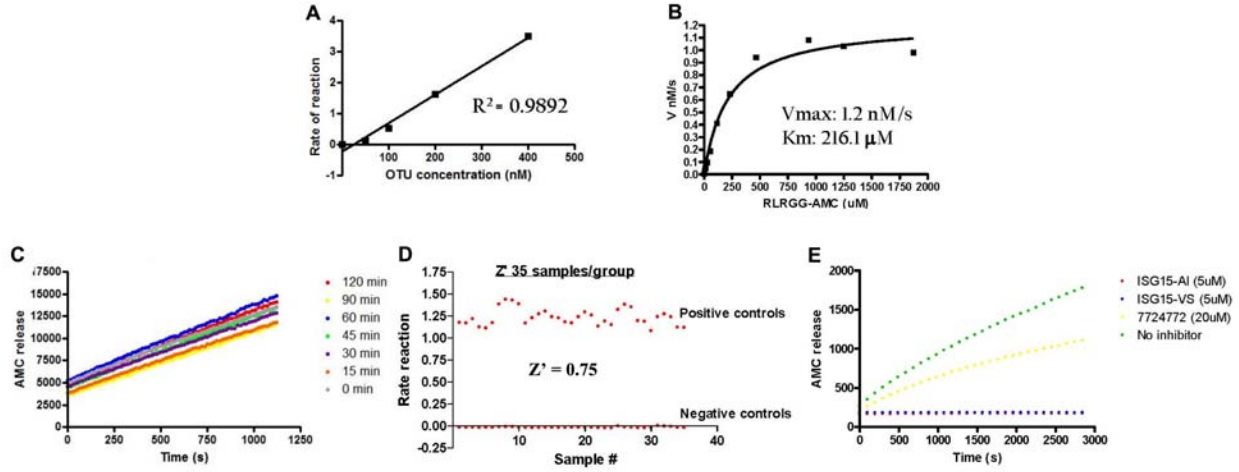

Figure 6. A. Linear rate of hydrolysis of RLRGG-AMC [100 µM] by CCHFV-L rOTU. B. Initial velocity of hydrolysis of RLRGG-AMC by CCHFV-L rOTU [50 nM]. C. Stability of RLRGG-AMC [100 µM] at room temperature overtime. D. Determination of Z' score to validate assay robustness for high throughput screen (HTS). E. Effect of CCHFV-L rOTU inhibitors on RLRGG-AMC hydrolysis. Assays done as in Figure 1. All reactions were done in a final volume of 50 µl HTS kinetic buffer [50mM Tris-HCl pH 7.6, 2mM DTT, 6% DMSO].

Using this assay we have now screened a small molecule library comprising 29,569 compounds, and come up with 10 small molecules with potent inhibitory activities in vitro. Interestingly, these compounds were specific for the OTU protease of CCHFV, as most of them did not inhibit the protease activity of mammalian proteases belonging to the same family, otubain1, otubain2, or A20 (Figure 7). We are now further characterizing these molecules for their activity in tissue culture and antiviral properties.

IC_{50} (uM)

Inhibitor No.	RLRGG-AMC	Ub-AMC	ISG15-AMC	NEDD8-AMC	OTUB1	OTUB2	ISOT/ A20
2	3.36	4.8	2.3	0.78	>100	>100	>100
3	2.47	3.9	3.6	37.8	>100	>100	>100
4	2.35	3.1	9.3	27.3	>100	>100	>100
5	15.3	1.2	8.5	>100	>100	>100	>100
6	16.12	1.1	11.4	50.1	25	50	>100
7	2.4	1.6	>100	2.67	>100	>100	>100
8	1	4	>100	1.09	>100	>100	>100
10	>100	6.25	>100	>100	>100	>100	>100
13	5.58	>100	35.1	>100	>100	50	>100
21	3.125	3.13	28	>100	>100	>100	>100

Figure 7. Inhibitory concentration 50 (IC50) in micromolar of our best hits. The IC50 has been calculated using substrates RLRGG-AMC, Ub-AMC, ISG15-AMC and Nedd8-AMC and CCHFV-L OTU. Most of these compounds did not demonstrate inhibition (IC50 > 100) against the mammalian enzymes otubain1 (OTUB1), otubain2 (OTUB2), isopeptidase T (ISOT) and A20.

During the last year, we have also conducted studies to identify cellular factors important to the replication of CCHFV and other bunyaviruses. In particular, we have focused on identifying host proteins than interact with the N proteins of these viruses. Given the known roles of bunyavirus N proteins in viral RNA replication, virion assembly, and suppression of host innate immune responses, we expect that protein-protein interactions among N proteins and host factors will be critical for viral replication. Currently, we have amassed of a list of approximately one hundred host proteins that interact with one or more of the nucleocapsid proteins of CCHFV, RVFV, ANDV and HTNV (Figure 8). Efforts are now in progress to also identify protein interactors for additional bunyavirus proteins as well.

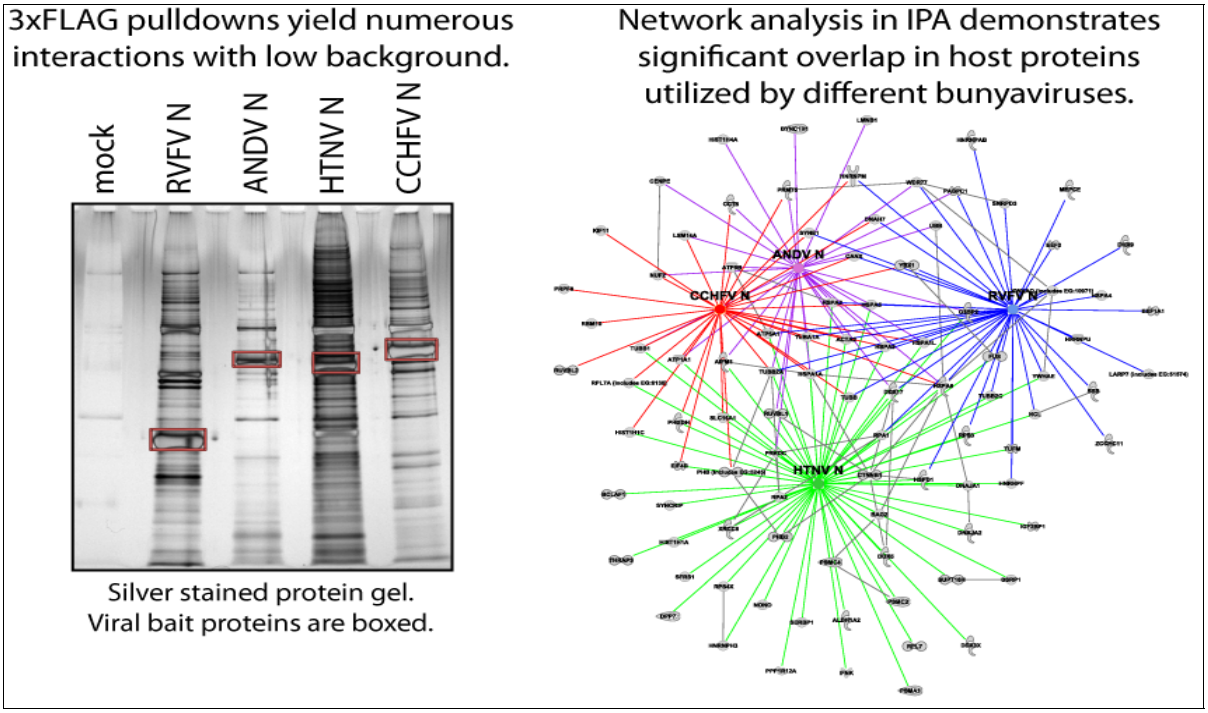

Figure 8. Isolation of interacting bunyavirus and host proteins, and network analysis of protein-protein interactions using the Ingenuity Pathway Analysis (IPA) program. Bunyavirus N proteins with N-terminal 3xFLAG affinity tags were transiently expressed in 293T cells and then virus-host protein complexes were isolated by co-immunoprecipitation. These complexes were separated by SDS-PAGE and then host proteins were identified by mass spectrometry.

In addition, in collaboration with Brian Mark, we have solved the crystal structures of a CCHFV OTU domain bound to Ub and to ISG15 at 2.5Å and 2.3Å resolution, respectively (see Figure 9, and also Figs 1and 2 in appended manuscript 5, James et al., PNAS 108:2222-2227). The complexes provide the first structural example of ISG15 bound to another protein and reveal the molecular mechanism of an ISG15 cross-reactive deubiquitinase. To accommodate structural differences between Ub and ISG15, the viral protease binds the β-grasp folds of Ub and C-terminal Ub-like domain of ISG15 in an orientation that is rotated nearly75 degrees with respect to that observed for Ub bound to a representative eukaryotic OTU domain from yeast. Distinct structural determinants in three regions (see Figure 9, and also Figs 1and 2 in appended manuscript 5, James et al., PNAS 108:2222-2227) necessary for binding either substrate were identified and allowed the re-engineering of the viral OTU protease into enzymes with increased substrate specificity, either for Ub or for ISG15. Our findings provide the basis for future studies to determine *in vivo* the relative contributions of deubiquitination and deISG15ylation to viral immune evasion tactics, and a structural template of a promiscuous deubiquitinase from a hemorrhagic fever virus that can be targeted for inhibition using small molecule based strategies.

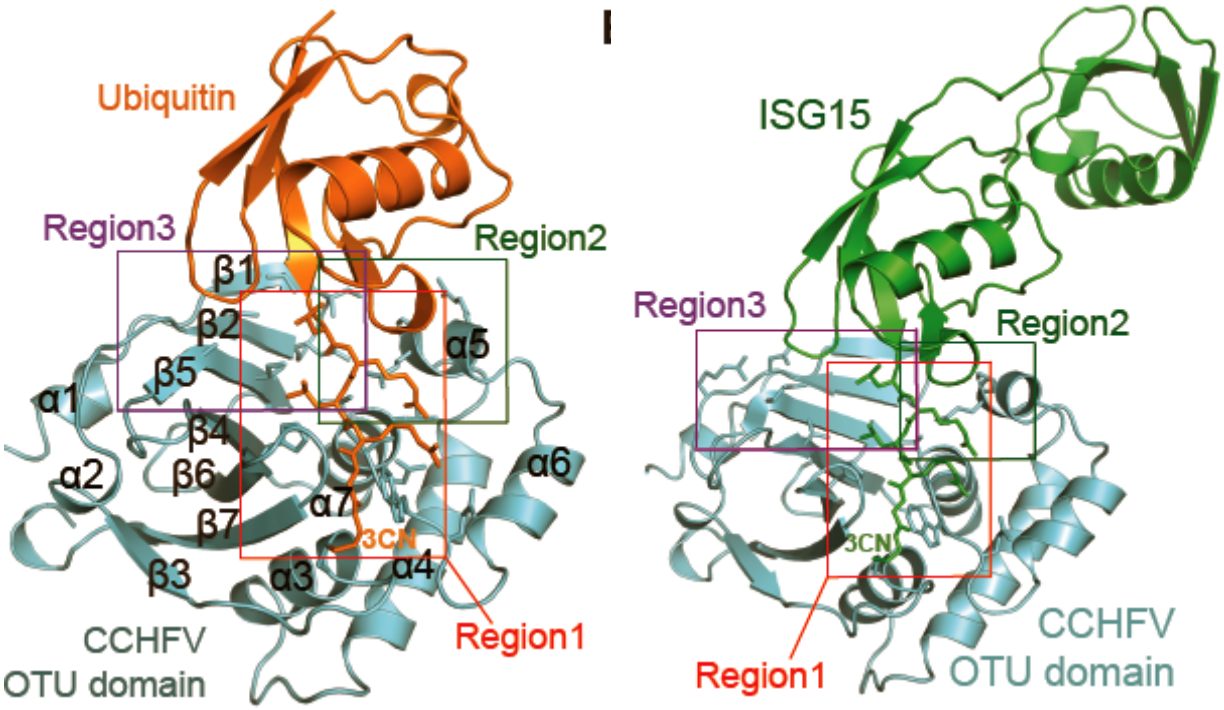

Figure 9. Crystal structure of CCHFV-OTU (cyan) bound to Ub (orange) and to ISG15 (green). Regions involved in protein-protein contacts (Regions 1, 2 and 3) are shown. Figures were drawn using PyMol.

Task 2. Generation of recombinant CCHFV from cDNA.

We have constructed CCHFV minigenomes containing a reporter gene flanked by the CCHFV S and L segment UTRs and shed that these reporter genes are activated upon infection with CCHFV, in collaboration with Dr. Schmaljohn, PI of subproject 3. Similar resutls were obtained by the laboratory of Dr. Nichols, at the CDC. We have also constructed and sequenced expression vectors for the 3 segments of CCHFV. Since we focused our last year in developing an assay for the identification of inhibitors of the CCHFV L OTU domain, we have not completed task 2, but we have constructed the rescue plasmids, and we hope to be able to rescue CCHFV in the near future in collaboration with Dr. Schmaljohn under BSL4 containment.

Task 3. Generation of attenuated CCHFV by reverse genetics.

Since no recombinant CCHFV was generated yet, this task has been postponed to future studies outside of the period of support of this grant. However, we have succeeded on establishing a screen assay for CCHFV inhibitors that may lead to efficient therapies against this viral agent (see task 1), which might provide an alternative to the use of attenuated CCHFV as vaccines for the prevention of disease associated with this virus.

Subproject #2: Cell Biology of CCHFV Glycoproteins

Work carried out under subproject #2 was performed in the laboratory of Dr. Robert W. Doms at the University of Pennsylvania, and was directed towards characterizing the envelope glycoproteins of CCHFV. There were two tasks:

Task 1. Analyze the assembly and processing of CCHFV G1 and G2 glycoproteins and characterize the mucin-like domain present at the amino terminus of the polyprotein.

In previous years, we developed antibodies and protein expression systems for the CCHFV glycoproteins. We produced a codon-optimized version of the CCHFV M segment that is now being used by Dr. Schmaljohn in DNA vaccination studies. We found that the codon optimized version of M segment produced (upon transfection) much higher levels of the Gn and Gc glycoproteins than did the native construct. This is perhaps not surprising – codon usage in ticks and mammals is quite different, and CCHFV has evolved to replicate in both of this disparate hosts.

To understand the processing and intracellular localization of the CCHFV glycoproteins as well as their neutralization and protection determinants, we produced and characterized monoclonal antibodies (MAbs) specific to both the G_N and G_C proteins. Using these MAbs, we found that G_N predominantly colocalized with a Golgi marker when expressed alone or with G_C (see Fig. 2, in appended manuscript 1, Bertolotti-Ciarlet et al., J.Virol. 79: 6152-6), while G_C was transported to the Golgi only in the presence of G_N (see Fig. 5A, in appended manuscript 1, Bertolotti-Ciarlet et al., J.Virol. 79: 6152-6). Both proteins remained Endo H sensitive, indicating that the CCHFV glycoproteins are most likely targeted to the *cis* Golgi (see Fig. 5B, in appended manuscript 1, Bertolotti-Ciarlet et al., J.Virol. 79: 6152-6). Golgi targeting information partly resides within the G_N ectodomain, because a soluble version of G_N lacking its transmembrane and cytoplasmic domains also localized to the Golgi (see Fig. 6, in appended manuscript 1, Bertolotti-Ciarlet et al., J.Virol. 79: 6152-6). The mucin-like and P35 domains, located at the N terminus of the G_N precursor protein and removed posttranslationally by endoproteolysis, were required for Golgi targeting of G_N when it was expressed alone but were dispensable when G_C was coexpressed.

In a paper published last year we showed that the C-terminal region of Gn is cleaved by a cellular protease, resulting in an NSm protein with a molecular weight of approximately 20 kDa (see Fig 2, in appended manuscript 3, Altamura et al., J. Virol. 81:6632-6642). We found that NSm is produced following M segment expression in a variety of cell types (for an example of NSm expression in 293T/17 cells, see Fig. 7A, in appended manuscript 3, Altamura et al., J. Virol. 81:6632-6642) and importantly found that it is also produced in cells following infection with live CCHFV (see Fig. 7B, in appended manuscript 3, Altamura et al., J. Virol. 81:6632-6642). We also found that that this protein is produced efficiently and shortly after synthesis of PreGn (see Fig. 3, in appended manuscript 3, Altamura et al., J. Virol. 81:6632-6642), that it is stable (see Fig. 3, in appended manuscript 3, Altamura et al., J. Virol. 81:6632-6642), and that at least some of it is transported to the Golgi (see Fig. 4, in appended manuscript 3, Altamura et al., J. Virol. 81:6632-6642). When we mutated the protein such that cleavage did not occur, the resulting protein proved to be non-functional as described under *Task 2*. This raised the possibility that the protease responsible for this event might be the target for antiviral compounds. By analogy, cathepsin L inhibitors are being tested in animal models to see if they will protect from ebola virus infection – cathepsin L cleaves the ebola virus glycoprotein, and this cleavage event is essential for its function.

Over the past year, much of our work has been directed towards identifying the cellular protease responsible for cleaving the C-terminal region of the Gn glycoprotein. This work is virtually ready to submit to the Journal of Virology. In our first paper on this topic, we identified the NSm protein of Crimean-Congo hemorrhagic fever virus (genus Nairovirus, family Bunyaviridae) as an approximately 15 kDa cell-associated nonstructural protein encoded between the Gn and Gc glycoproteins that is generated through endoproteolytic cleavage of the M polyprotein (see Fig. 1, in appended manuscript 3, Altamura et al., J. Virol. 81:6632-6642). Using transiently expressed M polyproteins lacking NSm, we found that gross deletion of NSm

results in improper trafficking and aberrant processing of the viral glycoproteins, and we believe that this phenotype is the result of inefficient processing at the PreGN-PreGC junction in the absence of NSm. Sequence analysis of the transmembrane domains flanking NSm has indicated that both are candidates for intramembrane proteolysis by signal peptidase (SPase). Mutagenesis of residues critical for SPase processing within the transmembrane domain N-terminal to NSm blocked Gn-NSm cleavage, confirming the importance of this domain to NSm generation. Similarly, mutation of residues in the transmembrane domain immediately C-terminal to NSm blocked cleavage at the NSm-PreGc junction. We have also found that small proteins comprising only the Gn-NSm junction and some flanking regions can be efficiently cleaved both in transfected cells and in rabbit reticulocyte lysates in the presence of microsomal membranes, thereby providing a convenient system for identifying the protease in vitro. These data support the notion that Gn-NSm cleavage occurs independently of the PreGN ectodomain and that the termini of NSm are defined by a microsome-associated protease, most likely SPase. Unfortunately, signal peptidase is not a good drug target, so we are not pursuing this line of work. However, the information gleaned from these studies is now being used to produce soluble versions of the CCHFV glycoproteins for structural studies.

Task 2. Identify cell receptors and attachment factors for CCHFV.

Despite the fact that the geographic distribution of CCHFV is quite broad, limited sequence information was available on the viral M segment, with sequences of isolates obtained outside of China or Russia being rare. This information is essential to understand possible attachment factors, as the glycoprotein encoded by the M segment is responsible for attachment and entry in the host cell. Our colleagues at USAMRIID had assembled a panel of CCHFV isolates from ticks, livestock infected by ticks, humans infected by ticks, humans who contracted the disease by contact with infected livestock, or humans who contracted the disease from another human. Strains include two isolates from human cases of CCHFV in South Africa (SPU 41/84 and SPU 94/87), two strains from Uzbekistan (U2-2-002 and M-20, a strain that was isolated from a fatal human case), and a strain isolated from *Hyalomma asiaticum* tick in China (Hy13). We fully sequenced the M segments and expressed the glycoproteins derived from the viral isolates. These new sequences showed high variability in the N-terminal region of G_N and more modest differences in the remainder of G_N and in G_C. Phylogenetic analyses placed these newly identified strains in three of the four previously described M segment groups (see Fig. 1, in appended manuscript 2, Ahmed et al., J. Gen. Virol., 86:3327-36).

We have developed an efficient and reproducible cell-cell fusion assay that has enabled us to examine the function of the CCHFV glycoproteins. We are using this assay to test a panel of glycoprotein mutants produced by Dr. Stuart Nichol's lab at the CDC. In this assay, human 293T cells are transfected with an expression plasmid containing our codon-optimized version of the CCHFV M segment, as well as a plasmid expressing the omega subunit of b-galactosidase. The next day, these cells are mixed with target cells that express the alpha subunit of b-galactosidase. The pH of the media is then adjusted to the desired value for two minutes, after which the cells are returned to normal media for 4 hours. At this point the cells are lysed with a nonionic detergent, and the amount of b-galactosidase activity present is measured with a luminometer. Fusion between the effector (CCHFV expressing) and target cells results in cytoplasmic mixing and b-galactosidase complementation – neither the alpha nor omega subunits are active on their own. We carry this assay out in deep 94 well plates, which makes this assay reasonably high throughput. We have found that CCHFV fusion is pH dependent, and can occur with a variety of cell types. At present, we are working with the Nichol lab at the CDC to test a variety of CCHFV glycoprotein mutants, and have also produced a panel of mutants in which amino acid changes were introduced into the putative fusion peptide within the Gc protein.

One area in which progress has not been good has been the production of CCHFV pseudotypes. We have succeeded in placing the Gn and Gc glycoproteins from a number of bunyaviruses, including Sin Nombre, Hantaan, Andes and Puumala, onto a VSV core. These high-titer virus pseudotypes are being used to test sera samples that have resulted from vaccine experiments with non-human primates conducted by Dr. Jay Hooper and colleagues at USAMRIID. The neutralization assay we have developed is much more rapid and quantitative than standard plaque assays, can be performed on a wide range of cell types, takes only 48 hours (vs. nearly a week for a plaque reduction neutralization titer test), uses smaller amounts of reagent, and can be performed under BSL2 conditions. However, we have not been able to produce CCHFV or Rift Valley Fever virus pseudotypes despite many attempts. At present, we suspect that there is some incompatibility between the cytoplasmic domains of the CCHFV glycoproteins and the underlying VSV core. We hope that the mutants we produce in the cell fusion assay will suggest new approaches: mutations in the cytoplasmic domains that either increase surface expression of the proteins or that have no effect on membrane fusion activity will then be tested in our pseudotype system.

If we can produce CCHFV pseudotypes, we will work with Dr. Sara Cherry and employ a whole genome RNAi screen to identify host genes that, when suppressed, lead to reduced CCHFV pseudotype infection. We have done this recently with Rift Valley Fever virus, and find that this virus triggers macropinocytosis upon binding the cell surface.

Subproject #3: Characterization of CCHFV strains and small animal model development

Work carried out under subproject #3 was performed in the laboratory of Dr. Connie Schmaljohn at the United States Army Medical Research Institute of Infectious Diseases (USAMRIID). These studies involve working with the intact virus in high biocontainment and supporting subprojects 1 and 2 with reagents and experiments with virus to complement in vitro work from subproject 1 and 2. Accomplishments for major tasks under this subproject follow:

Task 1. Characterization of CCHFV isolates and virulence factors

To accomplish the goal of characterizing CCHFV we developed methods to improve the yield and recovery of viruses propagated in cultured cells. For this, we performed studies aimed at: (1) identifying an optimal cell line for virus growth: (2) determining the time of highest virus yield from cells and supernatants; (3) developed a real time PCR method for quantifying viral genomes; (4) developed a FACS assay for measuring percentages of infected cells. To further improve yields of viruses and to attempt to recover additional primary isolates, we obtained a panel of 29 human cell lines from the National Cancer Institute. These include cell lines derived from tumors of colon, prostate, kidney, peripheral blood, lung, central nervous system, ascites, skin, pleural effusion, ovary, and lymph node. Preliminary work has started to characterize CCHFV growth parameters in these cells. These studies were not completed during the granting period, but will be continued under another research program.

As reported in the FY06 annual report, we developed a real time PCR for measuring viral genomes. These studies were reported in a peer reviewed publication during 2007 (Garrison, et al., 2007). We found that the genome copy number was far higher than actual levels of infectious virus, as detected by plaque assay. Consequently, additional studies were undertaken to develop better methods for recovering infectious virus. As reported in the FY07 annual report, we performed numerous growth curves to identify the optimal time for recovery of infectious virus. In addition, we developed a protocol for harvesting both cell culture

supernatants and cells, which greatly improved the yields of infectious virus obtained. In the past, we typically obtained virus in the range of 10^3-10^5 pfu/ml. In many cases, this meant that our experiments were limited to using at most a multiplicity of infection (MOI) of 0.1-1. The method that we developed involves freeze-thawing infected cells, allowing us to liberate virions retained within cells. By combining this cell lysate with supernatants from the infected cells, we have been able to obtain CCHFV titers in the range of 10^7-10^8 pfu/ml. As shown in Fig. 10, we found that maximum virus yield could be obtained from HepG2 and CER cells at 48 and 60 hours post infection respectively, with yields of 10^7 plaque forming units per ml.

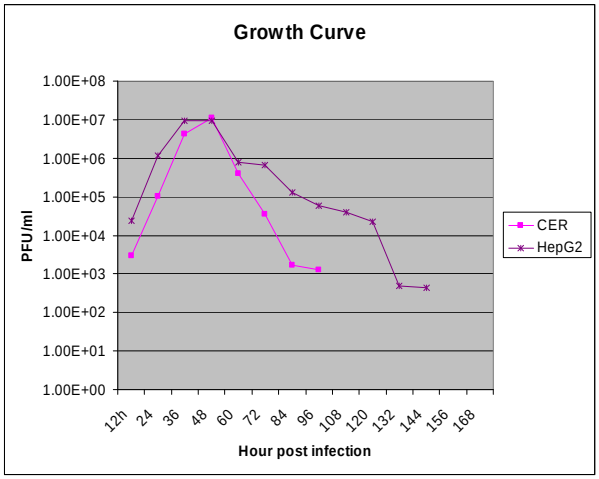

Fig. 10. CER and HepG2 cells were infected with an MOI of 0.003. Every 12 hours, for 7 days, the supernatant and infected cell lysate from one flask of each cell type was collected. Infectious virus yield of the combined lysate and supernatant from each time point was measured by plaque assay on Vero E6 cells.

To determine the extent of viral infections in cultured cells, we developed an immunofluorescent assay in which CCHFV-infected cells can be quantified by using a Fluorescence Activated Cell Sorter (FACS). Examples of results for mock infected cells and cells infected at MOIs of 0.1, 1 and 10 are shown in Fig. 11.

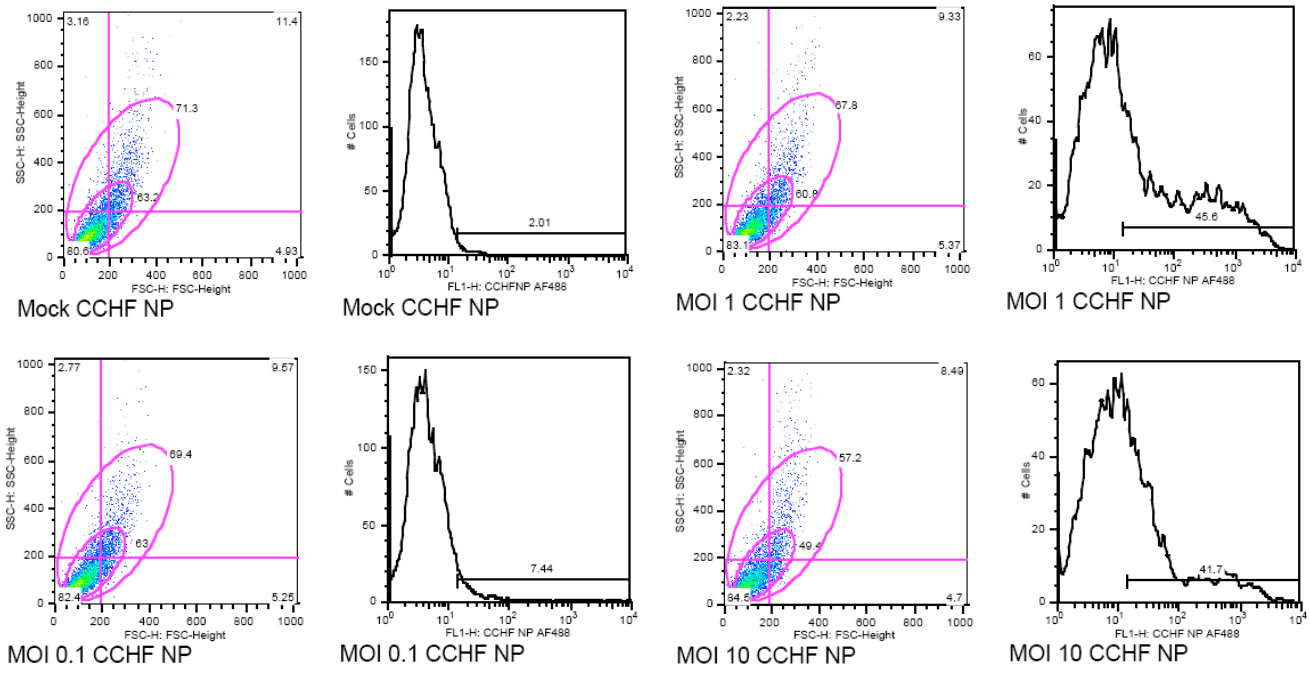

Fig. 11. 293T cells were infected with an MOI of 0.1, 1, or 10. Twenty-four hours post infection the cells were fixed in 10% formalin for 24 hours, followed by staining for CCHFV NP using a monoclonal antibody labeled with Alexa-Fluor 488. The percentage of infected cells was determined by flow cytometry. An antibody to an unrelated virus was used to determine background staining.

In addition to studies involving characterization of CCHFV strains, we also initiated experiments aimed at gaining a better understanding of virulence factors for CCHFV. Our studies focused on the potential of CCHFV to antagonize innate immune responses, such as the interferon (IFN) responses, of host cells. One of the most common methods of IFN antagonism by RNA virus is interference with the JAK-STAT signaling pathway. To determine if CCHFV was inhibiting this pathway, we infected (MOI of 5) or mock-infected 293T cells. On days 2 and 3 after infection, cells were either treated with 1000 IU of IFN-α/ml for 30 min or left untreated. At appropriate times, cells were lysed and lysates harvested and analyzed by western blotting to measure phosphorylation and activation of STAT1 and STAT2. We found that CCHFV did not inhibit phosphorylation of STAT1 and STAT2 following IFN treatment when compared to mock infected. Also, in infected cells that did not receive any IFN treatment, there were detectable levels of phosphorylated STATs indicating and viral infection alone was inducing IFN production.

To further characterize cellular response pathways that CCHFV might antagonize, we obtained profiler PCR Arrays from SuperArray Biosciences Corporation for use in analyzing the expression of a focused panel of genes for various cytokines and signaling pathways by real time PCR. Each 96-well plate includes SYBR Green-optimized primer assays for interferon or inflammatory pathway-focused genes. These arrays allow monitoring of the expression profiles of 84 genes per pathway that encode many important immunological molecules. In initial experiments, we tested Janus activated kinase/signal transducer and activator of transcription (JAK/STAT) and NF-kB arrays. We infected Liver cells (HepG2), which are permissive for CCHFV, at MOIs of 1 and 5. At 6, 12, and 24h postinfection, RNA from CCHFV-infected cells was processed according to manufacturer's recommendation. In these initial experiments, we found that these assay conditions resulted in an extremely high background, making interpretation of results suspect. Consequently, we began efforts to obtain highly purified CCHFV. We have experimented with CCHFV 10200 purification using PEG precipitation followed by purification on density gradients using Percoll and Optiprep matrices. To date the rate limiting step to virus recovery has been PEG precipitation, which is very infefficient. Banding of viable virus was obtained on the Percoll gradient, the purity of these bands are being assessed.

In addition to these studies, we supported work with Dr. García-Sastre's laboratory (subproject #1), to determine if interferon stimulated gene 15, a ubiquitin homologue is inhibited by infection with CCHFV. These findings are reported in the Subproject 1 results, and are detailed in a peer reviewed publication in 2007 (Frias-Staheli, et al., 2007).

Task 2. Epitope mapping of CCHFV monoclonal antibodies.

In collaboration with Subproject 2, we have conducted studies with a panel of monoclonal antibodies specific to G_N and G_C. These studies indicated that there were significant antigenic differences between the M segments from different CCHFV phylogenetic groups,

though several neutralizing epitopes in both G_N and in G_C were conserved among all strains examined (see Table 2, in appended manuscript 2, Ahmed et al., J. Gen. Virol., 86:3327-36). Thus, the genetic diversity exhibited by CCHFV strains results in significant antigenic differences that will need to be taken into consideration for vaccine development.

Since neutralizing MAb 11E7 was able to recognize G_C by Western blot under non-reducing conditions (see Fig. 3, in appended manuscript 1, Bertolotti-Ciarlet et al., J.Virol. 79: 6152-6), we were able, in collaboration with Subproject 2, to partially map its epitope by testing its ability to recognize fragments of G_C produced in 293T cells. This is of relevance because MAb 11E7 protects mice in vivo from challenge with CCHFV strain IbAr10200. Passive immunization can be effective for the treatment of CCHFV infection in humans, emphasizing the importance of identification of neutralizing antibodies and the epitopes to which they bind. The neutralizing epitope of MAb 11E7 is contained between amino acids 1443 and 1566 of the M segment of IbAr10200 strain, a highly conserved region of the protein.

Task 3 . Develop an animal model for CCHFV

As reported in the annual reports, we attempted to generate mouse and nonhuman primate models for CCHFV. For mice, we tested two approaches. The first approach involved serial passage of CCHFV from suckling mice (which are killed by CCHFV) through progressively older mice. The intent was to adapt the virus through passage for lethality. After 18 passes, we were unable to kill mice older than 6 days of age. Consequently, this approach was abandoned.

Our next approach involved CCHFV virus passage in SCID mice followed by passage in adult BALB/c mice to develop a lethal mouse-adapted CCHFV. In the initial adaptation, we sought to isolate the virus population that is capable of migrating to target tissues/organs (i.e. liver, peritoneal monocytes, Kupffer cells) at the earliest time point. The isolated virus was then used to infect new mice. Each group consisted of 10 mice that were inoculated intraperitoneally with 1000 pfu of CCHFV, strain 3010, which was isolated from a fatal human case in Uganda. Two mice were sacrificed each on days 2 and 3 and the tissues removed and virus isolated by homogenizing the tissues in 10 mls of PBS. To isolate virus, liver homogenates were centrifuged and the supernatants containing virus collected. The amount of virus in supernatants was quantified by plaque assay. Lethality was monitored in the remaining 8 mice. After 18 serial passes, we did not observe any increase in lethality in the SCID mice. Consequently, this effort was also temporarily abandoned. We plan to initiate similar new experiments but with different strains of CCHFV.

As an initial study of CCHFV in nonhuman primates, we injected three cynomolgus macaques intravenously with ~$1x10^4$ pfu of CCHFV strain 3010 and three others with ~$1x10^4$ pfu CCHFV strain I248 (isolated from a 1998 lethal human case of CCHFV in Uzbekistan). An additional group of two macaques serve as negative controls. Although some of the primates maintained the virus through six days post infection as measured by qPCR, none of them developed symptoms of disease. Although we were unsuccessful in obtaining a workable animal model of disease, we feel that these experiments suggest that it might be possible to develop an infection model in nonhuman primates and will continue efforts using higher challenge doses of virus. Additionally, in another project, we are attempting to develop a guinea pig model of disease and infection.

Recently, a STAT-1 mouse model for CCHFV strain IbAr 10200 was developed by Dennis Bente et al (J Virol. 2010 Nov;84(21):11089-100). To confirm that the CCHFV strain

IbAr 10200 in the USAMRIID repository was uniformly lethal in the reported model we infected 10 STAT-129, and 10 of the parent strain 129S6, with 100pfu via intra peritoneal injection. The virus was uniformly lethal in the STAT-129 mice by day 4 post infection, and as expected the parent strain showed no signs of infection.

Task 4. Support using live virus for projects 1 and 2.

Several support functions have already been detailed in tasks above. In addition to those, the following support tasks were accomplished:

We generated ELISA antigen by PEG precipitation of CCHFV, strain 10200, released into cell culture medium. This antigen was tested and shown to be reactive with mouse hyperimmune mouse ascitic fluid generated to CCHFV. These were provided to collaborators at both of the other laboratories. We also provided monoclonal antibodies to CCHFV to both of the collaborating laboratories.

Numerous attempts were made at optimizing and utilizing the reverse genetics system for CCHFV minigenome luciferase reporter assay. These tests were performed using Vero, 293T, and SW13 cell lines with CCHFV strains 10200 and U40. The information obtained during optimization of minigenome assays conducted under task 1, subproject 1, using supportive plasmids will hopefully generate the information required for the use of live CCHFV to drive higher levels of reporter gene expression.

We attempted to use a MuA transposon-based mutagenesis system to generate a fusion library in which a GFP encoding cassette is inserted randomly throughout the S RNA segment of the CCHFV genome. This reagent was intended for use in cell trafficking studies conducted under subproject 2. We screened the transfection/infection supernatants by RT-PCR to identify locations in CCHFV-S that will tolerate GFP fusions. We then constructed recombinant CCHFV-S RNA with GFP fusions in the identified locations, and repeated the process of transfection/infection several times. We were able to identify several clones that contained the GFP, but we had trouble recovering stable genes. Consequently, we contracted Geneart, Inc. to generate a codon optimized and stabilized clone. Although this clone was not available for use during this granting period, we believe that it will have great applicability in future studies, and once characterized will be provided to the collaborating labs.

We generated a baculovirus recombinant that produces the nucleocapsid protein of CCHFV, strain 10200. This was accomplished to provide a better characterized and more stable source of CCHFV antigen for ELISA. Although this was constructed late in the granting period, it should be of great value for continuing studies by us and our collaborators. An FPLC purification approach was undertaken (Fig. 12) to purify the NP to approximately 90%, and further refinement of purification in order to increase protein purity is ongoing. Collaborators will soon be testing this purified protein with positive human sera for reactivity.

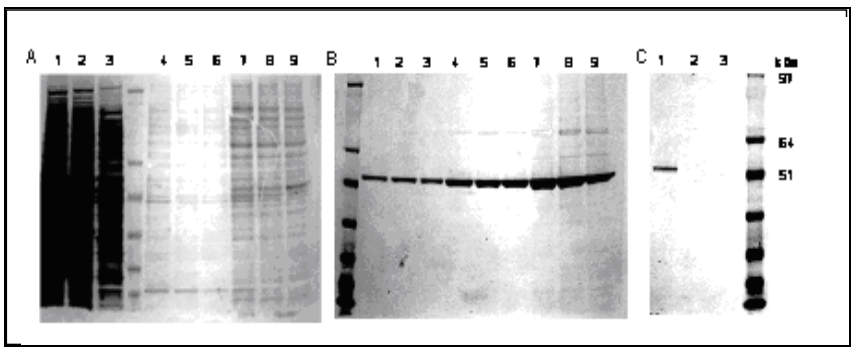

Fig. 12: A recombinant baculovirus was constructed to produce a His-tagged CCHF-NP protein. FPLC was used to purify the protein and increasing concentrations of imadazole were used to elute the proteins. A Western blot was performed with an anti-CCHFV-NP antibody (C) and the final purified product (C, lane 1) retention (C, lane 1) to confirm the identity of the purified protein.

3. Key research accomplishments.

Our key research accomplishments are also listed under **Conclusions** and in the papers and abstracts (listed under **Reportable Outcomes**). The major key research accomplishments reached during this project are as follows:

1. We found that IBR 10-200 is growth restricted in human macrophages unlike 3010.
2. We have determined cell cytokine levels in response to viral infection in a cell system
3. Intact virus support was provided to projects 1 and 2. A graduate student was fully trained to work at USMRIID in the high biocontainment laboratories.
4. The sequence of the L protein of CCHFV has been obtained
5. We found that the L protein of CCHFV is a cytoplasmic protein with an apparent molecular weight of 450kDa.
6. We found that a luciferase reporter gene construct flanked by the 3' and 5' UTR of the S segment of CCHFV is replicated and transcribed in CCHFV-infected cells.
7. We found that the N protein of CCHFV has a strong RNA-binding domain in the C-terminal half of the protein (amino acids 240 to 482) and a second weaker RNA-binding domain at the N-terminus (amino acids 1 to 160).
8. We reported that the GN and GC proteins are targeted to the Golgi when expressed together. When expressed alone, GN is transported to the Golgi while GC is retained in the ER.
9. We found that codon optimization of the CCHFV M segment makes it possible to over-express the GN and GC glycoproteins, resulting in the delivery of some of the proteins to the cell surface.
10. We found that the GN and GC proteins present on the cell surface can mediate cell-cell fusion at acid pH. This makes it possible to study the function of these proteins under BSL2 conditions.
11. We found that the GC protein forms a dimer.
12. We reported that there is significant antigenic variability between different CCHFV strains isolated from different parts of the world. While this has obvious implications for vaccine development, it is important to recognize that some neutralizing epitopes are highly conserved, making these important vaccine targets.
13. We found that the N protein has a predicted coiled-coiled domain that might be involved in oilgomerization.
14. We found that the N protein oligomerizes, and the first 160 amino acids are dispensable for N-N interactions.
15. We found that the N protein has a strong interaction with the N-terminal fragment of the L protein, and a weak interaction with the C-terminal fragment of the L protein.
16. We reported that the OTU-like domain of the L protein has isopeptidase activity and is able to overcome antiviral pathways regulated by ubiquitin and by the IFN-inducible ubiquitin-like molecule ISG15. This activity is common with the nsp2 protease of arteriviruses.
17. We reported that the Gn protein undergoes a C-terminal cleavage event that liberates an NSm protein. Cleavage appears to occur within the second transmembrane domain, making this an intramembranous cleavage event. 18. The NSm protein is stable, transported to the Golgi, and is produced in virus infected cells.
19. We found that it is possible to produce some soluble versions of the Gn protein that are secreted from cells, making it possible to begin crystallization trials.
20. We have established a collaboration with investigators at Lawrence Livermore National Laboratories (LLNL) for complete sequence analysis of CCHFV strains.

21. We found that CCHFV infection does not inhibit phosphorylation of STAT1 and STAT2 following IFN treatment.
22. We found that CCHFV infection resulted in IFN production, as detected by STAT phosphorylation.
23. We have optimized the tissue culture techniques to propagate strain 10200 of CCHFV and obtained CCHFV titers in the range of 10^7-10^8 pfu/ml.
24. We found that the 3' UTR of the L gene of CCHFV has an unusual G at position 10, not shared by the M and S genes.
25. Our evidence is most consistent with signal peptidase being responsible for NSm cleavage, but we have not proven this.
26. We reported that the NSm protein is stable, transported to the Golgi, and is produced in virus infected cells. When it is genetically ablated, the viral glycoproteins do not fold and assemble correctly.
27. We found that codon optimization of the CCHFV M segment makes it possible to express CCHFV glycoproteins at the cell surface.
28. We found that cells expressing the CCHFV glycoproteins mediate fusion with other cells quickly and efficiently following low pH treatment, thus providing us with a high throughput assess to study CCHFV glycoprotein function.
29. CCHFV has been successfully passaged 18 times in SCID mice.
30. We found that CCHFV replicates in non-human primates.
31. An enzymatically active OTU domain of the L of CCHFV has been expressed and purified from bacteria.
32. We have established a fluorometric enzymatic assay for the screen of inhibitors of the OTU domain of the L of CCHFV.
33. We have optimized and developed this enzymatic assay in a 386 format assay.
34. We have conducted a HTS for small compounds that inhibit the enzymatic activity of the OTU protease of the L protein of CCHFV and identified several specific inhibitors.
35. We generated a baculovirus recombinant that produces the nucleocapsid protein of CCHFV, strain 10200.
36. We developed an immunofluorescence assay in which CCHFV-infected cells can be quantified by using a Fluorescence Activated Cell Sorter
37. We have characterized the enzymatic activities of the OTU protease of the L protein of CCHFV against Ub-linked and ISG15-linked substrates
38. We have solved the structure of the OTU protease of the L protein bound to two of their substrates, Ub and ISG15, that can now be used to better refine the identified inhibitors, for possible use in vivo.
39. We have confirmed that STAT-1 knock-out mice can be used as a lethal animal model of CCHFV infection, opening the possibility of using a mouse model of this virus.

4. Reportable outcomes.

Over the four years of this DOD-sponsored project, plus two more years of no-cost extension, fove papers have been published, two in the Journal of Virology, one in Journal of General Virology, one in Cell Host and Microbe and one in PNAS. Mr. Lou Altamura, the graduate student who led the subproject at U Penn, visited USAMRIID approximately 4 times a year, spending 1-2 weeks each time to work with live CCHFV in the biocontainment suites. He graduated in early 2008 and has begun a postdoctoral fellowship with Dr. Schmaljohn at USAMRIID where he continues to work on CCHFV. We are particularly proud of the fact that this grant supported the work of one of the top students at the University of Pennsylvania in a manner that influenced his career choice such that he has chosen to continue working on

emerging viruses at USAMRIID. Ms Frias-Staheli, the graduate student that led the work at Mount Sinai School of Medicine, also graduated this year, and she has decided to stay working as a postdoc on emerging virus diseases in the laboratory of Charlie Rice.

Papers and abstracts that have resulted from this research project during the period of support are listed below.

PAPERS

Bertolotti-Ciarlet, A., Smith J., Strecker K., Paragas J., Altamura L., McFalls J., Frias-Staheli N., García-Sastre, A., Schmaljohn, C., and Doms, RW. (2005) Cellular localization and antigenic characterization of Crimean-Congo hemorrhagic fever virus glycoproteins. J.Virol. 79: 6152-61.

Ahmed, A., McFalls, J., Hoffmann, C., Filone, C.M., Stewart S. M., Paragas, J., Khodjaev S., Shermukhamedova D., Schmaljohn, C.S., Doms, R.W., and Bertolotti-Ciarlet, A. (2005) Presence of broadly reactive and group-specific neutralizing epitopes on newly described isolates of Crimean-Congo hemorrhagic fever virus. Journal of General Virology. 86:3327-36.

Altamura, L.A., A. Andrea Bertolotti-Ciarlet, J. Teigler, J.J. Paragas, C.S. Schmaljohn and R.W. Doms. (2007) Identification of a novel C-terminal cleavage of Crimean-Congo hemorrhagic fever virus PreGN that leads to generation of an NSM protein. J. Virol. 81:6632-6642.

Frias-Staheli, N., N. V. Giannakopoulos, M. Kikkert, S. L. Taylor, A. Bridgen, J. Paragas, J. A. Richt, R. R. Rowland, C. S. Schmaljohn, D. J. Lenschow, E. J. Snijder, A. Garcia-Sastre, and H. W. t. Virgin. 2007. Ovarian tumor domain-containing viral proteases evade ubiquitin- and ISG15-dependent innate immune responses. Cell Host Microbe 2:404-16.

James, T. W., N. Frias-Staheli, J.-P. Bacik, J. M. L. Macleod, M. Khajehpour, A. García-Sastre & B. L. Mark. Structural basis for the removal of ubiquitin and interferon-stimulated gene 15 by a viral ovarian tumor domain-containing protease. 2011. Proc. Natl. Acad. Sci. (USA),108:2222-2227.

ABSTRACTS TO MEETINGS

Frias-Staheli, N., Ratnakumar, K., and García-Sastre, A. (2006). The nucleocapsid of Crimean-Congo hemorrhagic fever virus is a ssRNA-binding protein that oligomerizes and can interact with the viral polymerase. XIII International Conference on Negative Strand Viruses. June 17-22 Salamanca, Spain.

Altamura, L.A., Stubbs, J., Schmaljohn, C.S., and Doms, R.W. (2007) Crimean-Congo hemorrhagic fever virus encodes an NSM protein. American Society for Tropical Medicine and Hygiene 56th Annual Meeting. November 4-8 Philadelphia, PA. Poster and oral presentations.

Altamura, L.A., Bertolotti-Ciarlet, A., Teigler, J., Paragas, J., Schmaljohn, C., and Doms, R.W. (2006) Identification of a novel C-terminal cleavage of Crimean-Congo hemorrhagic fever virus PreGN. American Society for Virology 25th Annual Meeting. July 15-19 Madison, WI.

Altamura, L.A., Bertolotti-Ciarlet, A., Teigler, J., Paragas, J., Schmaljohn, C., and Doms, R.W. (2006) Identification of a novel C-terminal cleavage of Crimean-Congo hemorrhagic fever virus PreGN. XIII International Conference on Negative Strand Viruses. June 17-22 Salamanca, Spain.

Altamura, L.A., Schmaljohn, C.S., and Doms, R.W. (2007) Crimean-Congo hemorrhagic fever virus encodes an NSM protein. American Society for Virology 26th Annual Meeting. July 14-18 Corvallis, OR. Oral presentation.

N. Frias-Staheli, N. V. Giannakopoulos, C. S. Schmaljohn, H. W. Virgin IV, A. García-Sastre (2007). The OTU Domain-containing L protein of Crimean Congo Hemorragic Fever Virus Has De-ISGylating and De-Ubiquitinating activities. American Society for Virology 26th Annual Meeting. July 14-18 Corvallis, OR. Oral presentation. Awarded with a prize for best presentation.

N. V. Giannakopoulos, N. Frias-Staheli, A. García-Sastre, H. W. Virgin IV (2007). Viral OTU domains: A new class of immune evasion proteases targeting both ubiquitin and ISG15 conjugates. Meeting on Ubiquitin and Ubiquitin-like Modifications in Viral Infection and Immunity. August 28-29. Natcher Conference Center. NIH Campus, Bethesda. Awarded with a prize for best poster.

Adolfo García-Sastre, Natalia Frías-Staheli and Rafael A. Medina (2009). Towards the development of a high throughput assay to identify inhibitors of the OTU protease encoded by Crimean-Congo hemorrhagic fever virus. Presented at the "Military Health Research Forum 2009", Kansas City, August 2009

Adolfo García-Sastre, Natalia Frías-Staheli, Maudry Laurent-Rolle, Juliet Morrison, Courtney Ray Plumlee, Dabeiba Bernal, Ana Fernandez-Sesma, Christian Schindler, Rafael Medina, Joseph Ashour. Inhibition of Innate Immunity by Hemorrhagic Fever Arboviruses. Presented at the Annual Biodefense Research Centers of Excellence Meeting, Las Vegas, 2010.

5. Conclusions.

The major conclusions reached during this project, also listed under research accomplishments, are as follows:

1. We found that IBR 10-200 is growth restricted in human macrophages unlike 3010.
2. We have determined cell cytokine levels in response to viral infection in a cell system
3. Intact virus support was provided to projects 1 and 2. A graduate student was fully trained to work at USMRIID in the high biocontainment laboratories.
4. The sequence of the L protein of CCHFV has been obtained
5. We found that the L protein of CCHFV is a cytoplasmic protein with an apparent molecular weight of 450kDa.
6. We found that a luciferase reporter gene construct flanked by the 3' and 5' UTR of the S segment of CCHFV is replicated and transcribed in CCHFV-infected cells.
7. We found that the N protein of CCHFV has a strong RNA-binding domain in the C-terminal half of the protein (amino acids 240 to 482) and a second weaker RNA-binding domain at the N-terminus (amino acids 1 to 160).
8. We reported that the GN and GC proteins are targeted to the Golgi when expressed together. When expressed alone, GN is transported to the Golgi while GC is retained in the ER.
9. We found that codon optimization of the CCHFV M segment makes it possible to over-express the GN and GC glycoproteins, resulting in the delivery of some of the proteins to the cell surface.
10. We found that the GN and GC proteins present on the cell surface can mediate cell-cell fusion at acid pH. This makes it possible to study the function of these proteins under BSL2 conditions.
11. We found that the GC protein forms a dimer.

12. We reported that there is significant antigenic variability between different CCHFV strains isolated from different parts of the world. While this has obvious implications for vaccine development, it is important to recognize that some neutralizing epitopes are highly conserved, making these important vaccine targets.
13. We found that the N protein has a predicted coiled-coiled domain that might be involved in oilgomerization.
14. We found that the N protein oligomerizes, and the first 160 amino acids are dispensable for N-N interactions.
15. We found that the N protein has a strong interaction with the N-terminal fragment of the L protein, and a weak interaction with the C-terminal fragment of the L protein.
16. We reported that the OTU-like domain of the L protein has isopeptidase activity and is able to overcome antiviral pathways regulated by ubiquitin and by the IFN-inducible ubiquitin-like molecule ISG15. This activity is common with the nsp2 protease of arteriviruses.
17. We reported that the Gn protein undergoes a C-terminal cleavage event that liberates an NSm protein. Cleavage appears to occur within the second transmembrane domain, making this an intramembranous cleavage event. 18. The NSm protein is stable, transported to the Golgi, and is produced in virus infected cells.
19. We found that it is possible to produce some soluble versions of the Gn protein that are secreted from cells, making it possible to begin crystallization trials.
20. We have established a collaboration with investigators at Lawrence Livermore National Laboratories (LLNL) for complete sequence analysis of CCHFV strains.
21. We found that CCHFV infection does not inhibit phosphorylation of STAT1 and STAT2 following IFN treatment.
22. We found that CCHFV infection resulted in IFN production, as detected by STAT phosphorylation.
23. We have optimized the tissue culture techniques to propagate strain 10200 of CCHFV and obtained CCHFV titers in the range of 10^7-10^8 pfu/ml.
24. We found that the 3' UTR of the L gene of CCHFV has an unusual G at position 10, not shared by the M and S genes.
25. Our evidence is most consistent with signal peptidase being responsible for NSm cleavage, but we have not proven this.
26. We reported that the NSm protein is stable, transported to the Golgi, and is produced in virus infected cells. When it is genetically ablated, the viral glycoproteins do not fold and assemble correctly.
27. We found that codon optimization of the CCHFV M segment makes it possible to express CCHFV glycoproteins at the cell surface.
28. We found that cells expressing the CCHFV glycoproteins mediate fusion with other cells quickly and efficiently following low pH treatment, thus providing us with a high throughput assess to study CCHFV glycoprotein function.
29. CCHFV has been successfully passaged 18 times in SCID mice.
30. We found that CCHFV replicates in non-human primates.
31. An enzymatically active OTU domain of the L of CCHFV has been expressed and purified from bacteria.
32. We have established a fluorometric enzymatic assay for the screen of inhibitors of the OTU domain of the L of CCHFV.
33. We have optimized and developed this enzymatic assay in a 386 format assay.
34. We have conducted a HTS for small compounds that inhibit the enzymatic activity of the OTU protease of the L protein of CCHFV and identified several specific inhibitors.
35. We generated a baculovirus recombinant that produces the nucleocapsid protein of CCHFV, strain 10200.

36. We developed an immunofluorescence assay in which CCHFV-infected cells can be quantified by using a Fluorescence Activated Cell Sorter
37. We have characterized the enzymatic activities of the OTU protease of the L protein of CCHFV against Ub-linked and ISG15-linked substrates
38. We have solved the structure of the OTU protease of the L protein bound to two of their substrates, Ub and ISG15, that can now be used to better refine the identified inhibitors, for possible use in vivo.
39. We have confirmed that STAT-1 knock-out mice can be used as a lethal animal model of CCHFV infection, opening the possibility of using a mouse model of this virus.

6. References.

Garrison, A. R., S. Alakbarova, D. A. Kulesh, D. Shezmukhamedova, S. Khodjaev, T. P. Endy, and J. Paragas. 2007. Development of a TaqMan minor groove binding protein assay for the detection and quantification of Crimean-Congo hemorrhagic fever virus. Am J Trop Med Hyg 77:514-20.

7. Appendices.

Original copies of journal articles published during this grant have been attached.

8. Supporting data.

Twelve figures with figure legends have been included in the body text.

JOURNAL OF VIROLOGY, May 2005, p. 6152–6161 Vol. 79, No. 10
0022-538X/05/$08.00+0 doi:10.1128/JVI.79.10.6152–6161.2005

Cellular Localization and Antigenic Characterization of Crimean-Congo Hemorrhagic Fever Virus Glycoproteins

Andrea Bertolotti-Ciarlet,[1] Jonathan Smith,[2] Karin Strecker,[1] Jason Paragas,[3] Louis A. Altamura,[1] Jeanne M. McFalls,[1] Natalia Frias-Stäheli,[4] Adolfo García-Sastre,[4] Connie S. Schmaljohn,[3] and Robert W. Doms[1]*

Department of Microbiology, University of Pennsylvania, Philadelphia, Pennsylvania 19104[1]; AlphaVax, Inc., 2 Triangle Drive, Research Triangle Park, North Carolina 27709[2]; Virology Division, U.S. Army Medical Research Institute for Infectious Diseases, Fort Detrick, Frederick, Maryland 21702[3]; and Department of Microbiology, Mount Sinai School of Medicine, One Gustav L. Levy Place, New York, New York 10029[4]

Received 30 July 2004/Accepted 21 December 2004

Crimean-Congo hemorrhagic fever virus (CCHFV), a member of the genus *Nairovirus* of the family *Bunyaviridae*, causes severe disease with high rates of mortality in humans. The CCHFV M RNA segment encodes the virus glycoproteins G_N and G_C. To understand the processing and intracellular localization of the CCHFV glycoproteins as well as their neutralization and protection determinants, we produced and characterized monoclonal antibodies (MAbs) specific for both G_N and G_C. Using these MAbs, we found that G_N predominantly colocalized with a Golgi marker when expressed alone or with G_C, while G_C was transported to the Golgi apparatus only in the presence of G_N. Both proteins remained endo-β-*N*-acetylglucosaminidase H sensitive, indicating that the CCHFV glycoproteins are most likely targeted to the *cis* Golgi apparatus. Golgi targeting information partly resides within the G_N ectodomain, because a soluble version of G_N lacking its transmembrane and cytoplasmic domains also localized to the Golgi apparatus. Coexpression of soluble versions of G_N and G_C also resulted in localization of soluble G_C to the Golgi apparatus, indicating that the ectodomains of these proteins are sufficient for the interactions needed for Golgi targeting. Finally, the mucin-like and P35 domains, located at the N terminus of the G_N precursor protein and removed posttranslationally by endoproteolysis, were required for Golgi targeting of G_N when it was expressed alone but were dispensable when G_C was coexpressed. In neutralization assays on SW-13 cells, MAbs to G_C, but not to G_N, prevented CCHFV infection. However, only a subset of G_C MAbs protected mice in passive-immunization experiments, while some nonneutralizing G_N MAbs efficiently protected animals from a lethal CCHFV challenge. Thus, neutralization of CCHFV likely depends not only on the properties of the antibody, but on host cell factors as well. In addition, nonneutralizing antibody-dependent mechanisms, such as antibody-dependent cell-mediated cytotoxicity, may be involved in the in vivo protection seen with the MAbs to G_C.

Crimean-Congo hemorrhagic fever virus (CCHFV) causes a hemorrhagic and toxic syndrome in humans with mortality rates of up to 50%. CCHFV infection was first described during an outbreak in Russia during the 1940s, when more than 200 cases of severe hemorrhagic fever were reported among agricultural workers and soldiers in the Crimean peninsula (15, 16). Since then, the virus has spread throughout many regions of the world, including sub-Saharan Africa (60, 61), Bulgaria, the Arabian Peninsula, Iraq, Pakistan, the former Yugoslavia, northern Greece, and northwest China (16, 23, 42–45).

CCHFV is a member of the genus *Nairovirus* within the family *Bunyaviridae* (52). Members of this enveloped-virus family have a tripartite, single-stranded RNA genome of negative polarity. The medium RNA segment (the M segment) encodes the viral glycoproteins G_N and G_C, which, like those of other *Bunyaviridae*, are synthesized as polyprotein precursors that undergo proteolytic cleavage events to yield mature glycoproteins (52). The CCHFV glycoproteins exhibit several unusual structural features and undergo several processing events. First, the CCHFV glycoproteins contain, on average, 78 to 80 cysteine residues, suggesting the presence of an exceptionally large number of disulfide bonds and a complex secondary structure. Second, the G_N precursor protein (Pre-G_N) contains a highly variable domain at its amino terminus that contains a high proportion of serine, threonine, and proline residues, and it is predicted to be heavily O glycosylated, thus resembling a mucin-like domain present in other viral glycoproteins, most notably the Ebola virus glycoprotein (56). The mucin-like region in the Ebola glycoprotein has been shown to play an important role in a cell-rounding phenotype and immunoevasion (39, 56). It is not known whether this domain plays an important role in CCHFV pathogenesis or whether it is even O glycosylated. A third unusual feature is

* Corresponding author. Mailing address: Department of Microbiology, University of Pennsylvania, 225 Johnson Pavilion, 3610 Hamilton Walk, Philadelphia, PA 19104. Phone: (215) 898-0890. Fax: (215) 898-9557. E-mail: doms@mail.med.upenn.edu.

that the G_N glycoprotein can undergo two posttranslational proteolytic cleavage events at the conserved motifs RSKR and RRLL, potentially releasing the mucin-like domain as well as a second N-terminal domain of approximately 35 kDa (P35, or the connector domain) (59). It is not known if the released domains traffic to an intracellular compartment, if they are secreted, or what effect they may have on viral pathogenesis and antigenic structure. Similar processing strategies have not been observed for other *Bunyaviridae* outside of the *Nairovirus* group.

As the only virally encoded membrane proteins, G_N and G_C must interact with cell surface receptors, mediate the entry of virus into cells, and serve as targets for neutralizing antibodies. Passive transfer of neutralizing antibodies can protect susceptible animals from hantavirus infection (8, 53–55, 62), and there is a report that convalescent-human sera can afford some protection in acutely infected individuals (58). Thus, characterizing the structures and functions of these proteins will be important for understanding CCHFV tropism and pathogenesis as well as for vaccine development. In this study, we describe the first monoclonal antibodies (MAbs) raised against the CCHFV glycoproteins, map the subunits to which they bind, and characterize their abilities to neutralize virus and to protect mice from a lethal CCHFV challenge. In addition, using these MAbs, we investigated the localization of G_N and G_C when expressed alone or together and have begun to map the regions involved in glycoprotein localization and interactions.

MATERIALS AND METHODS

Cells, antibodies, and viruses. CCHFV prototype strain IbAr10200, first isolated in 1976 from *Hyalomma excavatum* ticks from Sokoto, Nigeria, was grown in African green monkey kidney Vero cells or the E6 variant (51). African green monkey kidney fibroblast (CV-1), Vero, Vero E6, human cervix carcinoma (HeLa), and human embryonic kidney (HEK 293T) cells were maintained in Dulbecco's modified Eagle medium (DMEM) supplemented with 10% fetal bovine serum (Invitrogen, Carlsbad, CA). Similarly, the human tumor cell line SW-13 (adrenocortical carcinoma) was grown in DMEM supplemented with 2.5% fetal bovine serum. Work with CCHFV was performed in a biosafety level 4 laboratory at the U.S. Army Medical Research Institute for Infectious Diseases. A recombinant vaccinia virus expressing the T7 bacteriophage RNA polymerase (vTF1.1) was grown in HeLa cells, and titers were determined in CV-1 cells according to standard protocols (1).

Production of MAbs. MAbs were prepared against the G_N and G_C glycoproteins of the CCHFV strain IbAr10200 by fusion of SP2/0 myeloma cells with splenocytes from BALB/c inbred mice. We carried out five independent fusions in which mice were immunized with infected suckling mouse brain homogenates (fusions I and II; MAb 30F7), with affinity-purified virion glycoproteins precipitated from nonionic detergent lysates of gradient-purified virus preparations (fusions III and IV; MAbs 1H6, 5E3, 6C2, 5B5, 8C4, 9H3, 3E3, 8G7, 8A8, and 8F10), or with affinity-purified proteins from similar lysates of infected cells (fusion V; MAbs 8A1, 12A9, 11E7, 6C11, 13G8, 14B6, 10G4, 5A5, 6B12, 10E11, 3F3, 2C9, 7F5, 11F6, and 9C6). In earlier studies, we found that hybridoma fusions carried out with splenocytes from mice immunized with mouse brain homogenates resulted predominantly in MAbs that were reactive with the viral nucleocapsid protein. To produce immunogens enriched in viral glycoproteins, cultures of SW-13 cells in 34 T-150 flasks were infected with the IbAr10200 strain of CCHFV and incubated for 36 h at 37°C. Medium fractions were removed, clarified at 10,000 × *g*, and centrifuged in an SW28 rotor (Beckman) to pellet virus particles (25,000 rpm for 3 h). Virus pellets were lysed in immunoprecipitation buffer (50 mM Tris-HCl, pH 8.0, containing 150 mM NaCl, 2% Triton X-100, 1% sodium deoxycholate, and protease inhibitors) and subsequently centrifuged to equilibrium in CsCl gradients. This resulted in a separation of the viral nucleocapsid (density = 1.3 g/ml) from the viral glycoproteins which banded in a broad band at lower densities. Infected-cell monolayers were similarly lysed in immunoprecipitation buffer, clarified at 10,000 × *g*, and centrifuged in an SW41 rotor (Beckman) to sediment the viral nucleocapsid from the solubilized viral glycoproteins (40,000 rpm for 4 h). Fractions enriched for viral glycoproteins from both cell and virion samples were then collected on solid-phase immunoadsorbents prepared by saturating protein A-Sepharose with anti-CCHFV hyperimmune mouse ascitic fluid (D. Watts, U.S. Army Medical Research Institute for Infectious Diseases). Immunoadsorbents were then exhaustively washed with phosphate-buffered saline (PBS), emulsified directly in complete or incomplete Freund's adjuvant, and inoculated subcutaneously and intraperitoneally into mice as described below. With this procedure, the CCHFV glycoproteins were enriched but were not pure. Importantly, the viral nucleocapsid was not detectable under these conditions, and using these immunogens, we were able to prepare a large number of CCHFV glycoprotein-specific MAbs.

MAbs were produced essentially as described previously (28). Briefly, BALB/c mice were twice immunized intraperitoneally with 100 μl of antigen preparations emulsified in Freund's complete adjuvant for primary immunization and in Freund's incomplete adjuvant for secondary immunization. Mice were euthanized 3 to 5 days after a third immunization, and splenocytes were fused with Sp2/0-Ag14 myeloma cells. Hybridoma cultures were incubated at 37°C with several changes of hypoxanthine-aminopterin-thymidine medium, and the supernatant fluids were screened by immunofluorescence (IF) assays against CCHFV-infected Vero cells and by enzyme-linked immunosorbent assays (ELISA) with viral antigen from suckling mouse brain homogenates or gradient-purified virus preparations. Antigenic specificity was initially determined by immunoprecipitation from [^{35}S]methionine-labeled infected-cell lysates (as described below) and subsequently by IF microscopy. Positive-antibody-producing cells were cloned by limiting dilution and then expanded. The immunoglobulin G subclasses of the resulting MAbs were determined by indirect ELISA analysis using hybridoma supernatants. The ELISA was developed using immunoglobulin G subclass-specific immunoglobulins (Miles Laboratories) by following the manufacturer's instructions.

Neutralization assays. Eighty percent plaque reduction neutralization (PRN-80) tests were carried out on SW-13 cell monolayers. Twofold serial dilutions of the MAbs were mixed with 200 PFU of the CCHFV IbAr10200 strain and incubated for 1 h at 37°C. Confluent monolayers of SW-13 cells in six-well plates were incubated with the virus-antibody mixture for 1 h at 37°C. The inocula were removed, and 1 ml of overlay consisting of 1 part double-strength DMEM with 5% fetal bovine serum and 1 part low-gelling-temperature agarose (Bio-Rad Laboratories, Richmond, CA) in distilled water was added. After incubation at 35°C in a sealed chamber for 2 to 5 days, the plaques were visualized by neutral red staining.

Protection studies. To evaluate the protective activities of MAbs directed against the CCHFV glycoproteins in an animal model, suckling mice, which are susceptible to infection with CCHFV (24, 50), were challenged with live virus before or after passive immunization with the CCHFV-specific MAbs. Two- to 3-day-old suckling mice were inoculated in groups of five to eight by intraperitoneal injection with 50 μl of undiluted ascitic fluid containing the different MAbs. The ascitic fluids were administrated 24 h before or after the inoculation of 100 50% lethal-dose units of the CCHFV strain IbAr10200. Ascitic fluid from Sp2/0 cells that did not contain virus-specific antibodies was used as a negative control.

Construction of CCHFV glycoprotein clones. The pCAGGS-M clone was created by cloning the entire M segment of IbAr10200 into the NruI and XhoI sites found in the plasmid pCAGGS-MCSII (41). The M segment was digested using the unique restriction enzyme sites SnaBI and SalI located in the untranslated regions of the gene. This clone was used as a template for the generation of a panel of constructs used to map functional regions on CCHFV glycoproteins (Fig. 1). Primers were synthesized according to the published sequence for IbAr10200 (51), and standard PCR technology was performed for cloning into the pcDNA3.1D/V5-His-TOPO vector (Invitrogen, Carlsbad, CA). The 5′-end primers included the CACC sequence at the 5′ end and the start codon to allow for directional cloning. The 3′-end primers did not possess a stop codon to allow the inclusion of the V5 and His epitope tags at the C terminus of the protein. The cloning was performed as described by the manufacturer (Invitrogen), and all constructs were sequenced. All primer sequences are available upon request.

Protein analysis. To analyze protein expression, we transfected HEK 293T cells using Lipofectamine 2000 (Invitrogen). After 24 h, cell extracts were prepared in 50 mM Tris-HCl, pH 7.4, 5 mM EDTA, 1% Triton X-100, and Complete protease inhibitor cocktail (Roche Applied Sciences, Indianapolis, IN). Cell lysates were incubated at 4°C for 3 min and then centrifuged at 10,000 × *g* for 10 min. Sodium dodecyl sulfate-polyacrylamide gel electrophoresis (SDS-PAGE) was performed using 4 to 15% Tris-HCl gels (Bio-Rad, Hercules, CA), followed by Western blot analysis with mouse anti-V5 (Invitrogen) as the primary antibody and sheep anti-mouse horseradish peroxidase conjugate as the second-

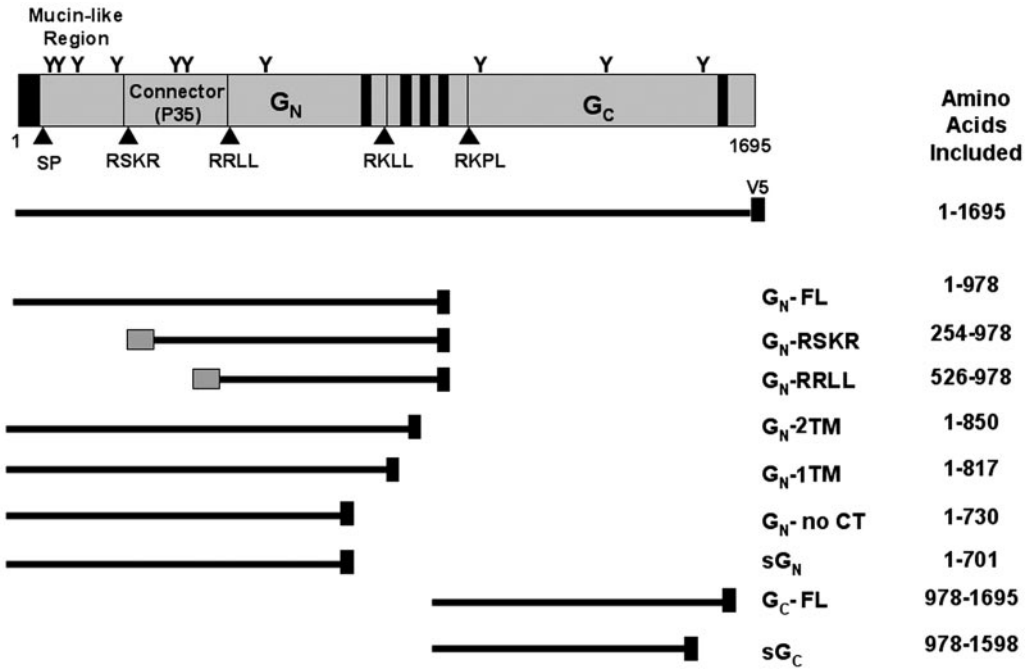

FIG. 1. Schematic representation of CCHFV M segment constructs. Predicted N-linked glycosylation sites are indicated with "Y." The filled triangles (▲) indicate the predicted conserved cleavage sites with the four conserved amino acid cleavage sites indicated (59), and the black bars indicate the predicted TMs. Specific constructs used in this study are also indicated by black lines, indicating which portions of the CCHFV M segment are included in each construct. The gray boxes on the constructs G_N-RSKR and G_N-RRLL indicate the inclusion of the hen egg white lysozyme signal peptide at the N terminus of the protein (6). A V5 epitope tag was positioned at the C terminus of each construct; these tags are represented as black boxes on the far-right side of each construct. Finally, the amino acids included in each construct are indicated on the right column, using the first methionine in the IbAr10200 strain as residue 1.

ary antibody (Amersham Pharmacia, Buckinghamshire, United Kingdom), followed by visualization with ECL-Plus Western blotting detection reagents (Bioscience, Piscataway, NJ).

IF microscopy. Localization of the CCHFV glycoproteins by indirect IF was performed as described previously (38). HeLa cells grown to 50% confluence on glass coverslips were infected with the recombinant vaccinia virus vTF1.1 (1), followed 40 min later by transfection with the different pcDNA3.1D/V5-His constructs (Fig. 1). When proteins were expressed with pCAGGS constructs, vTF1.1 infection was not utilized, since protein expression was obtained from the chicken beta-actin promoter. At 24 h posttransfection, the cells were fixed with 2% (wt/vol) paraformaldehyde in PBS, permeabilized with 0.5% Triton X-100, and stained with a G_N- or G_C-specific MAb ascites fluid (diluted 1:250) or with mouse anti-V5 MAb (diluted 1:500) (Invitrogen) in PBS containing 0.5 mM $MgCl_2$ and 4% fetal bovine serum. In addition, TGN46, a sheep antibody specific for a heavily glycosylated protein localized primarily in the trans-Golgi network, was included as a marker for Golgi localization (Serotec, Oxford, United Kingdom). Then, cells were washed with PBS and incubated for 1 h with the secondary antibodies conjugated to Alexa Flour 488 (goat anti-mouse) and Alexa Flour 594 (goat anti-sheep) (Molecular Probes, Eugene, OR) diluted 1:500 in PBS–4% fetal bovine serum. Finally, cells were washed in PBS, mounted in Fluoromount-G (Southern Biotechnology Associates, Birmingham, AL), and examined on a Nikon E600 microscope at a magnification of ×60 utilizing UV illumination.

Endoglycosidase treatment. The method of Trimble and Maley (57) was slightly modified for digesting glycosylated CCHFV glycoproteins with endo-β-*N*-acetylglucosaminidase H (endo-H). Cell lysates from transfected HEK 293T cells were boiled for 5 min in a 50 mM sodium citrate buffer (pH 5.5) containing 1% SDS and 200 μg/ml of phenylmethylsulfonyl fluoride. After cooling, the samples were supplemented with an equal volume of 0.02 U of endo-H (New England BioLabs Inc., Beverly, MA) in a 50 mM sodium citrate buffer (pH 5.5) or the same buffer without the enzyme before incubation at 37°C for 20 h. After this incubation, the samples were analyzed by SDS-PAGE. In addition, the glycoproteins were treated with peptide-*N*-glycosidase F (PNGase F) (New England Biolabs). A similar protocol was followed for PNGase F treatment, but the digestion was performed in 100 mM sodium phosphate, pH 7.5, with 0.75% NP-40, 0.1% SDS, and 50 mM β-mercaptoethanol.

Immunoprecipitations from infected cells. Immunoprecipitation assays were performed as previously described (38). Briefly, SW-13 cell monolayers (1×10^6 cells) were infected with the CCHFV strain IbAr10200 at a multiplicity of infection of 5. Infected SW-13 cells were placed in methionine-free DMEM at 28 h postinfection for 30 min, and then 30 μCi of [^{35}S]methionine (Trans-^{35}S-label; ICN, Irvine, CA) was added. After 1 h of labeling, 50 μg of unlabeled methionine per ml was added. Infected cells were collected 24 h postlabeling or 20 h posttransfection and lysed with 0.5 ml of lysis buffer containing 50 mM Tris, pH 7.4, 150 mM NaCl, 1% CHAPSO {3-[(3-cholamidopropyl)-dimethylammonio]-2-hydroxy-1-propanesulfonate}, 5 mM EDTA, and a Complete protease inhibitor mixture (Roche). Precleared lysates were incubated for 1 h at 4°C with the MAbs. Glycoproteins were immunoprecipitated using 7 μg of the MAbs generated in this study. The MAbs were previously coupled to protein A/G Plus-agarose beads (Santa Cruz Biotechnology, Santa Cruz, CA). Immunoprecipitated proteins were eluted at 100°C for 5 min with 20 μl of sample buffer (0.08 M Tris-HCl, pH 6.8, 2% SDS, 10% glycerol, 5% β-mercaptoethanol, 0.005% bromophenol blue). The immunoprecipitated proteins were detected after separation by 10% SDS-PAGE utilizing a personal densitometer (model 860; Molecular Dynamics, Inc., Sunnyvale, CA), and the data were analyzed with the ImageQuant NT software.

Immunoprecipitation from transfected cells. For the analysis of the different CCHFV glycoprotein constructs, HEK 293T cell monolayers (1×10^6) were transfected using Lipofectamine 2000 (Invitrogen) according to the manufacturer's instructions. The immunoprecipitation protocol utilized was in general the same as that described above for infected cells. The V5 epitope tag present at the C terminus of the recombinant proteins was detected using 7 μg of a MAb directed against the V5 tag (Invitrogen). Samples from transfected cells were analyzed by Western blotting as described above, using a rabbit anti-V5 tag hyperimmune serum diluted 1:5,000 (Sigma).

RESULTS

CCHFV M segment processing. Glycoproteins of the nairovirus group of bunyaviruses are processed in a distinctive and

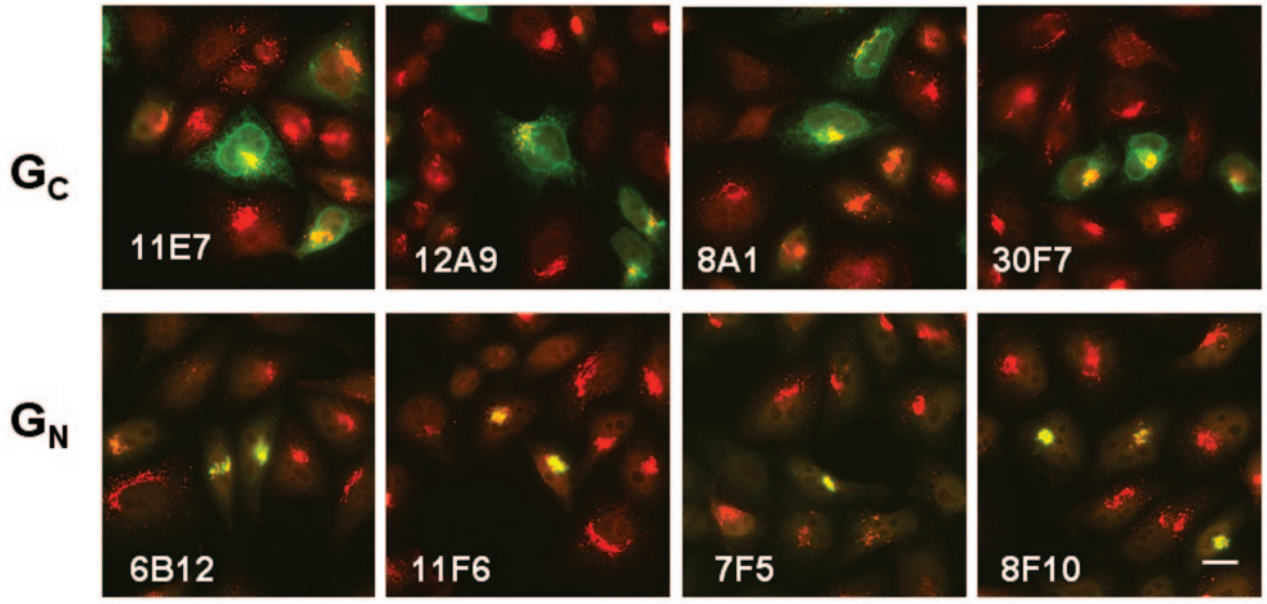

FIG. 2. Analysis of G_N and G_C cellular localization. HeLa cells were transfected with a pCAGGS vector expressing the full-length M segment of CCHFV. After 24 h, the cells were fixed and stained using the indicated MAbs in addition to an antibody specific for the Golgi resident protein TGN46 as described in Materials and Methods. The images show the Golgi apparatus (red) and the glycoproteins (green) merged. Yellow indicates colocalization. The secondary antibodies used were Alexa Fluor 488 (goat anti-mouse) and Alexa Fluor 594 (goat anti-sheep). Magnification, ×60; bar = 100 nm.

complex manner (51, 59). The M segment of CCHFV encodes a polyprotein that undergoes proteolytic processing to yield a 140-kDa Pre-G_N (termed G_N-FL in Fig. 1) and an 85-kDa precursor of G_C (Pre-G_C; termed G_C-FL in Fig. 1). Recently, it was shown that the N terminus of the mature G_N protein contains both a mucin-like and a P35 connector domain (Fig. 1) that are removed by specific cleavage with protease SKI-1, resulting in the generation of mature G_N (G_N-RRLL in Fig. 1) (59). However, how G_N and G_C are cleaved from each other is not clear, though it is thought that the N terminus of the mature G_C protein is generated by cleavage at a conserved RKPL site (59). Finally, cleavage between the mucin domain and the P35 region may be mediated by furin, which is consistent with the presence of a conserved RSKR sequence between these domains (Fig. 1) (59).

MAbs to CCHFV. To assist in our studies of CCHFV glycoprotein processing and localization, and to determine if antibodies can confer protection to CCHFV, we produced a panel of MAbs from mice immunized with a variety of CCHFV antigens as described in Materials and Methods. MAbs to CCHFV were identified by ELISA, after which both immunoprecipitation and immunofluorescence studies were done to identify the glycoprotein subunit to which each MAb bound. Only the 26 MAbs whose specificity could be clearly identified by both techniques are included in this study. For the immunofluorescence studies, HeLa cells were transfected with pcDNA3.1D/V5-His vectors expressing either G_N (G_N-FL, G_N-RSKR, or G_N-RRLL) or G_C (G_C-FL) and were infected with vTF1.1, a recombinant vaccinia virus that expresses the T7 RNA polymerase (1), in order to achieve high levels of protein expression. The cells were then fixed and processed for IF microscopy. All G_N antibodies recognized G_N-FL but most did not recognize G_N-RSKR or G_N-RRLL, with the exception of MAb 8F10, which recognized all the G_N constructs. Since neither G_N-RSKR nor G_N-RRLL was correctly transported to the Golgi apparatus (see below), the failure of most G_N MAbs to recognize these constructs could be due to protein misfolding rather than the loss of specific epitopes.

From the panel of 26 MAbs, we selected six directed against G_N and six directed against G_C for the detailed study of CCHFV glycoprotein processing and targeting. When analyzed by IF and when utilizing HeLa cells transfected with the entire M segment of CCHFV strain IbAr10200, all anti-G_C MAbs gave similar patterns, with G_C being localized to both the endoplasmic reticulum (ER) and Golgi regions as judged by colocalization with Golgi and ER markers (Fig. 2 and data not shown). The six anti-G_N MAbs recognized G_N only in the Golgi apparatus, suggesting that they recognize epitopes that are either formed after the protein reaches the Golgi apparatus or formed shortly before exit from the ER (Fig. 2). None of the MAbs detected G_N or G_C protein on the surfaces of unpermeabilized cells (data not shown). Our results indicate that the CCHFV glycoproteins are not delivered to the cell surface in appreciable quantities, which is consistent with studies that have shown that other *Bunyaviridae* bud into the Golgi apparatus and that their glycoproteins are targeted to this organelle and not delivered to the cell surface (13, 18, 29, 34, 37).

To determine if the MAbs could recognize G_N and G_C in different experimental contexts, both Western blot analysis and immunoprecipitation assay were performed. None of the MAbs recognized CCHFV proteins under fully denaturing conditions by Western blot analysis. However, in the absence of boiling, MAb 11E7 could recognize G_C obtained from transfected cells or from virus-infected cells by Western blot analysis (Fig. 3).

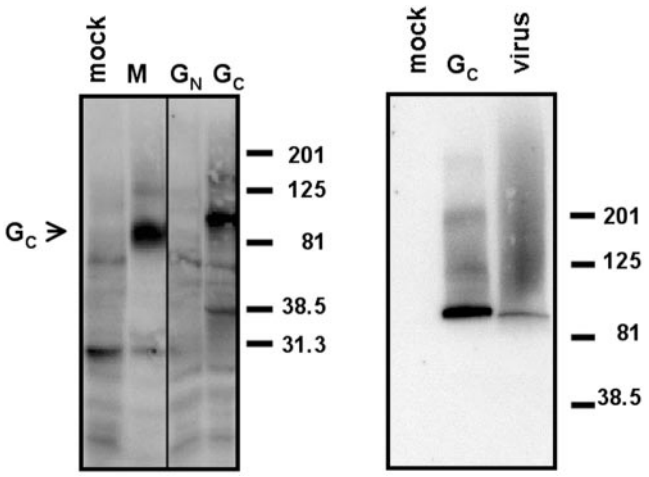

FIG. 3. MAb 11E7 directed against G_C recognizes a linear epitope. HEK 293T cells were transfected with the pCAGGS vector containing the entire CCHFV M segment (M), infected with vaccinia virus vTF1.1 and transfected with the pDNA3.1 constructs containing the G_N or G_C full-length gene with a V5 tag at the C terminus, or mock transfected. Alternatively, SW-13 cells infected with CCHFV were lysed and analyzed by Western blotting (lane labeled "virus"). Western blotting was performed utilizing MAb 11E7. Molecular size markers (in kilodaltons) are noted at the right of each blot.

The failure of most of the MAbs to recognize their antigens by Western blot analysis indicates that they bind to conformation-dependent determinants that are lost upon protein denaturation.

The MAbs were also used to immunoprecipitate G_N and G_C from lysates of cells infected with the IbAr10200 strain of CCHFV. All of the MAbs were able to immunoprecipitate the protein subunits to which they bound, which is consistent with their ability to recognize their epitopes by IF. In addition, four of the six G_C MAbs were able to immunoprecipitate both processed G_C (around 75 kDa) and its precursor protein (around 82 kDa), while all of the G_N MAbs analyzed were able to immunoprecipitate processed G_N (35 kDa) and its precursor (140 kDa), which contains both the mucin and the P35 connector domains (data not shown).

Virus neutralization and protection studies. To analyze the in vitro neutralization activities of the panel of MAbs directed against the CCHFV glycoproteins, we performed plaque reduction assays. Twofold serial dilutions of each MAb ascites fluid sample were incubated with 200 PFU of the IbAr10200 strain of CCHFV for 1 h at 37°C prior to addition to confluent SW-13 cells. Plaques were counted 3 to 5 days later, and PRN-80 titers were calculated. None of the MAbs directed against G_N exhibited neutralizing activity in this assay (Fig. 4B), though many of the MAbs directed against G_C neutralized CCHFV in vitro (Fig. 4A).

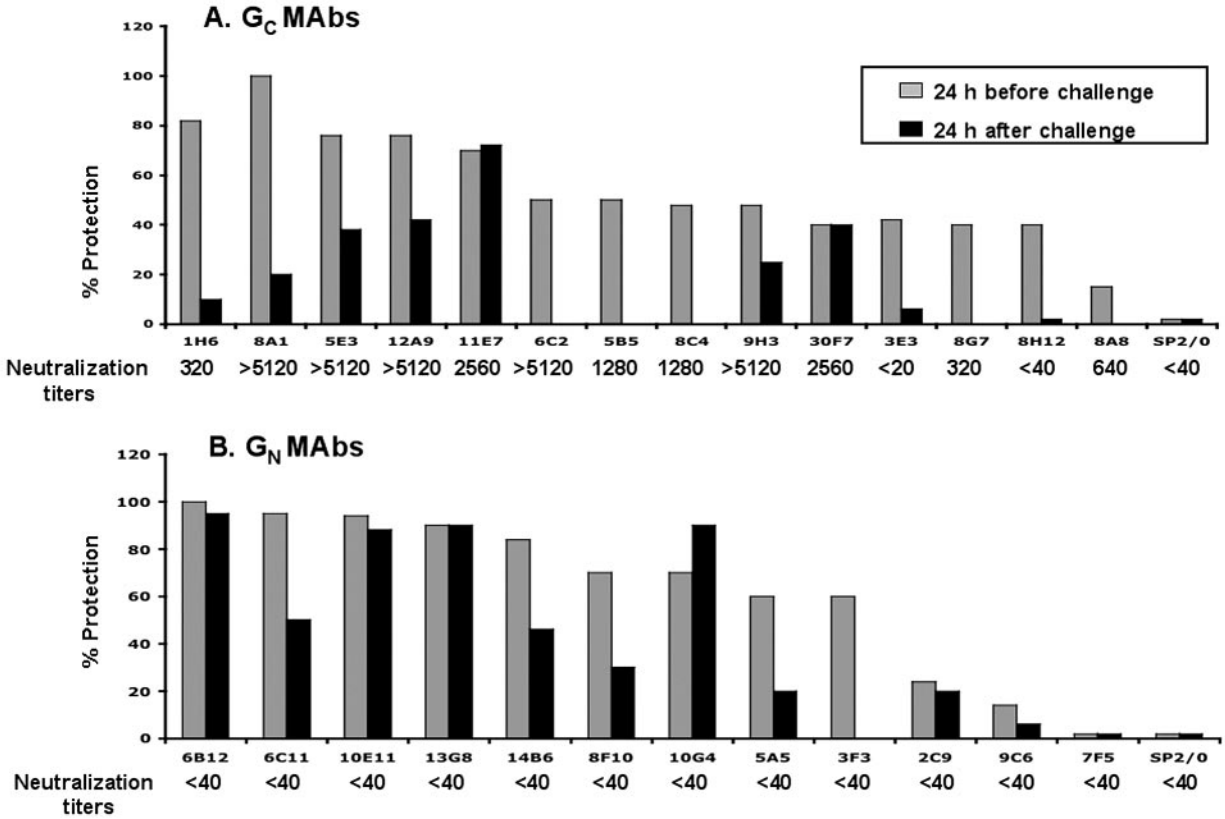

FIG. 4. Correlation between in vitro plaque reduction and in vivo protection. Passive immunization with CCHFV MAb against G_C (A) or against G_N (B). The percentage of protection represents the proportion of animals that survived challenge with respect to the total number of animals treated. Protection was determined in 2- to 3-day-old mice as described in Materials and Methods. The antibodies were provided 24 h before or 24 h after intraperitoneal challenge with the IbAr10200 strain of CCHFV. The plaque reduction neutralization titers are shown at the bottom of each plot for each antibody and represent 80% plaque reduction in SW-13 monolayer cells.

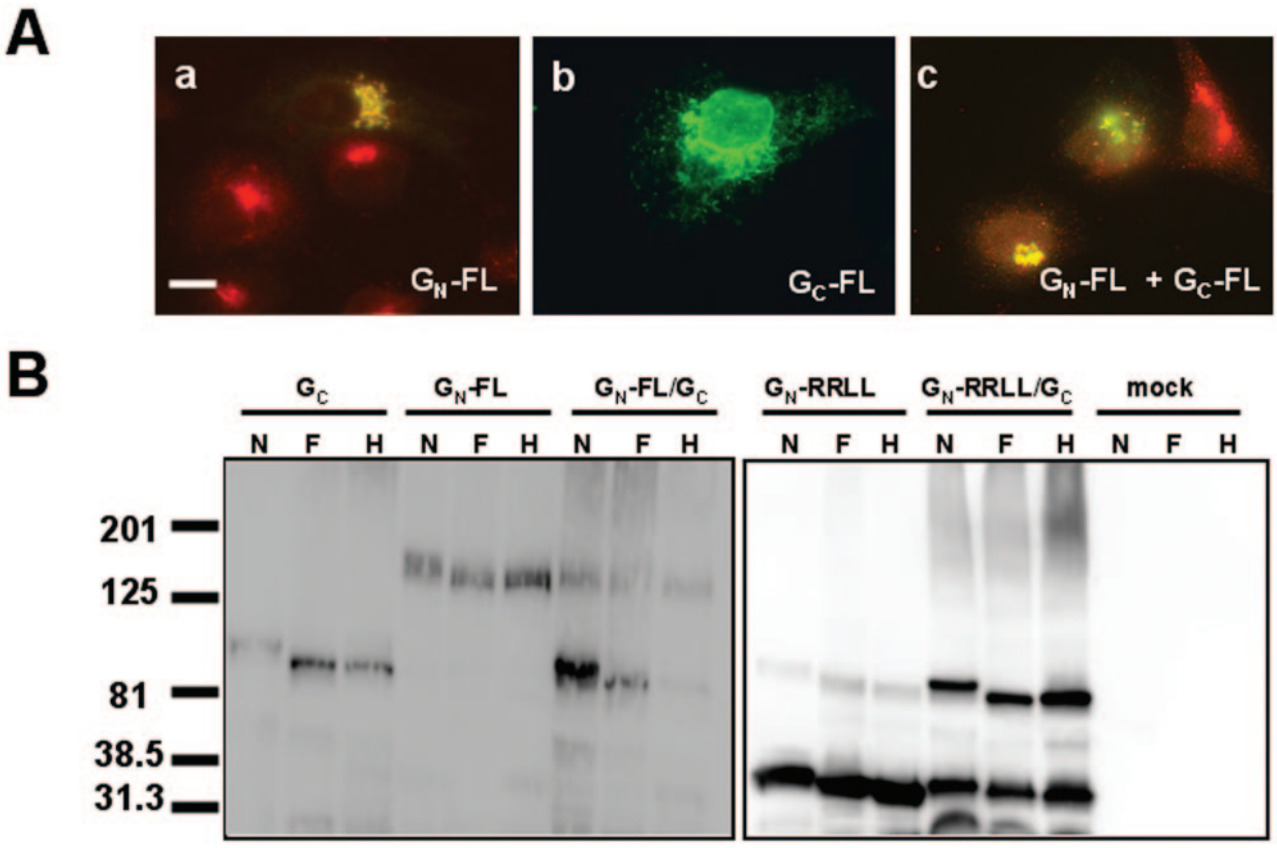

FIG. 5. (A) Localization of CCHFV glycoproteins expressed independently. HeLa cells were infected with recombinant vaccinia virus vTF1.1 and transfected with G_N-FL (a), G_C-FL (b), or both constructs (c). A schematic of the constructs is shown in Fig. 1. Twenty hours posttransfection, the cells were analyzed for the localization of the proteins by IF using MAbs specific for G_N (a) or G_C (b and c). The images show the glycoproteins (in green), the Golgi apparatus (in red), and the extent of colocalization (in yellow). Bar = 100 nm. (B) Endo-H treatment of CCHFV glycoproteins. HEK 293T cells were transfected with the G_N-FL, G_C-FL, or G_N-RRLL constructs separately or together in the presence of recombinant vaccinia virus-expressing T7 polymerase. The lysates were treated with PNGaseF (F) or endo-H (H) or were not treated (N). The lysates were analyzed by Western blotting with mouse anti-V5 antibody. Molecular size markers (in kilodaltons) are noted at the left.

Antibodies have been shown to be effective pre- and post-exposure to prophylaxis treatments for a number of viruses, including cytomegalovirus (9, 10) and respiratory syncytial virus (17, 32). Convalescent-phase serum has been shown to be of benefit to individuals acutely infected with CCHFV (57). Therefore, we tested the CCHFV MAbs for their ability to protect suckling mice challenged with the virus. The MAbs were individually administered by passive immunization to 2- to 3-day-old suckling mice either 24 h before or 24 h after challenge with 100 50% infective-dose units of the IbAr10200 strain of CCHFV (Fig. 4). Protection was registered as the percentage of animals that survived challenge with the live virus (Fig. 4). In general, anti-G_C MAbs that were capable of efficient neutralization in vitro protected mice to an appreciable degree when applied before and, to a lesser extent, after virus challenge (Fig. 4). In addition, anti-G_C MAbs that did not neutralize CCHFV infection of SW-13 cells afforded partial protection to mice from CCHFV provided that the MAbs were administered 24 h before viral challenge. When these MAbs were administered 24 h after virus challenge, protection was usually not observed. This suggests that these MAbs do possess some neutralizing activity that was not detected in our in vitro assay or that other antibody-based effector mechanisms, such as antibody-dependent cell-mediated toxicity or complement-mediated cell lysis, function in this context. Likewise, many of the anti-G_N MAbs conferred significant protection to CCHFV challenge, even when applied 24 h after virus challenge and even though they did not prevent virus infection of SW-13 cells in vitro (Fig. 4). These results show that there is an imperfect relationship between in vitro neutralization and in vivo protective ability, at least under the assay conditions used here, and that the ability of an antibody to neutralize CCHFV may depend in part on host factors, as has been observed for La Crosse virus (LACV), another bunyavirus (25–27).

G_N contains a Golgi targeting signal. To analyze the contribution of each CCHFV glycoprotein to Golgi localization, we expressed each protein independently in HeLa cells. IF analyses showed that, while G_N remained in the Golgi apparatus if expressed alone, G_C localized entirely in the ER in the absence of G_N (Fig. 5Aa and -b). When the proteins were expressed together from independent constructs, both G_C and G_N were localized in the Golgi apparatus (Fig. 5Ac). The restoration of G_C Golgi localization in the presence of G_N suggests that G_N possesses a Golgi localization signal and that G_C localizes to the Golgi apparatus through its interaction with G_N (Fig. 5A).

We further analyzed the localization of CCHFV glycoproteins when expressed independently or together by investigating their N-linked glycosylation. The G_N ectodomain of the IbAr10200 strain of CCHFV contains one predicted N-linked glycosylation site, while the G_C ectodomain contains three sites. To determine whether the CCHFV glycoproteins are glycosylated and, if so, modified by medial Golgi enzymes, we used PNGase F, which removes all N-linked carbohydrate chains, or endo-H, which removes immature carbohydrate chains. When G_C-FL was expressed alone, digestion with either endo-H or PNGase F caused the protein to migrate faster (Fig. 5B). When G_N-FL was expressed alone, it too migrated faster following digestion with either endo-H or PNGase F. To determine if the shift observed following glycosidase treatment of G_N-FL was the result of a loss of glycans on the mucin or P35 regions only, we treated the G_N-RRLL protein that lacks both the mucin and the P35 domains with endo-H. The G_N-RRLL protein also migrated faster after endo-H treatment, indicating the presence of N-linked carbohydrate chains on the ectodomain of the mature G_N as well. Similar results were obtained when the proteins were coexpressed (Fig. 5B). Thus, both proteins are N glycosylated, but neither appears to be processed in the medial Golgi apparatus when expressed alone or together.

Contribution of G_N N-terminal domains to protein localization. The CCHFV G_N protein is unusual in that it has two N-terminal domains, a mucin-like domain and the P35 domain, that appear to be cleaved from the G_N precursor in a posttranslational fashion (51). The function of these regions is unknown. A similar mucin-like domain has been found to be associated with the glycoprotein of Ebola virus and has been shown to induce cell rounding and detachment in vitro and possibly to be involved in the pathogenicity of the virus (56). To analyze the involvement of the mucin-like domain and P35 region in G_N cellular localization, we deleted these regions from constructs that contained only the G_N portion of the protein in order to generate a construct without the mucin-like domain (G_N-RSKR) and a construct without both the mucin-like domain and the P35 region (G_N-RRLL) (Fig. 1). In both cases, a signal sequence was introduced at the N terminus to ensure proper targeting to the ER. Upon expression in HeLa cells, IF analysis using a MAb to the G_N ectodomain showed that deletion of just the mucin-like domain (G_N-RSKR) resulted in a protein that localized to the Golgi apparatus in a manner similar to full-length G_N-FL (Fig. 6A). In contrast, the G_N-RRLL protein was not present in either the ER or the Golgi apparatus but was distributed in a punctuate pattern that resembled aggresomes, suggesting that it misfolds (Fig. 6B). Thus, the mucin-like domain is dispensable for Golgi targeting, while removal of the P35 connector region affected G_N localization and also led to enhanced degradation. Interestingly, localization of G_N-RRLL to the Golgi complex was recovered when the G_N-RRLL protein was coexpressed with G_C, suggesting that G_N-G_C interactions may promote the correct folding and transport of the proteins (Fig. 6C).

Mapping of the Golgi localization signal. In all *Bunyaviridae* glycoproteins that have been examined, the Golgi localization signal has been localized to G_N, generally in the cytoplasmic tail (CT) or transmembrane domain (TM) of the protein (3–5, 12, 14, 33, 34, 47, 49). The C-terminal domain of G_N contains a stretch of predicted TMs and cytoplasmic loops between the first amino acid of G_C and the predicted C terminus of G_N (59). The function of this unusual region on glycoprotein processing or any other step of the viral replication and cell cycle is unknown. To analyze the role of this region in G_N localization, we deleted two (G_N 2TM) or three (G_N 1TM) of the predicted four TMs at the G_N C terminus (Fig. 1). HeLa cells were transfected with the constructs and analyzed by IF (Fig. 6). We found that all of the C-terminally truncated G_N constructs localized to the Golgi apparatus (Fig. 6D and E). These results suggest that the Golgi localization signal is not located in this region.

Next, we designed soluble constructs that lacked the transmembrane and cytoplasmic domains of G_N (sG_N) or G_C (sG_C) or that lacked only the CT of G_N (G_N-no CT) (Fig. 1). When these constructs were expressed using the vaccinia virus T7 polymerase system in HeLa cells, both sG_N and G_N-no CT, although also present in the ER, localized to the Golgi apparatus when analyzed by IF microscopy using MAbs against G_N (Fig. 6F and G). In contrast, sG_C was restricted to the ER, just like full-length G_C (Fig. 6H). When sG_C and sG_N were coexpressed, sG_C was then targeted to the Golgi apparatus (Fig. 6I), indicating that the interaction of G_C and G_N occurs through their ectodomains, that the proteins can fold correctly when in their soluble forms, and that Golgi targeting information resides within the ectodomain of G_N.

DISCUSSION

Relatively little is known about the mechanisms by which bunyaviruses enter cells or how infection can be prevented by neutralizing antibodies, and MAbs that block CCHFV infection have not been described. Therefore, we developed a panel of MAbs to assist in our studies on CCHFV glycoprotein biology and to begin characterizing the antigenic structures of G_N and G_C. The large majority of MAbs bound to conformation-dependent epitopes in G_N or G_C. A number of MAbs against G_C, but not against G_N, were able to neutralize virus infection of SW-13 cells in vitro, suggesting that G_C plays an important role in virus entry. Similarly, MAbs directed against the G_C glycoproteins of LACV can inhibit virus infection, with some evidence indicating that this is due to a reduction in virus binding to the cell surface (19, 21, 22, 26). However, some antibodies against G_N can neutralize LACV infection in an insect cell line, though not in a mammalian cell line, suggesting that virus neutralization can be dependent on the cell type being infected and that virus entry mechanisms may differ between invertebrates and vertebrates (30). Consistent with this, proteolytic degradation of G_C with trypsin or pronase virtually eliminates the ability of LACV to bind to vertebrate, but not invertebrate, cell lines (30, 46).

Our results suggest that CCHFV neutralization mechanisms may be complex and context dependent. In general, MAbs directed against G_N were more effective at protecting mice from a lethal CCHFV challenge than were MAbs to G_C when administrated either 24 h before or after infection, even though G_N MAbs did not neutralize infection of SW-13 cells in vitro. In addition, not all G_C MAbs that neutralized CCHFV infection in vitro conferred high levels of protection in vivo, especially if administered after infection, as seen for the 8A1

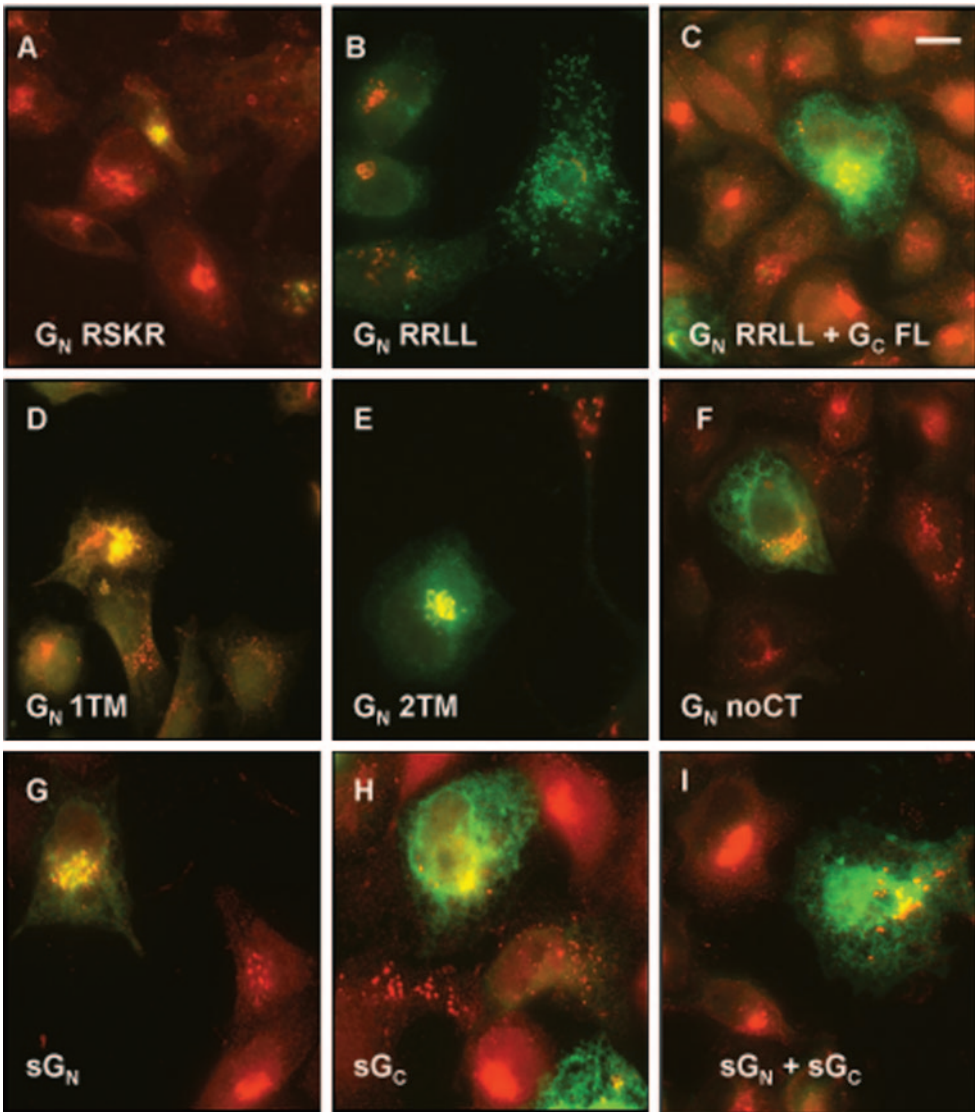

FIG. 6. Immunofluorescence analysis of the CCHFV glycoprotein constructs. HeLa cells were transfected with the indicated CCHFV constructs (shown schematically in Fig. 1) in the presence of recombinant T7 RNA polymerase expressed by vaccinia virus vTF1.1. Twenty hours posttransfection, the cells were fixed and stained using MAb 11E7 against G_C (panels H and I) and MAb 8F10 against G_N (panels A through G) (green) and the TGN46 antibody for Golgi localization (red). Nuclear staining is shown in blue. Bar = 100 nm.

and 1H6 MAbs. Thus, there was not a strict relationship between in vitro neutralization and in vivo protection. As noted above, these results resemble observations on the differential roles of LACV G_N and G_C glycoproteins in viral neutralization and protection. A soluble version of the G_C La Crosse glycoprotein is sufficient to block virus infection in mammalian cells, while antibodies against G_N neutralize infection in a mosquito cell line but not in a vertebrate cell line (31). The mechanisms that account for the differential inhibition of CCHFV infection are not currently clear. We assume that the conformational changes undergone by G_N and G_C to elicit membrane fusion and virus entry will likely be the same regardless of the cell type being infected and that these changes are likely to be induced by acid pH following endocytosis of the virus, as has been documented for La Crosse and Hantaan viruses (7, 20). However, it remains to be determined if CCHFV uses different cell surface receptors and attachment factors on different cell types. Without knowing the identity of any potential CCHFV receptors, it will be interesting to examine the ability of MAbs to neutralize CCHFV on cell lines derived from different species, including ticks.

One of the hallmarks of the *Bunyaviridae* family is that their glycoproteins are targeted to the Golgi apparatus from which they bud (48, 52). Based on this fact, a number of studies have sought to identify the signals responsible for targeting G_N and G_C to the Golgi apparatus for a number of bunyaviruses (2, 34, 36, 40, 47, 49). Generally, it has been found that the Golgi retention signals reside within the TM and/or CT of the glycoprotein closest to the N terminus of the glycoprotein precursor (18, 34, 35). However, no consensus Golgi localization motif appears to be shared among the glycoproteins of these viruses, and *Nairovirus* glycopro-

tein targeting signals and antigenic structures have not been analyzed so far.

We found that the CCHFV glycoproteins were targeted to the Golgi apparatus, as determined by IF microscopy. Since both G_N and G_C were sensitive to endo-H treatment, it is likely that the proteins are targeted to an early Golgi compartment. Similarly, hantavirus glycoproteins, although present in the Golgi apparatus, remain sensitive to endo-H treatment (49). When G_N and G_C were expressed together, G_N was localized to the Golgi complex while G_C was found in both the Golgi apparatus and the ER. It is obvious that G_N must also be present in the ER, but our conformation-dependent MAbs either do not recognize G_N in the ER or bind to epitopes that form just prior to exiting from this organelle. It is also possible that G_N is transported more quickly from the ER than G_C and, at steady state, is below our limit of detection in the ER. Indeed, some studies on the biosynthesis of Uukuniemi virus G_N and G_C proteins showed previously that G_N is transported faster than G_C from the ER to the site of virus budding at the Golgi complex (29). The apparent difference in transport kinetics is due to the fact that G_N folds and is transported from the ER to the Golgi apparatus ~30 to 45 min faster than G_C (4).

The ability of CCHFV G_N to localize to the Golgi apparatus when expressed independently of G_C indicates that G_N contains a Golgi targeting or retention motif. Since G_C is restricted to the ER in the absence of G_N, we conclude that its transport to the Golgi apparatus is dependent upon G_N and likely results from G_N-G_C oligomerization. Whether G_C fails to fold correctly in the absence of G_N, contains an ER retention signal that is masked by G_N association, or lacks a positive transport signal cannot be determined at present. Our results are in agreement with published data about other *Bunyaviridae* glycoproteins (3, 35, 36, 40, 47, 49) which localize to the Golgi apparatus in the absence of any other viral proteins (11, 14, 34, 47). Although for most of the *Bunyaviridae* glycoproteins analyzed to date, the Golgi targeting signal is contained in one of the glycoproteins, for the Hantaan virus, a member of the *Hantavirus* group, both glycoproteins are required to achieve Golgi apparatus targeting (49). Our results with CCHFV indicate that Golgi targeting information resides largely in the ectodomain of the G_N subunit, since a soluble version of G_N was largely restricted to the Golgi apparatus. However, small amounts of this protein were secreted from cells, indicating that the TM of G_N may also play a role in Golgi retention. It is also evident that the ectodomains of G_N and G_C interact with each other and that targeting of G_C to the Golgi apparatus is dependent upon its association with G_N, with ectodomain interactions being important.

In summary, although the CCHFV glycoproteins are unique in many aspects with respect to the glycoproteins from other members of the *Bunyaviridae* family, there are some similarities with regard to Golgi targeting and the glycoprotein subunits to which neutralizing antibodies are directed. Our studies indicate that CCHFV neutralization is likely to be context dependent and that more in-depth studies of various cell lines and animal models will be needed to characterize neutralization mechanisms and to identify antibodies that could be used therapeutically. Identification of regions on the CCHFV glycoproteins involved in viral neutralization, protection, and processing will contribute to our understanding of the tropism and pathogenesis of this emerging viral pathogen.

ACKNOWLEDGMENTS

We thank Nicolette Pesik, Randall Bethke, and Loreen Hodgson for superb technical assistance on the production and characterization of the MAbs. We also thank Aura Garrison and Donald Pijak for expert technical assistance.

This work was supported in part by National Institutes of Health training grant NIH T32 AI055400 and grant PR033269 from the Department of Defense Peer Reviewed Medical Research Program (PRMRP) of the Office of the Congressionally Directed Medical Research Programs.

REFERENCES

1. **Alexander, W. A., B. Moss, and T. R. Fuerst.** 1992. Regulated expression of foreign genes in vaccinia virus under the control of bacteriophage T7 RNA polymerase and the *Escherichia coli lac* repressor. J. Virol. **66:**2934–2942.
2. **Anderson, G. W., Jr., and J. F. Smith.** 1987. Immunoelectron microscopy of Rift Valley fever viral morphogenesis in primary rat hepatocytes. Virology **161:**91–100.
3. **Andersson, A. M., L. Melin, A. Bean, and R. F. Pettersson.** 1997. A retention signal necessary and sufficient for Golgi localization maps to the cytoplasmic tail of a *Bunyaviridae* (Uukuniemi virus) membrane glycoprotein. J. Virol. **71:**4717–4727.
4. **Andersson, A. M., L. Melin, R. Persson, E. Raschperger, L. Wikström, and R. F. Pettersson.** 1997. Processing and membrane topology of the spike proteins G1 and G2 of Uukuniemi virus. J. Virol. **71:**218–225.
5. **Andersson, A. M., and R. F. Pettersson.** 1998. Targeting of a short peptide derived from the cytoplasmic tail of the G1 membrane glycoprotein of Uukuniemi virus (*Bunyaviridae*) to the Golgi complex. J. Virol. **72:**9585–9596.
6. **Archer, D. B., D. J. Jeenes, D. A. MacKenzie, G. Brightwell, N. Lambert, G. Lowe, S. E. Radford, and C. M. Dobson.** 1990. Hen egg white lysozyme expressed in, and secreted from, *Aspergillus niger* is correctly processed and folded. Biotechnology (New York) **8:**741–745.
7. **Arikawa, J., I. Takashima, and N. Hashimoto.** 1985. Cell fusion by haemorrhagic fever with renal syndrome (HFRS) viruses and its application for titration of virus infectivity and neutralizing antibody. Arch. Virol. **86:**303–313.
8. **Arikawa, J., J. S. Yao, K. Yoshimatsu, I. Takashima, and N. Hashimoto.** 1992. Protective role of antigenic sites on the envelope protein of Hantaan virus defined by monoclonal antibodies. Arch. Virol. **126:**271–281.
9. **Aulitzky, W. E., T. F. Schulz, H. Tilg, D. Niederwieser, K. Larcher, L. Ostberg, M. Scriba, J. Martindale, A. C. Stern, P. Grass, et al.** 1991. Human monoclonal antibodies neutralizing cytomegalovirus (CMV) for prophylaxis of CMV disease: report of a phase I trial in bone marrow transplant recipients. J. Infect. Dis. **163:**1344–1347.
10. **Aulitzky, W. E., H. Tilg, D. Niederwieser, M. Hackl, B. Meister, and C. Huber.** 1988. Ganciclovir and hyperimmunoglobulin for treating cytomegalovirus infection in bone marrow transplant recipients. J. Infect. Dis. **158:**488–489.
11. **Bupp, K., K. Stillmock, and F. Gonzalez-Scarano.** 1996. Analysis of the intracellular transport properties of recombinant La Crosse virus glycoproteins. Virology **220:**485–490.
12. **Chen, S.-Y., and R. W. Compans.** 1991. Oligomerization, transport, and Golgi retention of Punta Toro virus glycoproteins. J. Virol. **65:**5902–5909.
13. **Chen, S.-Y., Y. Matsuoka, and R. W. Compans.** 1991. Assembly and polarized release of Punta Toro virus and effects of brefeldin A. J. Virol. **65:**1427–1439.
14. **Chen, S. Y., Y. Matsuoka, and R. W. Compans.** 1991. Golgi complex localization of the Punta Toro virus G2 protein requires its association with the G1 protein. Virology **183:**351–365.
15. **Chumakov, M. P., A. M. Butenko, N. V. Shalunova, L. I. Mart'ianova, S. E. Smirnova, N. Bashkirtsev, T. I. Zavodova, S. G. Rubin, E. A. Tkachenko, V. Karmysheva, V. N. Reingol'd, G. V. Popov, and A. P. Savinov.** 1968. New data on the viral agent of Crimean hemorrhagic fever. Vopr. Virusol. **13:**377. (In Russian.)
16. **Chumakov, M. P., S. E. Smirnova, and E. A. Tkachenko.** 1970. Relationship between strains of Crimean haemorrhagic fever and Congo viruses. Acta Virol. **14:**82–85.
17. **Englund, J. A., P. A. Piedra, and E. Whimbey.** 1997. Prevention and treatment of respiratory syncytial virus and parainfluenza viruses in immunocompromised patients. Am. J. Med. **102:**61–70, 75–76.
18. **Gerrard, S. R., and S. T. Nichol.** 2002. Characterization of the Golgi retention motif of Rift Valley fever virus G_N glycoprotein. J. Virol. **76:**12200–12210.
19. **Gonzalez-Scarano, F.** 1985. La Crosse virus G1 glycoprotein undergoes a conformational change at the pH of fusion. Virology **140:**209–216.

20. **Gonzalez-Scarano, F., R. S. Janssen, J. A. Najjar, N. Pobjecky, and N. Nathanson.** 1985. An avirulent G1 glycoprotein variant of La Crosse bunyavirus with defective fusion function. J. Virol. **54:**757–763.
21. **Grady, L. J., M. L. Sanders, and W. P. Campbell.** 1983. Evidence for three separate antigenic sites on the G1 protein of La Crosse virus. Virology **126:**395–397.
22. **Grady, L. J., S. Srihongse, M. A. Grayson, and R. Deibel.** 1983. Monoclonal antibodies against La Crosse virus. J. Gen. Virol. **64:**1699–1704.
23. **Hoogstraal, H.** 1979. The epidemiology of tick-borne Crimean-Congo hemorrhagic fever in Asia, Europe, and Africa. J. Med. Entomol. **15:**307–417.
24. **Huggins, J. W.** 1989. Prospects for treatment of viral hemorrhagic fevers with ribavirin, a broad-spectrum antiviral drug. Rev. Infect. Dis. **11** (Suppl. 4)**:** S750–S761.
25. **Kingsford, L.** 1984. Enhanced neutralization of La Crosse virus by the binding of specific pairs of monoclonal antibodies to the G1 glycoprotein. Virology **136:**265–273.
26. **Kingsford, L., K. H. Boucquey, and T. P. Cardoso.** 1991. Effects of specific monoclonal antibodies on La Crosse virus neutralization: aggregation, inactivation by Fab fragments, and inhibition of attachment to baby hamster kidney cells. Virology **180:**591–601.
27. **Kingsford, L., L. D. Ishizawa, and D. W. Hill.** 1983. Biological activities of monoclonal antibodies reactive with antigenic sites mapped on the G1 glycoprotein of La Crosse virus. Virology **129:**443–455.
28. **Kohler, G., S. C. Howe, and C. Milstein.** 1976. Fusion between immunoglobulin-secreting and nonsecreting myeloma cell lines. Eur. J. Immunol. **6:**292–295.
29. **Kuismanen, E., B. Bång, M. Hurme, and R. F. Pettersson.** 1984. Uukuniemi virus maturation: immunofluorescence microscopy with monoclonal glycoprotein-specific antibodies. J. Virol. **51:**137–146.
30. **Ludwig, G. V., B. A. Israel, B. M. Christensen, T. M. Yuill, and K. T. Schultz.** 1991. Monoclonal antibodies directed against the envelope glycoproteins of La Crosse virus. Microb. Pathog. **11:**411–421.
31. **Ludwig, G. V., B. A. Israel, B. M. Christensen, T. M. Yuill, and K. T. Schultz.** 1991. Role of La Crosse virus glycoproteins in attachment of virus to host cells. Virology **181:**564–571.
32. **Malley, R., J. DeVincenzo, O. Ramilo, P. H. Dennehy, H. C. Meissner, W. C. Gruber, P. J. Sanchez, H. Jafri, J. Balsley, D. Carlin, S. Buckingham, L. Vernacchio, and D. M. Ambrosino.** 1998. Reduction of respiratory syncytial virus (RSV) in tracheal aspirates in intubated infants by use of humanized monoclonal antibody to RSV F protein. J. Infect. Dis. **178:**1555–1561.
33. **Matsuoka, Y., S. Y. Chen, and R. W. Compans.** 1991. Bunyavirus protein transport and assembly. Curr. Top. Microbiol. Immunol. **169:**161–179.
34. **Matsuoka, Y., S. Y. Chen, and R. W. Compans.** 1994. A signal for Golgi retention in the bunyavirus G1 glycoprotein. J. Biol. Chem. **269:**22565–22573.
35. **Matsuoka, Y., S. Y. Chen, C. E. Holland, and R. W. Compans.** 1996. Molecular determinants of Golgi retention in the Punta Toro virus G1 protein. Arch. Biochem. Biophys. **336:**184–189.
36. **Matsuoka, Y., T. Ihara, D. H. Bishop, and R. W. Compans.** 1988. Intracellular accumulation of Punta Toro virus glycoproteins expressed from cloned cDNA. Virology **167:**251–260.
37. **Melin, L., R. Persson, A. Andersson, A. Bergström, R. Rönnholm, and R. F. Pettersson.** 1995. The membrane glycoprotein G1 of Uukuniemi virus contains a signal for localization to the Golgi complex. Virus Res. **36:**49–66.
38. **Morais, V. A., A. S. Crystal, D. S. Pijak, D. Carlin, J. Costa, V. M. Lee, and R. W. Doms.** 2003. The transmembrane domain region of nicastrin mediates direct interactions with APH-1 and the gamma-secretase complex. J. Biol. Chem. **278:**43284–43291.
39. **Nabel, G. J.** 1999. Surviving Ebola virus infection. Nat. Med. **5:**373–374.
40. **Nakitare, G. W., and R. M. Elliott.** 1993. Expression of the Bunyamwera virus M genome segment and intracellular localization of NSm. Virology **195:**511–520.
41. **Niwa, H., K. Yamamura, and J. Miyazaki.** 1991. Efficient selection for high-expression transfectants with a novel eukaryotic vector. Gene **108:**193–199.
42. **Olaleye, O. D., O. Tomori, and H. Schmitz.** 1996. Rift Valley fever in Nigeria: infections in domestic animals. Rev. Sci. Tech. Off. Int. Epizoot. **15:**937–946.
43. **Onishchenko, G. G., V. I. Efremenko, N. G. Kovalev, N. A. Shibkov, M. Fedorov, N. Zhilina, G. N. Fedosova, G. V. Sysoliatina, M. Evchenko, A. P. Beier, V. A. Popov, K. V. Shenetts, L. N. Marchukova, E. N. Afanas'ev, and N. V. Vasilenko.** 2001. Specific epidemiologic features of Crimean haemorrhagic fever in Stavropol' region in 1999–2000. Zh. Mikrobiol. Epidemiol. Immunobiol. **Nov., Dec.**(Suppl. 6)**:**86–89. (In Russian.)
44. **Onishchenko, G. G., M. Lomov, V. I. Markov, V. A. Merkulov, A. N. Mironov, I. V. Borisevich, A. A. Makhlai, N. T. Vasil'ev, S. O. Vodop'ianov, N. G. Tikhonov, T. P. Pashanina, V. V. Manankov, V. P. Smelianskii, S. T. Savchenko, and S. E. Smirnova.** 2000. The laboratory diagnosis of an outbreak of hemorrhagic fever at Oblivskaya village, Rostov Province: proof of the etiological role of the Crimean-Congo hemorrhagic fever virus. Zh. Mikrobiol. Epidemiol. Immunobiol. **Mar., Apr.**32–36. (In Russian.)
45. **Onishchenko, G. G., V. I. Markov, V. A. Merkulov, N. T. Vasil'ev, A. M. Berezhnoi, I. A. Androshchuk, and V. A. Maksimov.** 2001. Isolation and identification of Crimean-Congo hemorrhagic fever virus in the Stavropol territory. Zh. Mikrobiol. Epidemiol. Immunobiol. **Nov., Dec.**7–11. (In Russian.)
46. **Pekosz, A., C. Griot, K. Stillmock, N. Nathanson, and F. Gonzalez-Scarano.** 1995. Protection from La Crosse virus encephalitis with recombinant glycoproteins: role of neutralizing anti-G1 antibodies. J. Virol. **69:**3475–3481.
47. **Pensiero, M. N., and J. Hay.** 1992. The Hantaan virus M-segment glycoproteins G1 and G2 can be expressed independently. J. Virol. **66:**1907–1914.
48. **Pettersson, R. F., A. Andersson, and L. Melin.** 1995. Mapping a retention signal for Golgi localization of a viral spike protein complex. Cold Spring Harbor Symp. Quant. Biol. **60:**147–155.
49. **Ruusala, A., R. Persson, C. S. Schmaljohn, and R. F. Pettersson.** 1992. Coexpression of the membrane glycoproteins G1 and G2 of Hantaan virus is required for targeting to the Golgi complex. Virology **186:**53–64.
50. **Saluzzo, J.-F., and B. Le Guenno.** 1987. Rapid diagnosis of human Crimean-Congo hemorrhagic fever and detection of the virus in naturally infected ticks. J. Clin. Microbiol. **25:**922–924.
51. **Sanchez, A. J., M. J. Vincent, and S. T. Nichol.** 2002. Characterization of the glycoproteins of Crimean-Congo hemorrhagic fever virus. J. Virol. **76:**7263–7275.
52. **Schmaljohn, C. S.** 1996. *Bunyaviridae*: the viruses and their replication, p. 1447–1471. *In* B. N. Fields, D. M. Knipe, and P. M. Howley (ed.), Virology, 3rd ed., vol. 1. Lippincott-Raven, Philadelphia, Pa.
53. **Schmaljohn, C. S., J. Arikawa, S. E. Hasty, L. Rasmussen, H. W. Lee, P. W. Lee, and J. M. Dalrymple.** 1988. Conservation of antigenic properties and sequences encoding the envelope proteins of prototype Hantaan virus and two virus isolates from Korean haemorrhagic fever patients. J. Gen. Virol. **69:**1949–1955.
54. **Schmaljohn, C. S., Y.-K. Chu, A. L. Schmaljohn, and J. M. Dalrymple.** 1990. Antigenic subunits of Hantaan virus expressed by baculovirus and vaccinia virus recombinants. J. Virol. **64:**3162–3170.
55. **Schmaljohn, C. S., S. E. Hasty, and J. M. Dalrymple.** 1992. Preparation of candidate vaccinia-vectored vaccines for haemorrhagic fever with renal syndrome. Vaccine **10:**10–13.
56. **Simmons, G., R. J. Wool-Lewis, F. Baribaud, R. C. Netter, and P. Bates.** 2002. Ebola virus glycoproteins induce global surface protein down-modulation and loss of cell adherence. J. Virol. **76:**2518–2528.
57. **Trimble, R. B., and F. Maley.** 1984. Optimizing hydrolysis of N-linked high-mannose oligosaccharides by endo-beta-*N*-acetylglucosaminidase H. Anal. Biochem. **141:**515–522.
58. **Vassilenko, S. M., T. L. Vassilev, L. G. Bozadjiev, I. L. Bineva, and G. Z. Kazarov.** 1990. Specific intravenous immunoglobulin for Crimean-Congo haemorrhagic fever. Lancet **335:**791–792.
59. **Vincent, M. J., A. J. Sanchez, B. R. Erickson, A. Basak, M. Chretien, N. G. Seidah, and S. T. Nichol.** 2003. Crimean-Congo hemorrhagic fever virus glycoprotein proteolytic processing by subtilase SKI-1. J. Virol. **77:**8640–8649.
60. **Williams, R. J., S. Al-Busaidy, F. R. Mehta, G. O. Maupin, K. D. Wagoner, S. Al-Awaidy, A. J. Suleiman, A. S. Khan, C. J. Peters, and T. G. Ksiazek.** 2000. Crimean-Congo haemorrhagic fever: a seroepidemiological and tick survey in the Sultanate of Oman. Trop. Med. Int. Health **5:**99–106.
61. **Wood, O. L., V. H. Lee, J. S. Ash, and J. Casals.** 1978. Crimean-Congo hemorrhagic fever, Thogoto, Dugbe, and Jos viruses isolated from ixodid ticks in Ethiopia. Am. J. Trop. Med. Hyg. **27:**600–604.
62. **Zhang, X. K., I. Takashima, and N. Hashimoto.** 1989. Characteristics of passive immunity against hantavirus infection in rats. Arch. Virol. **105:**235–246.

Journal of General Virology (2005), **86**, 3327–3336 DOI 10.1099/vir.0.81175-0

Presence of broadly reactive and group-specific neutralizing epitopes on newly described isolates of *Crimean-Congo hemorrhagic fever virus*

Asim A. Ahmed,[1] Jeanne M. McFalls,[1] Christian Hoffmann,[1] Claire Marie Filone,[1] Shaun M. Stewart,[1] Jason Paragas,[2] Shabot Khodjaev,[3] Dilbar Shermukhamedova,[3] Connie S. Schmaljohn,[2] Robert W. Doms[1] and Andrea Bertolotti-Ciarlet[1]

Correspondence
Andrea Bertolotti-Ciarlet
aciarlet@mail.med.upenn.edu

[1]Department of Microbiology, University of Pennsylvania, Philadelphia, PA 19104, USA

[2]Virology Division, United States Army Medical Research Institute of Infectious Diseases, Fort Detrick, Frederick, MD 21702, USA

[3]Institute of Virology, Ministry of Health, Tashkent, Uzbekistan

Crimean-Congo hemorrhagic fever virus (CCHFV), a member of the genus *Nairovirus* of the family *Bunyaviridae*, causes severe disease in humans with high rates of mortality. The virus has a tripartite genome composed of a small (S), a medium (M) and a large (L) RNA segment; the M segment encodes the two viral glycoproteins, G_N and G_C. Whilst relatively few full-length M segment sequences are available, it is apparent that both G_N and G_C may exhibit significant sequence diversity. It is unknown whether considerable antigenic differences exist between divergent CCHFV strains, or whether there are conserved neutralizing epitopes. The M segments derived from viral isolates of a human case of CCHF in South Africa (SPU 41/84), an infected tick (*Hyalomma marginatum*) in South Africa (SPU 128/81), a human case in Congo (UG 3010), an infected individual in Uzbekistan (U2-2-002) and an infected tick (*Hyalomma asiaticum*) in China (Hy13) were sequenced fully, and the glycoproteins were expressed. These novel sequences showed high variability in the N-terminal region of G_N and more modest differences in the remainder of G_N and in G_C. Phylogenetic analyses placed these newly identified strains in three of the four previously described M segment groups. Studies with a panel of mAbs specific to G_N and G_C indicated that there were significant antigenic differences between the M segment groups, although several neutralizing epitopes in both G_N and G_C were conserved among all strains examined. Thus, the genetic diversity exhibited by CCHFV strains results in significant antigenic differences that will need to be taken into consideration for vaccine development.

Received 10 May 2005
Accepted 22 August 2005

INTRODUCTION

Crimean-Congo hemorrhagic fever virus (CCHFV) causes a haemorrhagic disease in humans with mortality rates that range from 10 to 80 % (Whitehouse, 2004). CCHFV can be isolated from ticks, livestock and humans (Whitehouse, 2004). Infection can occur through the bite of an infected tick, exposure to tissue and fluids from an infected animal or through contact with infected human bodily fluids. CCHFV infection was first described during an outbreak in Russia during the 1940s, when more than 200 cases of severe haemorrhagic fever were reported among agricultural workers and soldiers in the Crimean peninsula (Chumakov *et al.*, 1968, 1970). Since then, the virus has spread or has been recognized throughout many regions of the world, including sub-Saharan Africa (Williams *et al.*, 2000; Wood *et al.*, 1978), Bulgaria, the Arabian Peninsula, Iraq, Pakistan, the former Yugoslavia, northern Greece and north-west China (Chumakov *et al.*, 1970; Hoogstraal, 1979; Olaleye *et al.*, 1996; Onishchenko *et al.*, 2000, 2001a, b).

CCHFV is a member of the genus *Nairovirus* within the family *Bunyaviridae* (Schmaljohn, 1996). Members of this enveloped virus family have a tripartite, single-stranded RNA genome of negative polarity. The small segment (S) encodes the viral nucleocapsid, the medium segment (M) encodes the two glycoproteins, G_N and G_C, and the large segment (L) encodes an RNA-dependent RNA polymerase. The viral glycoproteins, like those of other members of the family *Bunyaviridae*, are synthesized as a polyprotein

The GenBank/EMBL/DDBJ accession numbers for the sequences described in this paper are AY900141–AY900145.

Supplementary figures are available in JGV Online.

precursor (Schmaljohn, 1996) that undergoes proteolytic cleavage events to yield the mature glycoproteins (Vincent *et al.*, 2003). The G_N precursor protein (Pre-G_N) contains an N-terminal domain with a high proportion of Ser, Thr and Pro residues. This region resembles the mucin-like domain present in the glycoproteins of other viruses, most notably the Ebola virus glycoprotein (Simmons *et al.*, 2002).

The G_N and G_C glycoproteins of CCHFV probably influence the host range, cell tropism and pathogenicity of this vertebrate and tick virus, and are the targets for neutralizing antibodies. Studies thus far indicate that portions of G_N are highly variable compared with other regions of G_N and with G_C (Chinikar *et al.*, 2004; Hewson *et al.*, 2004a, b; Morikawa *et al.*, 2002; Papa *et al.*, 2002). However, there is limited sequence information available on CCHFV isolates from regions outside China and the former Soviet Union (Chinikar *et al.*, 2004; Hewson *et al.*, 2004a, b; Morikawa *et al.*, 2002; Papa *et al.*, 2002). We previously described the first neutralizing mAbs to CCHFV (Bertolotti-Ciarlet *et al.*, 2005). In addition, some of these antibodies were shown to be protective in a suckling mouse animal model (Bertolotti-Ciarlet *et al.*, 2005). However, it is not clear whether significant antigenic differences exist between divergent CCHFV isolates or whether conserved neutralizing epitopes are present. This information is important for vaccine development, as the identification of conserved neutralizing epitopes may lead to the development of vaccines and entry inhibitors.

To further characterize the genetic diversity of the CCHFV M segment, we cloned and expressed glycoproteins from divergent CCHFV strains that were passaged a limited number of times. Additionally, to assess antigenic differences between CCHFV isolates, we cloned and fully sequenced the open reading frames from five CCHFV isolates obtained from humans or ticks in South Africa, Congo, Uzbekistan and China. Phylogenetic analyses indicated that one or more of these new strains segregated with three of the four previously described M segment groups (Hewson *et al.*, 2004b). The glycoproteins from each strain were expressed transiently in cell lines and their ability to be recognized by a panel of mAbs to G_N and G_C was determined. The genetic proximity of strains and their antigenic similarity were imperfectly correlated. Whilst some epitopes were conserved, others were not, indicating that CCHFV vaccines designed to induce neutralizing antibodies may have to include immunogens derived from several CCHFV strains, or in some way focus the immune response on conserved neutralizing epitopes.

METHODS

Virus strains and cells. African green monkey kidney fibroblast (CV-1), Vero, Vero E6, human cervix carcinoma (HeLa) and human embryonic kidney (HEK-293T) cells, obtained from the ATCC (Manassas, VA, USA), were maintained in Dulbecco's modified Eagle's medium (DMEM) supplemented with 10 % fetal bovine serum (FBS; Invitrogen). Similarly, the human tumour cell line SW-13 (adrenocortical carcinoma) was grown in DMEM supplemented with 2·5 % FBS. CCHFV strains Hy13, U2-2-002, SPU 41/84, SPU 128/81, SPU 94/87 and UG 3010 were used in this study. All of the viruses were passaged by intracerebral inoculation of 1-day-old mice with each CCHFV isolate, using a dose resulting in the death of 50 % of the mice. The mice were killed 24 h post-infection and the brains were harvested. Brains were homogenized to 10 % (w/v) with Hanks' salt solution and clarified by centrifugation at 10 000 r.p.m. in an SW41 rotor for 30 min. CCHFV prototype strain IbAr10200, first isolated in 1976 from ticks (*Hyalomma excavatum*) from Sokoto, Nigeria, was grown in African green monkey kidney Vero or Vero E6 cells (Sanchez *et al.*, 2002). Republic of South Africa CCHFV strain SPU 41/84 was isolated from an infected human in 1984 and passaged in suckling mice four times. Republic of South Africa CCHFV strain SPU 128/81 was isolated in 1981 from infected ticks (*Hyalomma marginatum rufipes*) and passaged in suckling mice three times. Congolese strain UG 3010 was isolated in 1956. This was one of the first 'Congo' strains isolated (Simpson *et al.*, 1967; Woodall *et al.*, 1967). Chinese strain Hy13 was isolated from infected ticks (*H. asiaticum*) in 1968 and was passaged in suckling mice three times. CCHFV strain U2-2-002/U-6415 from Uzbekistan was isolated from an infected human and passaged in suckling mice four times. All work with replication-competent CCHFV was conducted in a biosafety level 4 facility at the United States Army Medical Research Institute of Infectious Diseases (USAMRIID).

RNA purification, RT-PCR and sequencing. Consensus primers were designed based on an alignment of known full-length M segment sequences available in GenBank. In order to amplify the 5′ half of the M segment from each strain, primers CCHF 5′ (5′-TCTCAAAGAAACACGTGCCGC-3′) and CCHF 3519 R (5′-GTACTCRAAGACAGGRGARTACAT-3′) were designed. CCHF 2325 F (5′-AATGCAATAGAYGCTGARATGCA-3′) and CCHF 3′R (5′-TCTCAAAGAWATAGTGGCGGCACGCAGTC-3′) were designed to amplify the 3′ half of the M segment for each strain. Wobble code includes R = A or G, Y = C or T and W = A or T. The two designed amplicons share 1 kb overlapping sequence at the centre of the M segment. This strategy of amplification of the M segment in two halves was utilized for most of the strains. Total RNA was isolated from lysates of SW-13 cells infected with the different CCHFV strains by utilizing TRIzol LS (Invitrogen) and removed from biocontainment. The samples were chloroform-extracted, followed by high-speed centrifugation and isolation of the resulting aqueous layer. RNA was precipitated by using propan-2-ol and pellets were resuspended in RNase-free distilled water. RNA was further purified through the RNeasy system (Qiagen) according to the manufacturer's directions.

Reverse transcription of the entire M RNA segment was performed by using 5 µl RNA from above, CCHF 3′R (300 ng) and 1 µl of a mixture of the four dNTPs (at 10 µM each) in 12 µl. This mixture was heated to 65 °C for 5 min and chilled rapidly on ice. Four microlitres of 5 × RT buffer, 2 µl 0·1 M dithiothreitol and RNasin (40 U) were added to the mixture and heated to 42 °C for 2 min. Then, 1 µl Superscript II (Invitrogen) reverse transcriptase (RT, 200 U) was added to the reaction mixture and incubated at 42 °C for 1 h. The resultant cDNA generated from this reaction was used as a template in subsequent PCRs. PCR was performed by using 2 µl cDNA generated from the RT reaction, 5 µl CCHF primers (10 µM each), 5 µl 10 × PCR buffer, 1·5 µl dNTP mixture, 2 µl $MgSO_4$ (50 µM) and 0·6 µl Hi-Fidelity polymerase (5 U) in a 50 µl reaction. PCR thermocycler conditions were used as recommended by the manufacturer with an annealing temperature of 45 °C. When the consensus primer set was unable to generate a PCR product for one half of the M segment, a gene-specific internal primer was designed based on sequences from the half of the M segment that did yield a product. This was the case with UG 3010;

the 3′ half of the UG 3010 M segment was amplified by using a gene-specific internal primer, 3370F (5′-TGAACACAGGGGCAA-CAAAATC-3′), in combination with the 3′ external consensus primer CCHF 3′R. Resultant PCR products were TA-cloned into pCR4-TOPO using the TOPO cloning for sequencing system (Invitrogen) according to the manufacturer's instructions. Recombinant clones were confirmed by sequencing in both directions. On average, three clones from two PCRs were sequenced in both directions to generate a sequence for each M segment half. By using the data from the 5′ and 3′ ends of each M segment that shared a 1 kb overlap, the sequence of each strain's M segment was resolved. These two overlapping fragments were utilized for cloning a full-length M segment into the expression vector pCAGGS (Niwa *et al.*, 1991). The sequences have been deposited in GenBank (accession numbers AY900141–AY900145).

Mapping of mAb 11E7. In order to map the epitope recognized by mAb 11E7, we constructed expression plasmids that represent fragments of the G_C ectodomain. Primers were synthesized according to the published sequence for strain IbAr10200 (Sanchez *et al.*, 2002) and standard PCR technology was performed to clone the amplicons into the pcDNA3.1D/V5-His-TOPO vector (Invitrogen). The 5′ primers included the CACC sequence at the 5′ end and the start codon to allow for directional cloning. The 3′ primers did not possess a stop codon to allow the inclusion of the V5 cassette and polyhistidine epitope tags at the C terminus of the protein. Cloning was performed as described by the manufacturer (Invitrogen) and all constructs were sequenced. All primer sequences are available upon request.

Protein analysis. To analyse protein expression, HEK-293T cells were infected with recombinant vaccinia virus vTF1.1 expressing T7 polymerase (Alexander *et al.*, 1992) and transfected 40 min later by using Lipofectamine 2000 (Invitrogen). At 24 h post-transfection, cell extracts were prepared in 50 mM Tris/HCl (pH 7·4), 5 mM EDTA, 1 % Triton X-100 and Complete Protease Inhibitor cocktail (Roche Applied Sciences). Cell lysates were incubated at 4 °C for 3 min and then centrifuged at 10 000 ***g*** for 10 min. The supernatant was mixed with sample buffer [0·08 M Tris/HCl (pH 6·8), 2 % SDS, 10 % glycerol, 5 % β-mercaptoethanol, 0·005 % bromophenol blue] and incubated at 56 °C for 10 min before electrophoresis in a Criterion SDS-PAGE 4–15 % Tris/HCl gel (Bio-Rad). Western blot analysis was performed by using mouse anti-V5 (Invitrogen) or mAb 11E7 as primary antibodies and sheep anti-mouse horseradish peroxidase-conjugated secondary antibody (Amersham Biosciences) followed by visualization with ECL-Plus Western blotting detection reagents (Bioscience). In the case of Western blotting developed with mAb 11E7, samples were not treated with β-mercaptoethanol.

Immunofluorescence (IF) microscopy. To determine whether there were antigenic differences among glycoproteins from different CCHFV strains and to characterize their localization within cells, we performed indirect IF microscopy as described previously (Morais *et al.*, 2003). HeLa cells grown to 50 % confluence on glass coverslips were transfected with the different pCAGGS plasmids containing the CCHFV M segments. At 24 h post-transfection, the cells were fixed with 2 % (w/v) formaldehyde in PBS, permeabilized with 0·5 % Triton X-100 and stained with ascites containing a G_N- or G_C-specific mAb, diluted 1 : 250 in PBS containing 0·5 mM $MgCl_2$ and 4 % FBS. Then, cells were washed with PBS and incubated for 1 h with the secondary antibody conjugated to Alexa Fluor 488 (goat anti-mouse) (Molecular Probes) diluted 1 : 500 in PBS containing 4 % FBS. Finally, cells were washed in PBS, mounted with Fluoromount-G (Southern Biotechnology Associates) and examined on a Nikon E600 microscope at $\times 60$ magnification utilizing UV illumination.

Sequence analysis. We studied the relationships between the newly sequenced CCHFV M segments and previously published full-length isolates. The sequence alignments were produced by using CLUSTAL_X (Thompson *et al.*, 1997) and checked manually for accuracy. The phylogenetic trees were drawn by using the PHYLIP package version 3.57c (Felsenstein, 1997). Briefly, the trees were obtained by using distance methods; SEQBOOT was used to obtain 1000 bootstrap replications of the original sequence alignment. The bootstrapped alignments were used for construction of a consensus tree with NEIGHBOR and CONSENSE as described in the package documentation. Distance between species shown in Fig. 1 was obtained from the original alignment. Consensus trees were rooted with the Dugbe strain, using TREEVIEW version 1.6.1 (Page, 1996).

RESULTS AND DISCUSSION

Cloning and expression of M segments from diverse regions of the world

There is limited sequence information on CCHFV isolates from regions outside China and the former Soviet Union, with only one full-length M segment from an African strain described previously (Chinikar *et al.*, 2004; Hewson *et al.*, 2004a, b; Morikawa *et al.*, 2002; Papa *et al.*, 2002). It is not known whether divergent CCHFV strains exhibit significant antigenic variability or share neutralizing epitopes – information that is important for vaccine development. In addition, only the glycoproteins of the extensively passaged IbAr10200 and Matin strains have been well characterized with regard to processing and cellular localization (Sanchez *et al.*, 2002). To define the genetic and antigenic diversity of geographically diverse CCHFV strains, we cloned, sequenced and expressed the M segments from five isolates. Congolese strain UG 3010 was isolated in 1956 from a physician who became ill after handling blood taken from an infected boy at the Kisangani Hospital (Simpson *et al.*, 1967; Woodall *et al.*, 1967). Republic of South Africa CCHFV strain SPU 41/84 was isolated from a patient in South Africa in 1984 (Blackburn *et al.*, 1987), whilst Republic of South Africa strain SPU 128/81 was isolated from *H. marginatum* ticks (Shepherd *et al.*, 1985). Chinese strain Hy13 was isolated from *H. asiaticum* ticks in XinJiang, China, and Uzbekistan strain U2-2-002/U-6415 was isolated from an infected human. The viruses were passaged in suckling mice for between three and 11 times, as described in Methods.

M segment phylogeny

Hewson *et al.* (2004b) thoroughly described CCHFV phylogeny, revealing the existence of four M segment groups termed M1, M2, M3 and M4. We found that Chinese strain Hy13 clustered with group M1, along with several other Chinese strains and Pakistan strain Matin (Fig. 1a). South African strains SPU 41/84 and SPU 128/81 and Uzbekistan strain U2-2-002 clustered with group M2, along with previously described strains from China, Uzbekistan, Pakistan, Iraq and Nigeria (Hewson *et al.*, 2004b; Morikawa *et al.*, 2002; Sanchez *et al.*, 2002). Congo strain UG 3010 clustered with group M3, which contains two previously described Chinese strains (Fig. 1a) (Morikawa *et al.*, 2002). As noted previously, whilst there is some geographical clustering of CCHFV strains, there are also examples of geographically distant but genetically closely related virus

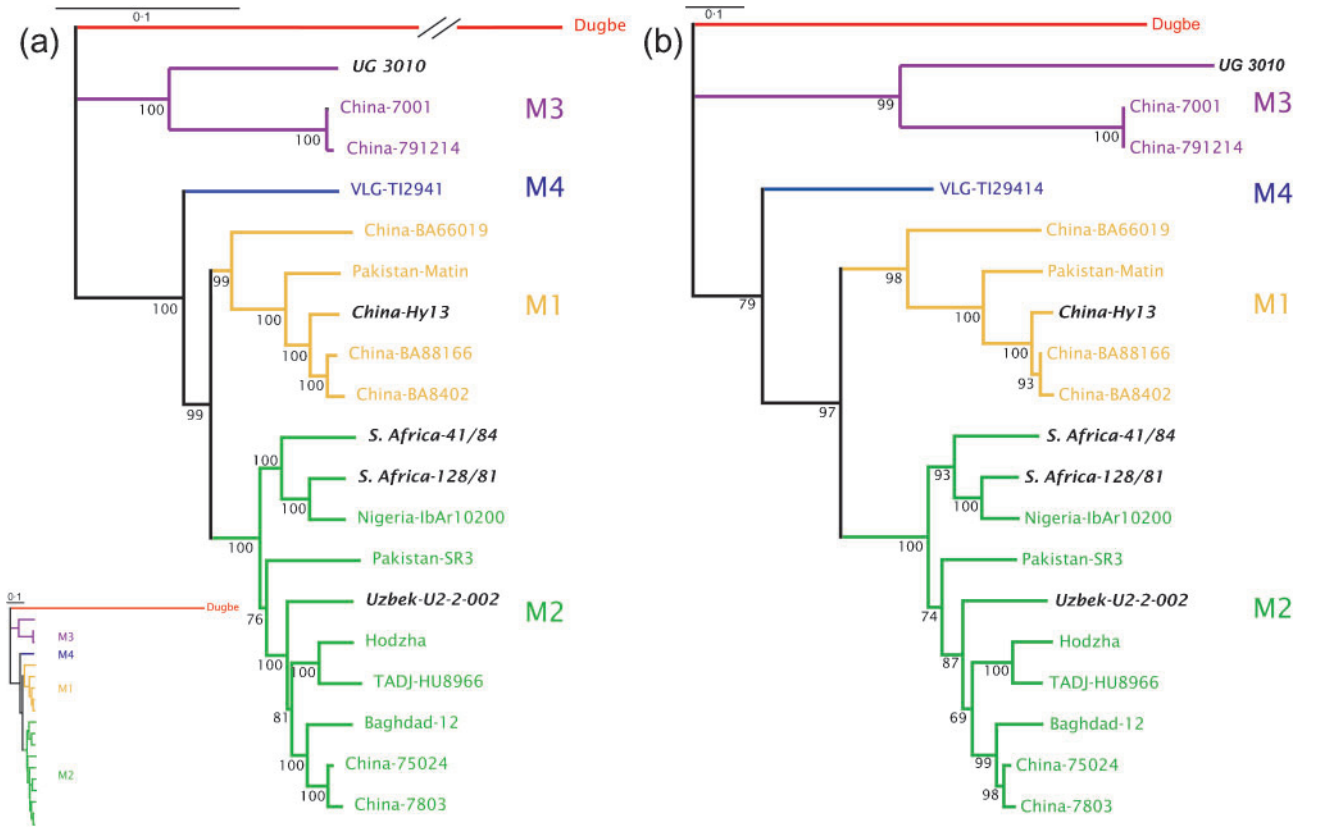

Fig. 1. Phylogenetic trees showing the relationships between CCHFV M segments. The bootstrap values shown are percentages of 1000 replications of the original dataset. All sequences were retrieved from GenBank. Strains marked in bold were sequenced as part of this study (GenBank accession numbers AY900141–AY900145). (a) Phylogenetic tree constructed by utilizing the full-length M segment sequence. The branch length for the Dugbe sequence (outgroup) was cropped for presentation purposes. The small tree at the bottom left of the figure shows the correct branch-length relationship between Dugbe and the remaining sequences. (b) Phylogenetic tree constructed with only the mucin-like domain sequence. Bars, 0·1 substitution per base position.

isolates, perhaps reflecting trade in livestock or dispersal of infected ticks by migratory birds (Hewson *et al.*, 2004b).

We repeated the phylogenetic analysis of the strains using different regions of the M segment (the mucin-like domain or P35 domains of G_N, G_N lacking these domains, and G_C). The same phylogenetic tree was obtained in all cases (data not shown), even when only the highly variable mucin-like domain was used (Fig. 1b). This indicates that sequencing only a small portion of the M segment should make it possible to categorize new CCHFV isolates accurately.

Pairwise analysis of M segments sequences

The five completed M segment sequences had lengths ranging from 1684 to 1699 aa. The CCHFV glycoprotein precursor has been described to contain 78–80 cysteine residues on average, suggesting the presence of an exceptionally large number of disulfide bonds and a complex secondary structure. Cysteine residues were highly conserved, as were the sequences at the predicted proteolytic cleavage sites that have been described previously (Vincent *et al.*, 2003). The number of potential *N*-linked glycosylation sites ranged from nine to 14. The M segments of the newly described strains were aligned with published sequences by using the CLUSTAL_X program (Jeanmougin *et al.*, 1998; Thompson *et al.*, 1997), and an identity matrix was constructed by using the program BioEdit (Tippmann, 2004). The G_N precursor protein (Pre-G_N) contains a highly variable domain at its N terminus that contains a high proportion of serine, threonine and proline residues, and it is predicted to be heavily *O*-glycosylated, thus resembling a mucin-like domain (Table 1) (Hewson *et al.*, 2004a, b; Morikawa *et al.*, 2002; Sanchez *et al.*, 2002). When the identity values for the M segments were calculated based only on the mucin domain, the M1, M2, M3 and M4 strains were clearly distinct, consistent with the phylogenetic analyses (Table 1). When the same type of comparison was performed by using the full-length sequences or other portions of G_N or G_C, distinctions between the subgroups were not as obvious (data not shown), although the M3

Table 1. Complete M segment deduced amino acid identities of CCHFV virus strains

ID, Identical. □ ⩾0·8 ⩾0·6 ⩾0·4 ⩾0·2 ■ <0·2

	Mucin sequence																					Full-length sequence																					
Strain		**M3**			**M4**	**M1**					**M2**												**M3**			**M4**	**M1**					**M2**										
	1	**2**	**3**	**4**	**5**	**6**	**7**	**8**	**9**	**10**	**11**	**12**	**13**	**14**	**15**	**16**	**17**	**18**	**19**	**20**	**1**	**2**	**3**	**4**	**5**	**6**	**7**	**8**	**9**	**10**	**11**	**12**	**13**	**14**	**15**	**16**	**17**	**18**	**19**	**20**
1. Dugbe	ID	0.08	0.09	0.09	0.11	0.10	0.11	0.12	0.12	0.11	0.10	0.12	0.10	0.11	0.11	0.09	0.09	0.09	0.10	0.10	ID	0.32	0.32	0.32	0.33	0.33	0.33	0.33	0.33	0.33	0.33	0.32	0.32	0.33	0.32	0.32	0.32	0.32	0.32	0.32
2. **UG 3010**	0.08	ID	0.35	0.35	0.21	0.21	0.23	0.23	0.23	0.23	0.17	0.18	0.20	0.21	0.19	0.19	0.20	0.19	0.21	0.21	0.32	ID	0.82	0.82	0.72	0.72	0.73	0.73	0.73	0.73	0.72	0.72	0.72	0.72	0.72	0.72	0.72	0.72	0.72	0.72
3. China-7001	0.09	0.35	ID	1.00	0.27	0.22	0.23	0.25	0.25	0.24	0.24	0.24	0.25	0.23	0.21	0.23	0.23	0.21	0.22	0.23	0.32	0.82	ID	1.00	0.73	0.72	0.74	0.74	0.74	0.73	0.73	0.73	0.73	0.73	0.73	0.73	0.73	0.73	0.72	0.73	0.73
4. China-791214	0.09	0.35	1.00	ID	0.27	0.22	0.23	0.25	0.25	0.24	0.24	0.24	0.25	0.23	0.21	0.23	0.23	0.21	0.22	0.23	0.32	0.82	1.00	ID	0.73	0.72	0.73	0.74	0.73	0.73	0.72	0.72	0.73	0.73	0.72	0.73	0.72	0.73	0.73	0.72
5. VLG-TI29414	0.11	0.21	0.27	0.27	ID	0.39	0.39	0.41	0.43	0.41	0.43	0.39	0.39	0.42	0.40	0.39	0.38	0.40	0.41	0.41	0.33	0.72	0.73	0.73	ID	0.82	0.82	0.83	0.83	0.83	0.82	0.83	0.83	0.82	0.83	0.83	0.82	0.83	0.83	0.83
6. China-BA66019	0.10	0.21	0.22	0.22	0.39	ID	0.61	0.58	0.58	0.57	0.44	0.49	0.48	0.52	0.46	0.43	0.44	0.47	0.46	0.47	0.33	0.72	0.72	0.72	0.82	ID	0.88	0.88	0.88	0.88	0.86	0.84	0.85	0.85	0.85	0.85	0.84	0.85	0.85	0.85
7. Pakistan-Matin	0.11	0.23	0.23	0.23	0.39	0.61	ID	0.78	0.77	0.76	0.42	0.47	0.47	0.47	0.46	0.46	0.45	0.46	0.47	0.47	0.33	0.73	0.74	0.73	0.82	0.88	ID	0.94	0.94	0.94	0.86	0.85	0.86	0.85	0.85	0.86	0.85	0.86	0.86	0.86
8. **China-Hy13**	0.12	0.23	0.25	0.25	0.41	0.58	0.78	ID	0.94	0.92	0.42	0.43	0.45	0.46	0.43	0.46	0.43	0.44	0.44	0.44	0.33	0.73	0.74	0.74	0.83	0.88	0.94	ID	0.97	0.97	0.85	0.85	0.85	0.85	0.85	0.86	0.85	0.86	0.86	0.85
9. China-BA88166	0.12	0.23	0.25	0.25	0.43	0.58	0.77	0.94	ID	0.98	0.42	0.45	0.46	0.48	0.46	0.47	0.45	0.46	0.46	0.46	0.33	0.73	0.74	0.73	0.83	0.88	0.94	0.97	ID	0.99	0.85	0.85	0.85	0.85	0.86	0.86	0.85	0.86	0.86	0.86
10. China-BA8402	0.11	0.23	0.24	0.24	0.41	0.57	0.76	0.92	0.98	ID	0.42	0.44	0.45	0.47	0.45	0.47	0.44	0.45	0.45	0.45	0.33	0.73	0.73	0.73	0.83	0.88	0.94	0.97	0.99	ID	0.85	0.85	0.85	0.85	0.85	0.86	0.85	0.85	0.86	0.85
11. **S. Africa 128/81**	0.10	0.17	0.24	0.24	0.43	0.44	0.42	0.42	0.42	0.42	ID	0.72	0.72	0.65	0.60	0.62	0.62	0.63	0.65	0.64	0.33	0.72	0.73	0.72	0.82	0.86	0.86	0.85	0.85	0.85	ID	0.92	0.96	0.90	0.90	0.91	0.90	0.90	0.92	0.91
12. **S. Africa 41/84**	0.12	0.18	0.24	0.24	0.39	0.49	0.47	0.43	0.45	0.44	0.72	ID	0.86	0.71	0.66	0.67	0.66	0.65	0.72	0.71	0.32	0.72	0.73	0.72	0.83	0.84	0.85	0.85	0.85	0.85	0.92	ID	0.92	0.89	0.89	0.90	0.89	0.90	0.90	0.90
13. Nigeria-IbAr10200	0.10	0.20	0.25	0.25	0.39	0.48	0.47	0.45	0.46	0.45	0.72	0.86	ID	0.69	0.65	0.65	0.66	0.65	0.71	0.71	0.32	0.72	0.73	0.73	0.83	0.85	0.86	0.85	0.85	0.85	0.96	0.92	ID	0.90	0.90	0.90	0.90	0.90	0.91	0.91
14. Pakistan-SR3	0.11	0.21	0.23	0.23	0.42	0.52	0.47	0.46	0.48	0.47	0.65	0.71	0.69	ID	0.69	0.72	0.73	0.72	0.75	0.74	0.33	0.72	0.73	0.73	0.82	0.85	0.85	0.85	0.85	0.85	0.90	0.89	0.90	ID	0.90	0.90	0.90	0.90	0.91	0.91
15. **Uzbek-U2-2-002**	0.11	0.19	0.21	0.21	0.40	0.46	0.46	0.43	0.46	0.45	0.60	0.66	0.65	0.69	ID	0.69	0.72	0.73	0.77	0.76	0.32	0.72	0.73	0.72	0.83	0.85	0.85	0.85	0.86	0.85	0.90	0.89	0.90	0.90	ID	0.93	0.92	0.93	0.94	0.94
16. Hodzha	0.09	0.19	0.23	0.23	0.39	0.43	0.46	0.46	0.47	0.47	0.62	0.67	0.65	0.72	0.69	ID	0.87	0.73	0.78	0.78	0.32	0.72	0.73	0.73	0.83	0.85	0.86	0.86	0.86	0.86	0.91	0.90	0.90	0.90	0.93	ID	0.96	0.93	0.95	0.94
17. TADJ-HU8966	0.09	0.20	0.23	0.23	0.38	0.44	0.45	0.43	0.45	0.44	0.62	0.66	0.66	0.73	0.72	0.87	ID	0.74	0.81	0.81	0.32	0.72	0.72	0.72	0.82	0.84	0.85	0.85	0.85	0.85	0.90	0.89	0.90	0.90	0.92	0.96	ID	0.92	0.94	0.94
18. Baghdad-12	0.09	0.19	0.21	0.21	0.40	0.47	0.46	0.44	0.46	0.45	0.63	0.65	0.65	0.72	0.73	0.73	0.74	ID	0.89	0.88	0.32	0.72	0.73	0.73	0.83	0.85	0.86	0.86	0.86	0.85	0.90	0.90	0.90	0.90	0.93	0.93	0.92	ID	0.96	0.96
19. China-75024	0.10	0.21	0.22	0.22	0.41	0.46	0.47	0.44	0.46	0.45	0.65	0.72	0.71	0.75	0.77	0.78	0.81	0.89	ID	0.97	0.32	0.72	0.73	0.73	0.83	0.85	0.86	0.86	0.86	0.86	0.92	0.90	0.91	0.91	0.94	0.95	0.94	0.96	ID	0.99
20. China-78033	0.10	0.21	0.23	0.23	0.41	0.47	0.47	0.44	0.46	0.45	0.64	0.71	0.71	0.74	0.76	0.78	0.81	0.88	0.97	ID	0.32	0.72	0.72	0.72	0.83	0.85	0.86	0.85	0.86	0.85	0.91	0.90	0.91	0.91	0.94	0.94	0.94	0.96	0.99	ID

group was the best defined and differentiated of the four subgroups (Table 1).

Antigenic analysis of G_N and G_C

Antigenic variation of arboviruses is of relevance because it may provide clues on the possible directions of epidemics or endemic spread. Little is known about antigenic relationships among CCHFV strains, in part because of the lack of adequate reagents. Early studies have shown that strains from diverse parts of the world have close antigenic relationships (Tignor *et al.*, 1980). However, these studies were performed by utilizing polyclonal serum obtained from animals inoculated with infected mouse-brain tissue, which usually results mainly in antibodies directed against the nucleocapsid (Blackburn *et al.*, 1987). Indeed, with the exception of a recent report from our laboratory (Bertolotti-Ciarlet *et al.*, 2005), the CCHFV mAbs described thus far are directed against the nucleocapsid (Blackburn *et al.*, 1987). The viral glycoproteins might exhibit a degree of higher antigenic variability than the nucleocapsid protein as a result of immune selection and the adaptation needed to efficiently bind to and enter diverse cell types. Therefore, we determined antigenic differences between G_N and G_C from different strains, utilizing a panel of eight mAbs to G_N and nine mAbs to G_C (Bertolotti-Ciarlet *et al.*, 2005). These mAbs bind to conformation-dependent epitopes and so were characterized for their ability to recognize the different G_N and G_C proteins by IF microscopy utilizing constructs expressing only one of the glycoproteins (Bertolotti-Ciarlet *et al.*, 2005). The G_N and G_C proteins from each of the five strains were recognized by a subset of the mAbs and were localized to both the endoplasmic reticulum and the Golgi, consistent with correct processing and transport (Table 2 and Fig. 2) (Andersson & Pettersson, 1998; Andersson *et al.*, 1997a, b; Chen & Compans, 1991; Chen *et al.*, 1991; Gerrard & Nichol, 2002). The Golgi localization was confirmed by IF microscopy using a marker for TGN46 (Serotec), a sheep antibody specific for a heavily glycosylated protein localized primarily in the trans-Golgi network (data not shown). The M segments from each of the five virus strains appeared to be expressed at similar levels, as they were all recognized well by mAb 11E7 (see Supplementary Fig. S1, available in JGV Online). In addition, by using a rabbit polyclonal serum, we were able to show that the G_N glycoproteins from each of the five CCHFV strains were expressed and processed properly (see Supplementary Fig. S2, available in JGV Online). With regards to mAb reactivity, two of the M2 group strains (SPU 128/81 and U2-2-002) were virtually identical to IbAr10200, which itself is an M2 group strain. However, the closely related SPU 41/84 M2 strain was not recognized by two of the G_C mAbs or by two of the G_N mAbs (Table 2). On the other hand, the M1 group strain Hy13 was recognized by seven of the eight G_N mAbs, but by only three of nine G_C mAbs. The M3 strain UG 3010, which was genetically the most distantly related to IbAr10200, shared a high degree of antigenic similarity with this prototype CCHFV strain.

Table 2. Reactivity of IbAr10200 mAbs with different CCHFV strains

The characterization of neutralization and protection has been described previously (Bertolotti-Ciarlet *et al.*, 2005). Neutralization is shown as the plaque-reduction neutralization titre (PRNT 80 %) and protection data as the number of surviving mice compared with the total number of mice treated. +, Positive signal by IF; −, negative result. The identity of the antibodies was determined by IF analysis using constructs that contain G_N or G_C alone (Bertolotti-Ciarlet *et al.*, 2005).

Target	mAb	Neutralization	Protection (%)	Hy13 M1	IbAr10200 M2	U2-2-002 M2	SPU 128/81 M2	SPU 41/84 M2	UG 3010 M3
G_C	11E7	2560	70	+	+	+	+	+	+
	3E3	<20	45	+	+	+	+	+	+
	12A9	>5120	75	−	+	+	+	+	−
	8A1	>5120	100	−	+	+	+	+	+
	30F7	2560	40	−	+	+	+	+	+
	7C12	<40	40	−	+	+	+	+	+
	9H3	>5120	50	−	+	+	+	+	+
	5B5	1280	50	−	+	+	+	−	+
	4C1	>5120	41	+	+	+	+	−	+
G_N	5A5	<40	60	+	+	+	+	+	+
	9C6	<40	20	+	+	+	+	+	+
	8F10	<40	70	+	+	+	+	+	+
	11F6	<40	30	−	+	−	+	+	+
	7F5	<40	10	+	+	+	+	−	+
	2C9	<40	30	+	+	+	+	−	−
	3F3	<40	60	+	+	+	+	+	−
	10G4	<40	75	+	+	+	+	+	−

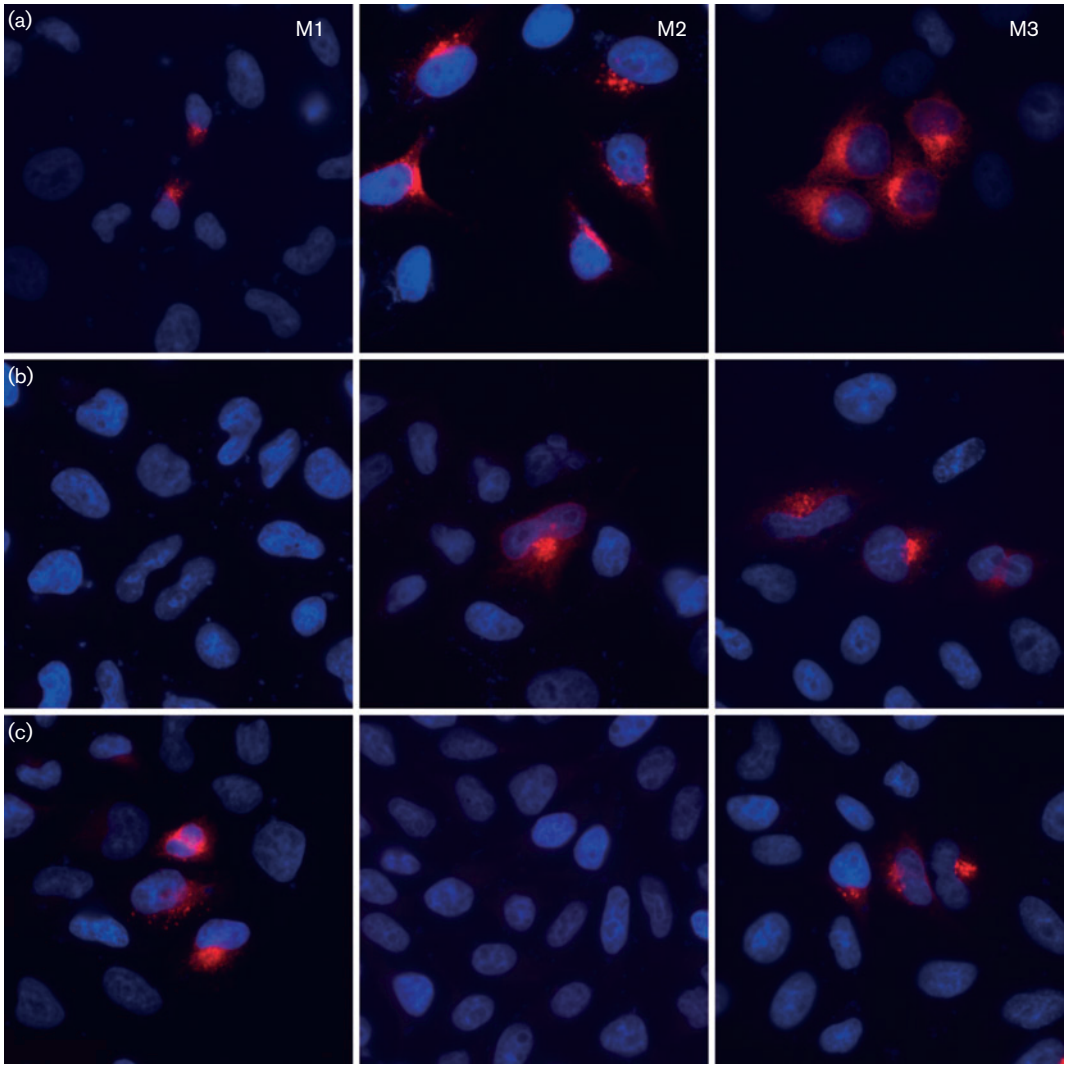

Fig. 2. IF analysis of CCHFV G_N and G_C glycoproteins. Transfected HeLa cells expressing CCHFV glycoproteins from different virus strains were processed for IF microscopy and stained with each of 17 different mouse anti-CCHFV mAbs (red) as described previously (Bertolotti-Ciarlet *et al*., 2005). Nuclei were stained with 4′,6-diamidino-2-phenylindole (DAPI; blue). Representative examples are shown in the following panels: (a) 11E7 anti-G_C mAb, from left to right: CCHFV strains M1 Hy13, M2 SPU 128/81, M3 UG 3010; (b) 8A1 anti-G_C mAb, from left to right: M1 Hy13, M2 U2-2-002, M3 UG 3010; (c) 7F5 anti-G_N mAb, from left to right: M1 Hy13, M2 SPU 41/84, M3 UG 3010. HeLa cells were transfected with CCHFV M segments by using Lipofectamine 2000 (Invitrogen) and processed 24 h later.

Altogether, the mAbs exhibited eight different reactivity patterns, including some mAbs that recognized only M2 virus strains and others that recognized all strains tested. Of the seven mAbs known to neutralize IbAr10200 potently *in vitro* (Bertolotti-Ciarlet *et al*., 2005), only 11E7 bound to all six virus strains. Of the five mAbs described previously to be able to protect at least 70 % of suckling mice challenged with IbAr10200 (Bertolotti-Ciarlet *et al*., 2005), 11E7 and 8F10 could bind to all six virus strains. It is important to note that, in each experiment, we used the parental IbAr10200 strain as a positive control (as it was recognized by all of the mAbs) and mock-transfected cells as a negative control (see Supplementary Fig. S3, available in JGV Online). These results suggest that there are significant antigenic differences between CCHFV strains that may not correlate well with genotypic or geographical characteristics. In addition, a number of epitopes to which neutralizing or protective mAbs can be directed are not highly conserved. However, at least one broadly cross-reactive, potently neutralizing mAb that can protect mice from a lethal CCHFV challenge (11E7) was identified.

Mapping of the 11E7 mAb epitope

As the neutralizing mAb 11E7 was able to recognize G_C by Western blot under non-reducing conditions, we were able

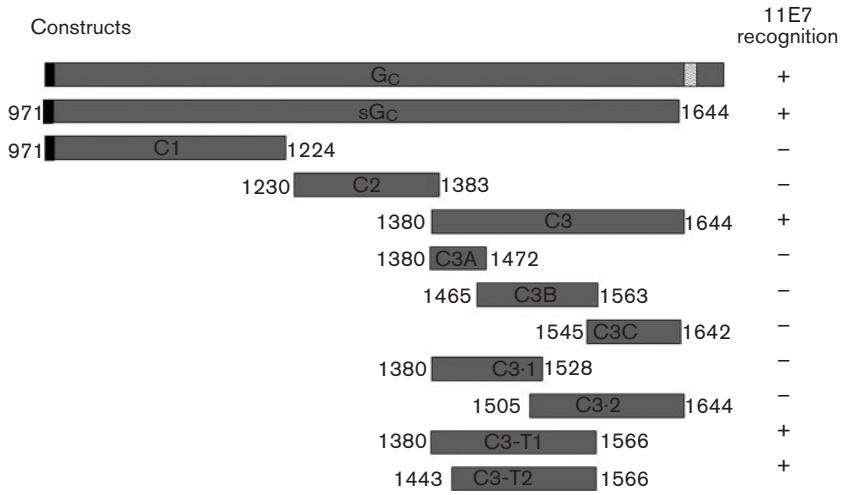

Fig. 3. Mapping of the epitope recognized by neutralizing mAb 11E7. A schematic representation of the different IbAr10200 G_C fragments utilized to map the 11E7 epitope is shown. All of the constructs were expressed in mammalian cells and included a V5 epitope tag at the C terminus to control for expression. The numbers at the end of each construct represent the amino acid numbers based on the full-length IbAr10200 M segment.

to partially map its epitope by testing its ability to recognize fragments of G_C produced in HEK-293T cells. This is of relevance because mAb 11E7 protects mice *in vivo* from challenge with CCHFV strain IbAr10200 (Bertolotti-Ciarlet *et al.*, 2005). Passive immunization can be effective for the treatment of CCHFV infection in humans, emphasizing the importance of identification of neutralizing antibodies and the epitopes to which they bind (Vassilenko *et al.*, 1990).

We found that a G_C construct lacking the transmembrane and cytoplasmic domains was recognized by mAb 11E7 (Fig. 3). Therefore, we constructed three fragments that covered the length of the G_C ectodomain (C1, C2 and C3). All fragments contained a V5 epitope tag at the C terminus to allow detection of the fragment and to confirm their expression (Fig. 4). Most of the constructs, when expressed, formed SDS-resistant oligomers to some extent (Fig. 4). However, the relevance of this oligomerization is not clear, as the fragments represent only small portions of the protein and may therefore aggregate. Nonetheless, of these three fragments, only construct C3, located at the C terminus of the G_C ectodomain, was recognized by 11E7. Therefore, we focused our attention on this area, further dividing it into three new fragments (C3A, C3B and C3C). The antibody recognized none of these fragments. Next, we decided to divide the C3 fragment into two overlapping regions (C3.1 and C3.2); however, this resulted in disruption of the 11E7 epitope (Figs 3 and 4). Therefore, we performed a small deletion within the C3 C terminus (C3-T1). The antibody recognized this construct. Additionally, a small deletion of the N terminus of the C3 region also yielded a fragment recognized by mAb 11E7 (C3-T2) (Figs 3 and 4). Therefore, we conclude that the neutralizing epitope of mAb 11E7 is contained between aa 1443 and 1566 of the M segment of IbAr10200 strain, a highly conserved region of the protein (Figs 3 and 4).

Conclusion

In summary, we report the first description of CCHFV glycoprotein antigenic structure and relatedness, as well as initial mapping of a cross-reactive neutralizing epitope present on divergent CCHFV strains. CCHFV strains can exhibit considerable genetic variability, with the mucin-like domain in G_N in particular being highly divergent. We also found a considerable amount of antigenic variability, which may not follow phylogenetic groupings of CCHFV strains. Even the highly conserved G_C protein exhibited antigenic

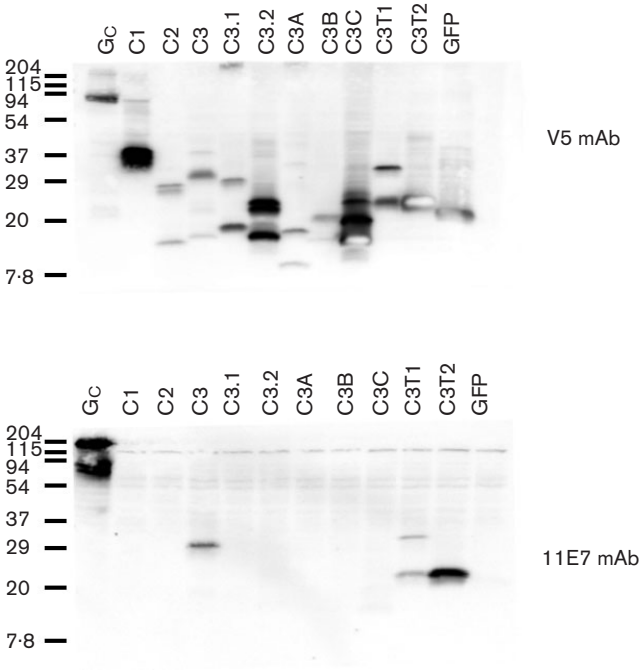

Fig. 4. Western blot analyses for mapping of the mAb 11E7 epitope. Western blotting was performed by using lysates of HEK-293T cells transfected with some of the constructs shown in Fig. 3 and developed by using mAb 11E7 in parallel with a mAb for the V5 tag (Invitrogen). Some of the smaller fragments ran as both monomers and oligomers in SDS-PAGE. Molecular markers are shown in kDa (Prestained SDS-PAGE standards, broad range; Bio-Rad). GFP, Green fluorescent protein.

variability, suggesting that CCHFV glycoproteins are subject to immune selection. Nonetheless, at least some epitopes to which neutralizing and/or protective antibodies bind are conserved between divergent CCHFV strains, and definition of these antibody-binding sites may be useful for vaccine design.

ACKNOWLEDGEMENTS

We thank Aura Garrison, Louis Altamura and Donald Pijak for expert technical assistance. This work was supported in part by training grant NIH T32 AI055400, Department of Defense Peer Reviewed Medical Research Program grant PRMRP PR033269 and R21-AI-063308.

REFERENCES

Alexander, W. A., Moss, B. & Fuerst, T. R. (1992). Regulated expression of foreign genes in vaccinia virus under the control of bacteriophage T7 RNA polymerase and the *Escherichia coli lac* repressor. *J Virol* **66**, 2934–2942.

Andersson, A. M. & Pettersson, R. F. (1998). Targeting of a short peptide derived from the cytoplasmic tail of the G1 membrane glycoprotein of Uukuniemi virus (*Bunyaviridae*) to the Golgi complex. *J Virol* **72**, 9585–9596.

Andersson, A. M., Melin, L., Bean, A. & Pettersson, R. F. (1997a). A retention signal necessary and sufficient for Golgi localization maps to the cytoplasmic tail of a *Bunyaviridae* (Uukuniemi virus) membrane glycoprotein. *J Virol* **71**, 4717–4727.

Andersson, A. M., Melin, L., Persson, R., Raschperger, E., Wikström, L. & Pettersson, R. F. (1997b). Processing and membrane topology of the spike proteins G1 and G2 of Uukuniemi virus. *J Virol* **71**, 218–225.

Bertolotti-Ciarlet, A., Smith, J., Strecker, K. & 7 other authors (2005). Cellular localization and antigenic characterization of Crimean-Congo hemorrhagic fever virus glycoproteins. *J Virol* **79**, 6152–6161.

Blackburn, N. K., Besselaar, T. G., Shepherd, A. J. & Swanepoel, R. (1987). Preparation and use of monoclonal antibodies for identifying Crimean-Congo hemorrhagic fever virus. *Am J Trop Med Hyg* **37**, 392–397.

Chen, S.-Y. & Compans, R. W. (1991). Oligomerization, transport, and Golgi retention of Punta Toro virus glycoproteins. *J Virol* **65**, 5902–5909.

Chen, S.-Y., Matsuoka, Y. & Compans, R. W. (1991). Golgi complex localization of the Punta Toro virus G2 protein requires its association with the G1 protein. *Virology* **183**, 351–365.

Chinikar, S., Persson, S.-M., Johansson, M. & 7 other authors (2004). Genetic analysis of Crimean-Congo hemorrhagic fever virus in Iran. *J Med Virol* **73**, 404–411.

Chumakov, M. P., Butenko, A. M., Shalunova, N. V. & 10 other authors (1968). New data on the viral agent of Crimean hemorrhagic fever. *Vopr Virusol* **13**, 377 (in Russian).

Chumakov, M. P., Smirnova, S. E. & Tkachenko, E. A. (1970). Relationship between strains of Crimean haemorrhagic fever and Congo viruses. *Acta Virol* **14**, 82–85.

Felsenstein, J. (1997). An alternating least squares approach to inferring phylogenies from pairwise distances. *Syst Biol* **46**, 101–111.

Gerrard, S. R. & Nichol, S. T. (2002). Characterization of the Golgi retention motif of Rift Valley fever virus G_N glycoprotein. *J Virol* **76**, 12200–12210.

Hewson, R., Chamberlain, J., Mioulet, V. & 9 other authors (2004a). Crimean-Congo haemorrhagic fever virus: sequence analysis of the small RNA segments from a collection of viruses world wide. *Virus Res* **102**, 185–189.

Hewson, R., Gmyl, A., Gmyl, L., Smirnova, S. E., Karganova, G., Jamil, B., Hasan, R., Chamberlain, J. & Clegg, C. (2004b). Evidence of segment reassortment in Crimean-Congo haemorrhagic fever virus. *J Gen Virol* **85**, 3059–3070.

Hoogstraal, H. (1979). The epidemiology of tick-borne Crimean-Congo hemorrhagic fever in Asia, Europe, and Africa. *J Med Entomol* **15**, 307–417.

Jeanmougin, F., Thompson, J. D., Gouy, M., Higgins, D. G. & Gibson, T. J. (1998). Multiple sequence alignment with Clustal X. *Trends Biochem Sci* **23**, 403–405.

Morais, V. A., Crystal, A. S., Pijak, D. S., Carlin, D., Costa, J., Lee, V. M.-Y. & Doms, R. W. (2003). The transmembrane domain region of nicastrin mediates direct interactions with APH-1 and the γ-secretase complex. *J Biol Chem* **278**, 43284–43291.

Morikawa, S., Qing, T., Xinqin, Z., Saijo, M. & Kurane, I. (2002). Genetic diversity of the M RNA segment among Crimean-Congo hemorrhagic fever virus isolates in China. *Virology* **296**, 159–164.

Niwa, H., Yamamura, K. & Miyazaki, J. (1991). Efficient selection for high-expression transfectants with a novel eukaryotic vector. *Gene* **108**, 193–199.

Olaleye, O. D., Tomori, O. & Schmitz, H. (1996). Rift Valley fever in Nigeria: infections in domestic animals. *Rev Sci Tech* **15**, 937–946.

Onishchenko, G. G., Lomov, Iu. M., Markov, V. I. & 12 other authors (2000). The laboratory diagnosis of an outbreak of hemorrhagic fever at Oblivskaya village, Rostov Province: proof of the etiological role of the Crimean-Congo hemorrhagic fever virus. *Zh Mikrobiol Epidemiol Immunobiol* 32–36 (in Russian).

Onishchenko, G. G., Efremenko, V. I., Kovalev, N. G. & 12 other authors (2001a). Specific epidemiologic features of Crimean haemorrhagic fever in Stavropol' region in 1999–2000. *Zh Mikrobiol Epidemiol Immunobiol* 86–89 (in Russian).

Onishchenko, G. G., Markov, V. I., Merkulov, V. A., Vasil'ev, N. T., Berezhnoi, A. M., Androshchuk, I. A. & Maksimov, V. A. (2001b). Isolation and identification of Crimean-Congo hemorrhagic fever virus in the Stavropol territory. *Zh Mikrobiol Epidemiol Immunobiol* 7–11 (in Russian).

Page, R. D. M. (1996). TREEVIEW: an application to display phylogenetic trees on personal computers. *Comput Appl Biosci* **12**, 357–358.

Papa, A., Ma, B.-J., Kouidou, S., Tang, Q., Hang, C.-S. & Antoniadis, A. (2002). Genetic characterization of the M RNA segment of Crimean Congo hemorrhagic fever virus strains, China. *Emerg Infect Dis* **8**, 50–53.

Sanchez, A. J., Vincent, M. J. & Nichol, S. T. (2002). Characterization of the glycoproteins of Crimean-Congo hemorrhagic fever virus. *J Virol* **76**, 7263–7275.

Schmaljohn, C. S. (1996). *Bunyaviridae*: the viruses and their replication. In *Fileds Virology*, 3rd edn, pp. 1447–1471. Edited by B. N. Fields, D. M. Knipe & P. M. Howley. Philadelphia, PA: Lippincott-Raven.

Shepherd, A. J., Swanepoel, R., Shepherd, S. P., Leman, P. A., Blackburn, N. K. & Hallett, A. F. (1985). A nosocomial outbreak of Crimean-Congo haemorrhagic fever at Tygerberg Hospital. Part V. Virological and serological observations. *S Afr Med J* **68**, 733–736.

Simmons, G., Wool-Lewis, R. J., Baribaud, F., Netter, R. C. & Bates, P. (2002). Ebola virus glycoproteins induce global surface protein down-modulation and loss of cell adherence. *J Virol* **76**, 2518–2528.

Simpson, D. I., Knight, E. M., Courtois, G., Williams, M. C., Weinbren, M. P. & Kibukamusoke, J. W. (1967). Congo virus: a hitherto undescribed virus occurring in Africa. I. Human isolations – clinical notes. *East Afr Med J* **44**, 86–92.

Thompson, J. D., Gibson, T. J., Plewniak, F., Jeanmougin, F. & Higgins, D. G. (1997). The CLUSTAL_X windows interface: flexible strategies for multiple sequence alignment aided by quality analysis tools. *Nucleic Acids Res* **25**, 4876–4882.

Tignor, G. H., Smith, A. L., Casals, J., Ezeokoli, C. D. & Okoli, J. (1980). Close relationship of Crimean hemorrhagic fever-Congo (CHF-C) virus strains by neutralizing antibody assays. *Am J Trop Med Hyg* **29**, 676–685.

Tippmann, H.-F. (2004). Analysis for free: comparing programs for sequence analysis. *Brief Bioinform* **5**, 82–87.

Vassilenko, S. M., Vassilev, T. L., Bozadjiev, L. G., Bineva, I. L. & Kazarov, G. Z. (1990). Specific intravenous immunoglobulin for Crimean-Congo haemorrhagic fever. *Lancet* **335**, 791–792.

Vincent, M. J., Sanchez, A. J., Erickson, B. R., Basak, A., Chretien, M., Seidah, N. G. & Nichol, S. T. (2003). Crimean-Congo hemorrhagic fever virus glycoprotein proteolytic processing by subtilase SKI-1. *J Virol* **77**, 8640–8649.

Whitehouse, C. A. (2004). Crimean–Congo hemorrhagic fever. *Antiviral Res* **64**, 145–160.

Williams, R. J., Al-Busaidy, S., Mehta, F. R. & 7 other authors (2000). Crimean-Congo haemorrhagic fever: a seroepidemiological and tick survey in the Sultanate of Oman. *Trop Med Int Health* **5**, 99–106.

Wood, O. L., Lee, V. H., Ash, J. S. & Casals, J. (1978). Crimean-Congo hemorrhagic fever, Thogoto, Dugbe, and Jos viruses isolated from ixodid ticks in Ethiopia. *Am J Trop Med Hyg* **27**, 600–604.

Woodall, J. P., Williams, M. C. & Simpson, D. I. (1967). Congo virus: a hitherto undescribed virus occurring in Africa. II. Identification studies. *East Afr Med J* **44**, 93–98.

JOURNAL OF VIROLOGY, June 2007, p. 6632–6642 Vol. 81, No. 12
0022-538X/07/$08.00+0 doi:10.1128/JVI.02730-06

Identification of a Novel C-Terminal Cleavage of Crimean-Congo Hemorrhagic Fever Virus $PreG_N$ That Leads to Generation of an NS_M Protein▽

Louis A. Altamura,[1] Andrea Bertolotti-Ciarlet,[1] Jeffrey Teigler,[2] Jason Paragas,[3]† Connie S. Schmaljohn,[3] and Robert W. Doms[1]*

Department of Microbiology, University of Pennsylvania, Philadelphia, Pennsylvania 19104[1]; Ursinus College, Collegeville, Pennsylvania 19426[2]; and United States Army Medical Research Institute for Infectious Diseases, Fort Detrick, Frederick, Maryland 21702[3]

Received 12 December 2006/Accepted 29 March 2007

The structural glycoproteins of Crimean-Congo hemorrhagic fever virus (CCHFV; genus *Nairovirus*, family *Bunyaviridae*) are derived through endoproteolytic cleavage of a 1,684-amino-acid M RNA segment-encoded polyprotein. This polyprotein is cotranslationally cleaved into the $PreG_N$ and $PreG_C$ precursors, which are then cleaved by SKI-1 and a SKI-1-like protease to generate the N termini of G_N and G_C, respectively. However, the resulting polypeptide defined by the N termini of G_N and G_C is predicted to be larger (58 kDa) than mature G_N (37 kDa). By analogy to the topologically similar M segment-encoded polyproteins of viruses in the *Orthobunyavirus* genus, the C-terminal region of $PreG_N$ that contains four predicted transmembrane domains may also contain a nonstructural protein, NS_M. To characterize potential $PreG_N$ C-terminal cleavage events, a panel of epitope-tagged $PreG_N$ truncation and internal deletion mutants was developed. These constructs allowed for the identification of a C-terminal endoproteolytic cleavage within, or very proximal to, the second predicted transmembrane domain following the G_N ectodomain and the subsequent generation of a C-terminal fragment. Pulse-chase experiments showed that $PreG_N$ C-terminal cleavage occurred shortly after synthesis of the precursor and prior to generation of the G_N glycoprotein. The resulting fragment trafficked to the Golgi compartment, the site of virus assembly. Development of an antiserum specific to the second cytoplasmic loop of $PreG_N$ allowed detection of cell-associated NS_M proteins derived from transient expression of the complete CCHFV M segment and also in the context of virus infection.

Crimean-Congo hemorrhagic fever virus (CCHFV) causes a hemorrhagic syndrome in humans with fatality rates varying between 5 and 30% but generally causes subclinical disease in animals (12). CCHFV is a member of the genus *Nairovirus* within the family *Bunyaviridae* and, like all members of this family, has a tripartite genome consisting of large (L), medium (M), and small (S) negative-sense RNA segments that encode the viral RNA polymerase, the glycoproteins, and the nucleocapsid protein, respectively (6, 33). As with other *Bunyaviridae*, the G_N and G_C glycoproteins of CCHFV are derived from an M segment-encoded polyprotein. Unique to the *Nairovirus* genus, however, is the fact that the M polyprotein requires processing through a series of intermediate precursors prior to generation of the mature glycoproteins found in virions (4, 5, 27, 32, 40). For CCHFV, several seminal studies have illustrated the complexity of these endoproteolytic events (Fig. 1). First, the M polyprotein is cotranslationally cleaved into the $PreG_N$ (140-kDa) and $PreG_C$ (85-kDa) precursors, presumably by signal peptidase. $PreG_N$ is then cleaved by the protease SKI-1 in the endoplasmic reticulum/*cis*-Golgi to generate the N terminus of G_N (39) and release a mucin-GP38 domain that is further processed by furin to generate the secreted glycoproteins GP38, GP85, and GP160 and possibly also a mucin-like protein (31). The $PreG_C$ precursor may also undergo trimming by a SKI-1-like protease to expose the N terminus of G_C.

One uncertain aspect of CCHFV glycoprotein processing is the site of C-terminal cleavage for the G_N glycoprotein. While G_N migrates in sodium dodecyl sulfate (SDS)-polyacrylamide gels as a 37-kDa protein, the predicted mass of the polypeptide defined by its N-terminal SKI-1 cleavage site to the beginning of G_C is approximately 58 kDa (Fig. 1). This discrepancy suggests that an additional cleavage event(s) is required to generate the G_N protein. If so, then cleavage likely occurs somewhere within the topologically complex C-terminal portion of $PreG_N$, which contains four predicted transmembrane domains, the last of which appears to function as a signal sequence for G_C. A potential SKI-1-like protease substrate (RKLL) and a polybasic motif (KKRKK) within the cytoplasmic loops of the M polyprotein of CCHFV have been proposed for this putative cleavage event, but mutagenesis of these domains failed to influence G_N maturation (39).

Cleavage within the C-terminal portion of $PreG_N$ could result in the generation of a discrete membrane protein. The M segments of viruses in the *Orthobunyavirus* genus, which have identical membrane topologies to those predicted for *Nairovirus* members such as CCHFV, encode a nonstructural membrane protein termed NS_M within the region between their G_N and G_C glycoproteins (10, 14, 17, 24, 28, 41). These NS_M proteins have been shown to accumulate in the Golgi compart-

* Corresponding author. Mailing address: Department of Microbiology, University of Pennsylvania, 225 Johnson Pavilion, 3610 Hamilton Walk, Philadelphia, PA 19104. Phone: (215) 898-0890. Fax: (215) 898-9557. E-mail: doms@mail.med.upenn.edu.

† Present address: National Institute for Allergy and Infectious Diseases, National Institutes of Health, Bethesda, MD 20892.

▽ Published ahead of print on 11 April 2007.

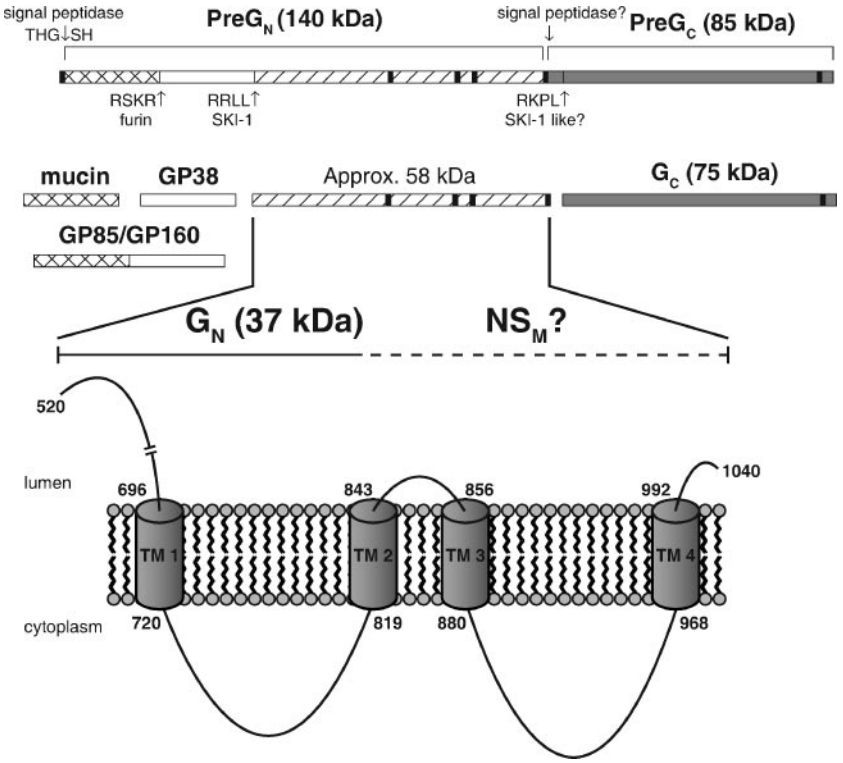

FIG. 1. Processing of the M segment-encoded polyprotein of CCHFV strain IbAr10200. A schematic of the CCHFV M segment-encoded polyprotein is shown, with known and suspected cleavage sites indicated. Signal peptidase is thought to generate the N terminus of the polyprotein and may also liberate PreG$_C$ as indicated (32). The mucin-GP38 domains are liberated by SKI-1 cleavage following the RRLL cleavage site to generate the N terminus of G$_N$ at amino acid 520 (32, 39). A second cleavage event, perhaps also mediated by SKI-1 or a similar protease, produces the N terminus of G$_C$ at residue 1041 following the sequence RKPL (32). Further cleavage by furin following the RSKR motif separates the mucin-like domain from GP38 (31). The region defined by the N termini of G$_N$ and G$_C$ encodes a 58-kDa polypeptide having four predicted transmembrane domains, indicated by black bars. Since mature G$_N$ is approximately 37 kDa, an additional C-terminal processing site may exist between G$_N$ and G$_C$, leading to the generation of an NS$_M$ protein. The uncertain boundaries of this putative NS$_M$ protein are indicated by a dashed line. The cylinders labeled TM 1 to TM 4 represent the four predicted transmembrane helices between the ectodomains of G$_N$ and G$_C$. Amino acid boundaries for each helix were predicted with TMHMM 2.0 (37).

ment along with the viral glycoproteins, pointing to a possible role for NS$_M$ in virus assembly. Indeed, in Bunyamwera virus, deletions of the entire NS$_M$ or its N-terminal regions prevented the plasmid rescue of virus by reverse genetics (34). A similar NS$_M$ protein has been proposed to exist for CCHFV (18, 31). However, no such protein has yet been identified for this or for any other member of the genus *Nairovirus*.

To address the hypothesis that CCHFV PreG$_N$ undergoes a C-terminal cleavage event to generate an NS$_M$ protein, an extensive series of PreG$_N$ truncation and deletion constructs were designed, and new detection reagents were developed. Using these tools, we defined the topology of the C-terminal region of PreG$_N$ and found that it efficiently underwent an endoproteolytic cleavage event that liberated a C-terminal fragment that trafficked to the Golgi compartment. Furthermore, the chronology and independence of this cleavage event in relation to the N-terminal proteolytic events that define G$_N$ were addressed, and a probable location of this cleavage site was identified. This C-terminal fragment was also found to constitute a cell-associated NS$_M$ protein that was generated from the full-length M polyprotein, both by transient plasmid expression and by virus infection.

MATERIALS AND METHODS

Cells and viruses. 293T/17, BHK-21, BSC-1, HeLa, Huh-7, and Vero E6 cells were grown in Dulbecco's modified Eagle medium (DMEM) supplemented with 10% fetal bovine serum (FBS; Invitrogen, Carlsbad, CA), 2 mM L-glutamine (Invitrogen), and 1% penicillin-streptomycin (P/S; Invitrogen). SW-13 cells were grown in Eagle's minimum essential medium (Invitrogen) supplemented with 5% FBS, 2 mM L-glutamine, and 1% P/S. Recombinant vaccinia virus vTF1.1 expressing bacteriophage T7 RNA polymerase (2) was propagated in HeLa cells, and titers were determined in BSC-1 cells according to standard protocols. CCHFV strain IbAr10200 was propagated and titers were determined in SW-13 cells. All CCHFV IbAr10200 infections were conducted in a biosafety level 3+ (BSL-3+) containment suite at the United States Army Medical Research Institute for Infectious Diseases (USAMRIID; Fort Detrick, Frederick, MD). While working with CCHFV, laboratory personnel wore standard personal protective equipment and powered air-purifying respirators.

Plasmids. An expression plasmid encoding the CCHFV IbAr10200 M segment (M [G$_C$V5]) was generated by PCR amplification of the open reading frame, followed by ligation of the amplicon into the pcDNA3.1D/V5-His TOPO expression vector, which encodes an in-frame C-terminal V5-His$_6$ epitope cassette. Thus, G$_C$ possessed a C-terminal epitope cassette in this context. To generate the panel of plasmids encoding C-terminal V5-His$_6$ epitope-tagged PreG$_N$ truncation mutants and derivative mutants thereof, the CCHFV IbAr10200 M segment was used as a template for PCR amplification of DNA fragments beginning with the M segment start codon and ending with the codon of the terminal amino acid of each construct. These amplicons were also introduced into the pcDNA3.1D/V5-His TOPO expression vector. The PreG$_N$V5(961)-NST mutant, as well as all

of the $PreG_N$V5(961) internal deletion mutants, was generated by using standard overlapping PCR approaches to introduce or delete nucleotides from the template plasmid. The cloning of the M segment of CCHFV strain IbAr10200 into the pCAGGS vector was described previously (3). All plasmids were propagated in MAX Efficiency Stbl2 competent cells (Invitrogen) and then confirmed by DNA sequencing. All primer sequences are available upon request.

Antibodies. Antipeptide antisera specific to the G_N ectodomain ($_{611}$TQEGR GHVKLSRGSE$_{625}$) and to the second cytoplasmic domain of $PreG_N$ ($_{926}$STD KEIHKLHLSIC$_{939}$) from CCHFV strain IbAr10200 were generated in rabbits and affinity purified in collaboration with ProSci Inc. (Poway, CA). The anti-N monoclonal antibody 9D5-1-1A was produced by Jonathan Smith (formerly of USAMRIID) during previously described efforts to produce CCHFV-specific antibodies (3). A mouse anti-V5 monoclonal antibody (Invitrogen) was used for protein immunoblot assays, and a rabbit polyclonal serum specific to the V5 epitope was used for immunoprecipitations (16).

Transfection. For protein immunoblot analysis of cell lysates transiently transfected with pcDNA3.1 plasmids, confluent monolayers of 293T/17 cells in six-well cluster plates were first infected with vTF1.1 vaccinia virus diluted in DMEM (2.5% FBS, 1% P/S) at a multiplicity of infection (MOI) of 5 for 30 min at 37°C prior to transfection. The virus inoculum was then removed, and DMEM (10% FBS) was added to the cells. For pCAGGS vector-based expression of CCHFV glycoproteins, no vTF1.1 was needed. In both cases, the cells were transfected with 6 μg per well of each expression plasmid using Lipofectamine 2000 (Invitrogen) and then incubated for 18 to 24 h prior to subsequent analysis.

Preparation of transfected cell lysates. The cell culture medium was aspirated, and the cells were washed briefly with Dulbecco's phosphate-buffered saline (DPBS; Invitrogen) and then lysed with buffer consisting of 1% Triton X-100, 150 mM NaCl, 5 mM EDTA, 50 mM Tris-HCl pH 7.4, and Complete protease inhibitor cocktail (Roche, Indianapolis, IN) for 10 min on ice. Insoluble material was removed from the lysates by centrifugation at 20,800 × *g* for 10 min at 4°C.

Enzymatic deglycosylation of proteins. To assess the N-linked glycosylation of CCHFV glycoproteins, transfected cell lysates were incubated overnight at 37°C with PNGase F, endoglycosidase H (Endo H), or no enzyme according to the manufacturer's instructions (New England Biolabs, Beverly, MA). In order to prevent complex glycosylation of proteins in vivo prior to enzymatic deglycosylation, transfected 293T/17 cells were cultured in DMEM (10% FBS) supplemented with 1 μM deoxymannojirimycin (DMJ; Sigma, St. Louis, MO) for 20 to 22 h prior to lysing the cells.

SDS-polyacrylamide gel electrophoresis (SDS-PAGE) and immunoblotting. Protein electrophoresis was performed using the NuPAGE precast gel system (Invitrogen). Specifically, proteins were denatured under reducing conditions at 70°C for 10 min and then separated on 10% Bis-Tris gels using either morpholineethanesulfonic acid (MES) or morpholinepropanesulfonic acid (MOPS) running buffers. Protein molecular weights were estimated by comparison to Full-Range Rainbow molecular weight standards (GE Healthcare Biosciences, Piscataway, NJ). Protein gels were electroblotted onto an Immobilon-P polyvinylidene difluoride membrane (PVDF; Millipore, Billerica, MA) at 30 V for 1 h. The PVDF membranes were then incubated with blocking buffer (PBS, 5% [wt/vol] powdered milk, 0.1% [vol/vol] Tween 20, 0.1% [wt/vol] NaN_3) for 30 min at room temperature. Primary antibodies were diluted in blocking buffer and used to probe the membranes overnight at 4°C. After washing with PBST buffer (PBS, 0.2% [vol/vol] Tween 20), horseradish peroxidase-conjugated sheep anti-mouse or sheep anti-rabbit secondary antibodies (GE Healthcare Biosciences) were diluted in blocking buffer lacking NaN_3 and used to probe the membranes for an additional 1.5 h at room temperature. The secondary antibody solution was then washed away with additional PBST. Proteins were detected by chemiluminescence using the SuperSignal West Femto kit (Pierce, Rockford, IL), and the immunoblots were imaged using a LAS-1000 Plus gel documentation system (Fujifilm, Tokyo, Japan).

Metabolic radiolabeling of proteins and immunoprecipitation. To analyze the kinetics of CCHFV glycoprotein proteolytic cleavage events, pulse-chase experiments were performed. Briefly, 293T/17 cells expressing CCHFV glycoproteins were pulsed with [^{35}S]cysteine-methionine labeling medium for 15 min, washed briefly with DPBS, and then chased for the indicated time periods with complete DMEM supplemented with 15 μg/ml unlabeled cysteine and methionine. CCHFV proteins were immunoprecipitated as previously described (32) and then separated by SDS-PAGE on NuPAGE 10% Bis-Tris gels. The ^{35}S signal was enhanced with Amplify fluorographic reagent (GE Healthcare Biosciences), collected on storage phosphor screens, and detected using a Typhoon 9410 variable mode imager (GE Healthcare Biosciences). Protein bands were quantified using ImageQuant TL (GE Healthcare Biosciences). For each protein analyzed ($PreG_N$, G_N, or C-term$_{961}$), the values were normalized as percentages of the peak time point for that protein.

CCHFV infections and preparation of viral material. Confluent monolayers of 293T/17 cells in 10-cm culture dishes were infected with CCHFV IbAr10200 at an MOI of 5. At 24 h postinfection, the culture medium was collected and clarified through 0.45-μm syringe filters, Complete protease inhibitor cocktail was added, and the pH was adjusted to 8.0 with 1 M Tris. Virions were semipurified by ultracentrifugation in a Beckman model SW41Ti rotor at 30,000 rpm for 3.5 h at 4°C. Afterwards, the virion pellet was resuspended in 150 μl 1% TX-100 lysis buffer (see above). The cell monolayers were washed once with DPBS and then lysed with 1.5 ml TX-100 lysis buffer as described above. Prior to removal from BSL-3+ containment, cell and virion lysates were inactivated in NuPAGE sample buffer containing 50 mM dithiothreitol for 10 min at 70°C.

Bioinformatics analysis of CCHFV glycoprotein sequences. The transmembrane domains for CCHFV M polyproteins were predicted using the TMHMM server, version 2.0 (37) available from the Center for Biological Sequence Analysis at the Technical University of Denmark. The molecular weights of polypeptide sequences were estimated using MacVector 9.0 (Accelerys, San Diego, CA).

RESULTS

$PreG_N$ is cleaved at its C terminus. The structural glycoproteins of CCHFV are derived from the polyprotein precursor encoded by its M RNA segment through a series of endoproteolytic cleavage events. The M polyprotein is first cleaved into two intermediate precursors, $PreG_N$ and $PreG_C$, though the precise boundary between them remains poorly defined. The $PreG_N$ precursor is subject to extensive proteolytic processing, with the N-terminal mucin-like and GP38 domains being removed by furin and SKI-1-mediated proteolysis, respectively (Fig. 1). SKI-1 cleavage generates the N terminus of mature G_N at amino acid 520 (in strain IbAr10200), and a related protease is thought to cleave the N terminus of $PreG_C$ to yield a mature G_C beginning at amino acid 1041. There are four predicted transmembrane helices between the G_N and G_C ectodomains, which define two relatively large (99 and 148 amino acids, respectively) cytoplasmic loops separated by a short (14-amino-acid) lumenal domain (Fig. 1). If G_N were defined as comprising amino acids 520 to 1040, then this protein would have a predicted mass of 58 kDa, excluding posttranslational modifications. However, G_N migrates with an approximate molecular mass of 37 kDa in SDS-polyacrylamide gels, suggesting that an additional cleavage event(s) in the topologically complex region between $PreG_N$ and $PreG_C$ must occur.

To test this hypothesis, a plasmid [$PreG_N$V5(961)] was constructed that encoded amino acids 1 to 961 of the IbAr10200 M polyprotein and a C-terminal V5-His_6 cassette (Fig. 2A). This version of $PreG_N$, which included three of the four predicted transmembrane helices following the G_N ectodomain and most of the second cytoplasmic loop, was designed based upon a previous report which operationally defined $PreG_C$ as amino acids 962 to 1684 of the polyprotein (32). Additionally, by truncating $PreG_N$ prior to the $PreG_C$ signal sequence, we hoped to avoid the complication of detecting additional product(s) generated from the $PreG_N$-$PreG_C$ cleavage site.

When lysates of 293T/17 cells expressing $PreG_N$V5(961) were analyzed by SDS-PAGE followed by immunoblotting with a polyclonal antiserum specific to the G_N ectodomain, both $PreG_N$ (140 kDa) and G_N (37 kDa) species were observed, as previously reported (1). These bands were of similar apparent size to those generated from a full-length IbAr10200 M polyprotein possessing a V5-His_6 cassette at the C terminus of G_C (M [G_CV5]) (Fig. 2B), indicating that $PreG_N$ and G_N were processed similarly in these two contexts.

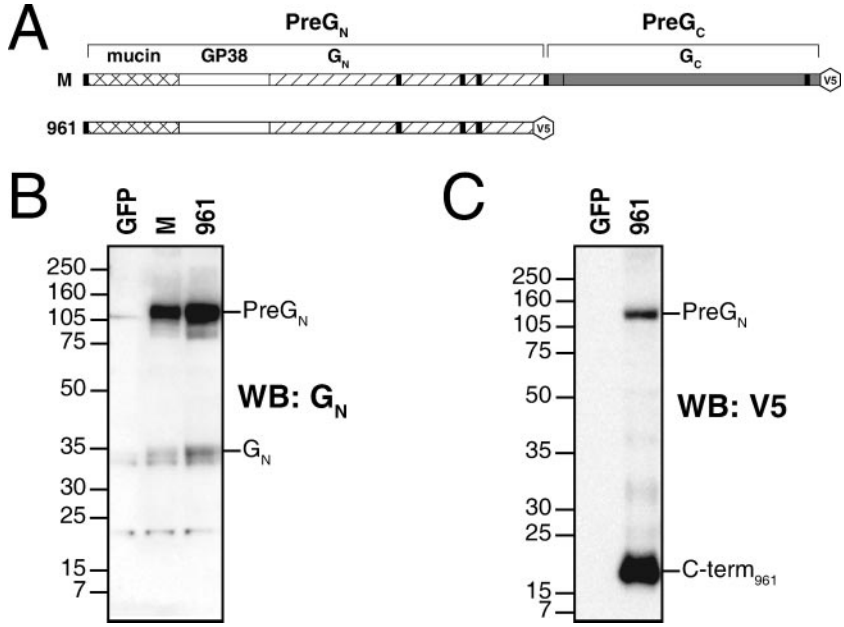

FIG. 2. PreG$_N$ is cleaved at its C terminus. (A) Schematic of CCHFV full-length M polyprotein and PreG$_N$ glycoprotein constructs. "M" and "961" refer to the constructs M[G$_C$V5] and PreG$_N$V5(961), respectively, that are described in the text. Each construct possessed a C-terminal V5-His$_6$ epitope cassette. 293T/17 cells were transfected with the indicated constructs and then cell lysates were prepared at 18 to 22 h posttransfection. A plasmid expressing green fluorescent protein (GFP) was used as a negative control. The samples were separated by SDS-PAGE using 10% Bis-Tris NuPAGE gels and MOPS-based running buffer. Proteins in cell lysates were immunoblotted with an anti-G$_N$ ectodomain polyclonal antiserum (B) or a monoclonal antibody directed against the V5 epitope tag (C). The locations of PreG$_N$, G$_N$, and the C-terminal fragment are indicated.

When a blot of the PreG$_N$V5(961) lysate was probed with an antibody specific to the C-terminal V5 epitope tag (Fig. 2C), PreG$_N$ was detected in addition to a band with a molecular mass of approximately 20 kDa, indicating that a cleavage event had occurred somewhere within the C-terminal region of PreG$_N$. Although several species greater than 20 kDa were faintly visible, the absence of these bands in the anti-G$_N$ immunoblot suggests that these are not processing intermediates. It seems more likely that these are degradation products of PreG$_N$ or aggregates of the hydrophobic C-terminal fragment. Furthermore, the lack of processing intermediates demonstrated that C-terminal cleavage occurred efficiently and prior to the N-terminal cleavage events that liberate the mucin-like and GP38 glycoproteins from G$_N$. To determine if this C-terminal cleavage event might be specific to 293T/17 cells, PreG$_N$V5(961) was expressed in additional cell lines known to support CCHFV replication (BHK, CHO-K1, HeLa, Huh-7, Vero E6, and SW-13) (15, 32, 39) (personal observations). Indeed, C-terminal cleavage of PreG$_N$ occurred efficiently in all cell lines tested (data not shown). Thus, the addition of an epitope cassette at the C terminus of PreG$_N$ allowed for the identification of a novel, C-terminal proteolytic fragment.

Chronology of PreG$_N$ processing. Although the preceding data suggested that PreG$_N$ underwent an efficient C-terminal cleavage event, they did not formally show that a precursor-product relationship exists between PreG$_N$ and the fragment. Therefore, a pulse-chase experiment was performed to investigate the kinetics with which the C-terminal fragment was generated relative to other posttranslational processing events. Cells expressing PreG$_N$V5(961) were metabolically radiolabeled with [^{35}S]cysteine-methionine for 15 min and then placed in normal growth medium with excess unlabeled cysteine and methionine for the times indicated (Fig. 3). At each time point, cell lysates were prepared, divided equally, and then immunoprecipitated using antibodies specific to either the C-terminal V5 epitope tag or to the G$_N$ ectodomain. Using either antibody, the maximum amount of PreG$_N$ was immunoprecipitated after 5 min of chase and then decreased through the chase period. As shown in Fig. 3A, the C-terminal fragment was efficiently immunoprecipitated with the V5 antiserum after metabolic labeling for as little as 10 min, indicating that this processing event begins very shortly after the synthesis of PreG$_N$, or perhaps even cotranslationally. However, C-terminal cleavage of PreG$_N$ appeared to be somewhat asynchronous, as evidenced by the fact that the fragment did not reach its peak abundance until approximately 1 hour into the chase (Fig. 3A). This variation could be due to a variety of factors, including limiting amounts of protease or asynchrony in the folding of this extensively disulfide-linked glycoprotein, both of which could be exacerbated by the levels of overexpression achieved in the vaccinia virus-T7 expression system used here. The greatest amount of mature G$_N$ was only precipitated after 3 to 4 hours (Fig. 3B), in agreement with previous reports (32, 39). Together, these data show that, in the context of this expression construct, PreG$_N$ is C-terminally cleaved shortly after its synthesis to generate the C-terminal fragment, followed by N-terminal SKI-1 cleavage to liberate G$_N$.

Interestingly, the C-terminal fragment was also precipitated with the G$_N$ ectodomain antiserum (Fig. 3B), suggesting a

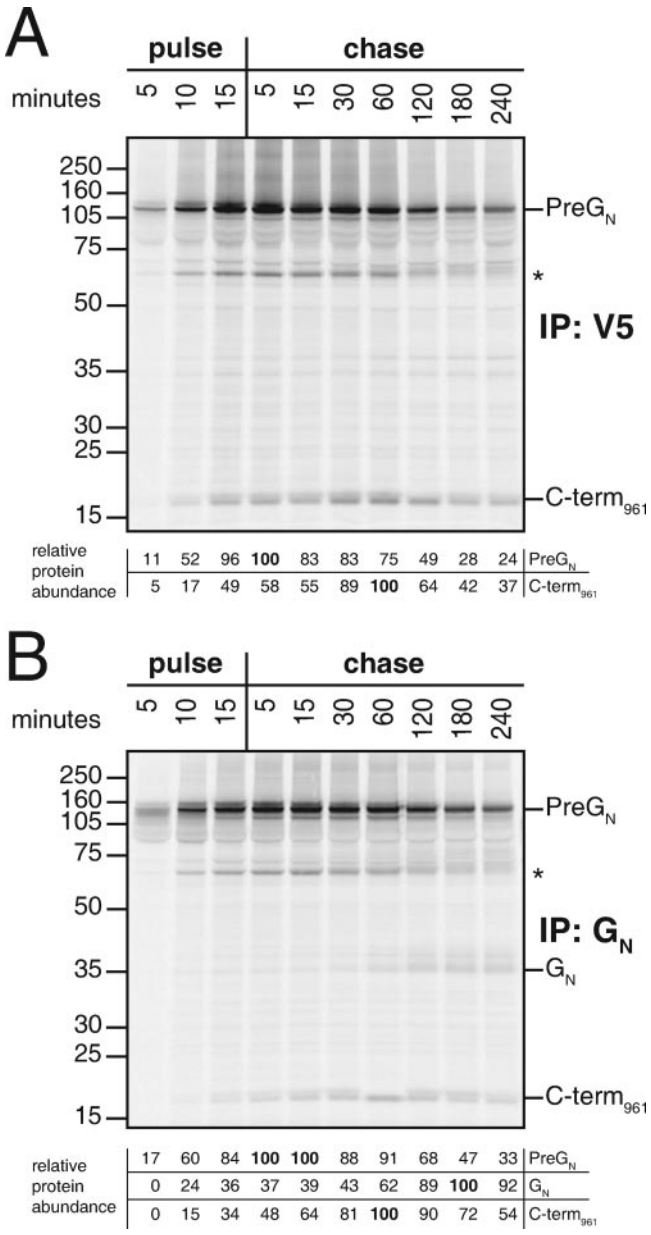

FIG. 3. Pulse-chase analysis of $PreG_N$ cleavage events. 293T/17 cells were transfected with a plasmid expressing $PreG_N$V5(961), metabolically labeled with [^{35}S]cysteine-methionine for 15 min, and then placed in normal growth medium containing excess cysteine-methionine for the times indicated at the tops of the gels. The cells were then lysed and immunoprecipitated with anti-V5 epitope polyclonal serum (A) or an anti-G_N ectodomain polyclonal serum (B). Some cells were labeled for only 5 or 10 min prior to lysis (left side of gel, as indicated). The samples were separated by SDS-PAGE using 10% Bis-Tris NuPAGE gels and MOPS-based running buffer. An asterisk indicates the location of the unidentified coprecipitating protein described in the text. The abundance of $PreG_N$, G_N, and the C-terminal fragment at each time point was determined by storage phosphor screen image analysis. Relative protein abundance represents the percentage of the maximum signal intensity obtained for each protein over the course of the experiment.

possible interaction between this protein and either $PreG_N$ or the G_N glycoprotein. Additional studies are warranted to confirm this observation. There was also a 60-kDa species that was immunoprecipitated throughout the pulse and chase periods using both antisera. The fact that this band was not detected by immunoblotting using either the V5 or G_N ectodomain antiserum (Fig. 2B and C) suggests that this is not a $PreG_N$ processing intermediate but may instead be a coimmunoprecipitating cellular protein. However, further studies will be required to identify this protein.

The C-terminal fragment traffics to the Golgi compartment. If the C-terminal fragment constituted an NS_M protein for CCHFV, then by analogy to *Orthobunyavirus* NS_M proteins (24, 28, 34) one might expect it to accumulate in the Golgi compartment, the site of virus assembly (9, 11, 23). The presence of complex N-linked glycans on glycoproteins is one indicator of transport to the Golgi compartment. Thus, to characterize the intracellular trafficking of the C-terminal fragment, we introduced an N-linked glycosylation site within the lumenal loop of $PreG_N$, which we hypothesized to be a part of the C-terminal fragment based upon amino acid mass predictions. However, since the glycosyltransferase machinery can only add N-linked sugars to sites greater than 12 to 14 amino acids away from the membrane (29), and since the predicted CCHFV lumenal domain is only 14 amino acids in length, an expression plasmid [$PreG_N$V5(961)-NST] was produced in which the lumenal loop was duplicated and an NST glycosylation sequon was inserted at the middle of the loop (Fig. 4A).

Analysis of $PreG_N$V5(961)- and $PreG_N$V5(961)-NST-transfected 293T/17 cell lysates separated by SDS-PAGE and immunoblotted with anti-V5 antibody showed that both constructs generated $PreG_N$ and C-terminal fragments (Fig. 4B, top panel). Immunoblotting with the G_N ectodomain antiserum demonstrated that the mature G_N glycoprotein was also generated in both contexts (data not shown). Untreated lysates showed that the $PreG_N$V5(961)-NST C-terminal fragment migrated more slowly than that from the parental construct. Treatment of these cell lysates with PNGase F had no effect on the parental C-terminal fragment but increased the mobility of the $PreG_N$V5(961)-NST fragment, confirming the utilization of the introduced glycosylation site. The deglycosylated $PreG_N$V5(961)-NST C-terminal fragment still migrated more slowly than the parental fragment, consistent with the increased length of the lumenal domain in the mutant. When samples were treated with Endo H, an enzyme that only removes immature N-linked carbohydrate domains, deglycosylation of the $PreG_N$V5(961)-NST C-terminal fragment was incomplete. To control for inefficient deglycosylation by Endo H, these constructs were also expressed in 293T/17 cells treated with DMJ, which prevents trimming of high-mannose sugars to more complex glycans. Incubation of DMJ-treated $PreG_N$V5(961)-NST lysates with Endo H led to complete deglycosylation of the C-terminal fragment (Fig. 4B, bottom panel). Thus, we concluded that a fraction of the $PreG_N$V5(961)-NST C-terminal fragment pool contained a complex N-linked glycan indicative of transport to the medial Golgi or beyond. Furthermore, the utilization of the introduced glycosylation site confirmed the predicted lumenal membrane topology of this domain within $PreG_N$, as well as its presence within the C-terminal fragment.

Mapping of the G_N C terminus. To more precisely define the G_N C-terminal cleavage site, a series of plasmids was constructed that encoded $PreG_N$ molecules of varying lengths truncated at their C termini and each appended with a V5-His_6

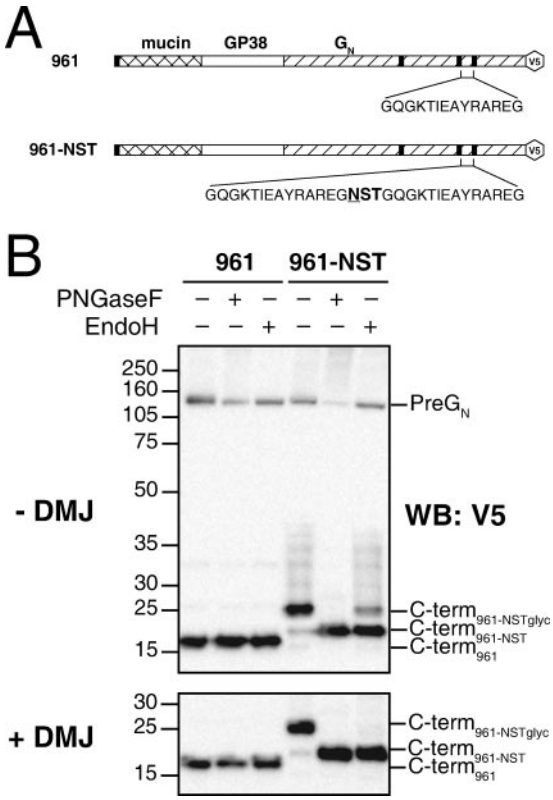

FIG. 4. Trafficking and topology of the PreG$_N$ C-terminal fragment. (A) Schematic of PreG$_N$V5 lumenal loop constructs. Using the PreG$_N$V5(961) construct as a template, the lumenal loop was duplicated and an NST glycosylation sequon was added at the junction to make PreG$_N$V5(961)-NST. Each construct possessed a C-terminal V5-His$_6$ epitope cassette. (B) 293T/17 cells were transfected with the indicated constructs and cultured in the absence (top panel) or presence (bottom panel) of 1 μM DMJ, and then cell lysates were prepared at 18 to 22 h posttransfection. The samples were then treated with PNGase F, Endo H, or mock digested as indicated prior to separation by SDS-PAGE using 10% Bis-Tris NuPAGE gels and MOPS-based running buffer. Proteins in cell lysates were immunoblotted with a monoclonal antibody directed against the V5 epitope. The locations of PreG$_N$, the C-terminal fragment of PreG$_N$V5(961) (C-term$_{961}$), and the deglycosylated (C-term$_{961\text{-}NST}$) and glycosylated (C-term$_{961\text{-}NSTglyc}$) C-terminal fragments of PreG$_N$V5(961)-NST are indicated.

epitope cassette (Fig. 5A). These plasmids were transiently transfected into 293T/17 cells, and the expressed proteins were analyzed by SDS-PAGE and immunoblotting using antibodies specific to the G$_N$ ectodomain or to the V5 epitope tag. When the immunoblot was probed with the G$_N$ antiserum (Fig. 5B), PreG$_N$ species were detected in each of the lysates, but efficient processing of PreG$_N$ to mature G$_N$ was only observed from the four largest constructs, PreG$_N$V5(881) to PreG$_N$V5(1036).

When the immunoblot of these constructs was probed with an antibody to the C-terminal V5 epitope tag (Fig. 5C), PreG$_N$ species were again observed in all of the lysates. The molecular weights of these V5-reactive species varied in proportion to their total length, whereas PreG$_N$ species detected with the G$_N$ antiserum migrated more similarly (Fig. 5B). This discrepancy could reflect differences in epitope accessibility between the two antisera and that these two antisera might detect slightly different PreG$_N$ species. The V5-specific antibody also recognized C-terminal fragments of constructs PreG$_N$V5(881) and larger, though these migrated at different positions, consistent with their variable lengths. In the Bis-Tris–MOPS gel system used here, proteins smaller than 7 kDa could not be detected. To resolve proteins less than 7 kDa in size, we also employed Bis-Tris–MES and Tris-Tricine SDS-PAGE systems, which can resolve proteins as small as 2 kDa. Even with these systems, no C-terminal fragments were detected in the lysates of cells expressing the four shortest constructs. Given the predicted membrane topology of PreG$_N$V5(842) and PreG$_N$V5(856) (Fig. 1), we reasoned that C-terminal cleavage might liberate a soluble, secreted C-terminal fragment. To address this, supernatants of cells transfected with these constructs were immunoprecipitated with an anti-V5 polyclonal antiserum and then immunoblotted for the V5 epitope tag. As shown in Fig. 5D, appropriately sized C-terminal fragments of PreG$_N$V5(842) and PreG$_N$V5(856) were found in the supernatants of these cells. Together, the increasing size of C-terminal fragments generated by this panel of PreG$_N$ truncation mutants suggested that they were all generated by proteolysis at a single common cleavage site.

The PreG$_N$V5(1036) construct was unique in that two V5-reactive species were generated from PreG$_N$. Amino acid 1036 is the last residue before the RKPL cleavage motif preceding the N terminus of mature G$_C$. This motif was omitted so as to prevent proteolytic removal of the V5-His$_6$ epitope cassette. Thus, PreG$_N$V5(1036) includes some fraction of PreG$_C$, although the precise number of amino acids is unknown because the N terminus of PreG$_C$ has yet to be identified. Sanchez et al. proposed that signal peptidase might cotranslationally cleave the nascent M segment-encoded polyprotein into PreG$_N$ and PreG$_C$ during its translocation into the ER lumen (32). This cleavage site is thought to exist proximal to the fourth predicted transmembrane helix (amino acids 969 to 991) following the G$_N$ ectodomain, though no direct evidence for this location exists. The predicted mass of the polypeptide spanning residues 991 to 1036 and including the V5-His$_6$ cassette is 10.3 kDa. Thus, the smaller (<15 kDa) C-terminal fragment generated from PreG$_N$V5(1036) is appropriately sized to confirm the presence of the PreG$_N$-PreG$_C$ cleavage site within, or C-terminal to, the fourth predicted transmembrane domain.

From these data, we concluded that the first three predicted transmembrane domains following the G$_N$ ectodomain, along with their associated lumenal and cytoplasmic loops, are minimally required for efficient SKI-1 processing of PreG$_N$. Truncation beyond this point (i.e., PreG$_N$V5 856, 842, 805, and 719) resulted in proteins that did not undergo the SKI-1 cleavage event, or at least did so very inefficiently. In addition, the C-terminal cleavage event did not occur in the two shortest truncations, suggesting that cleavage occurs C-terminal to amino acid 805 of PreG$_N$.

Next, a panel of internal deletion mutants was generated based upon the PreG$_N$V5(961) vector (Fig. 6A). The goal of this approach was to delete the putative cleavage site and to prevent the generation of a C-terminal fragment. Sequential deletions of 18 to 22 amino acids were made in the first and second cytoplasmic loops (amino acids 720 to 819 and 880 to 961, respectively). Additionally, a mutant was constructed in which the lumenal loop (amino acids 843 to 856) was deleted and replaced with six glycine residues in order to maintain the

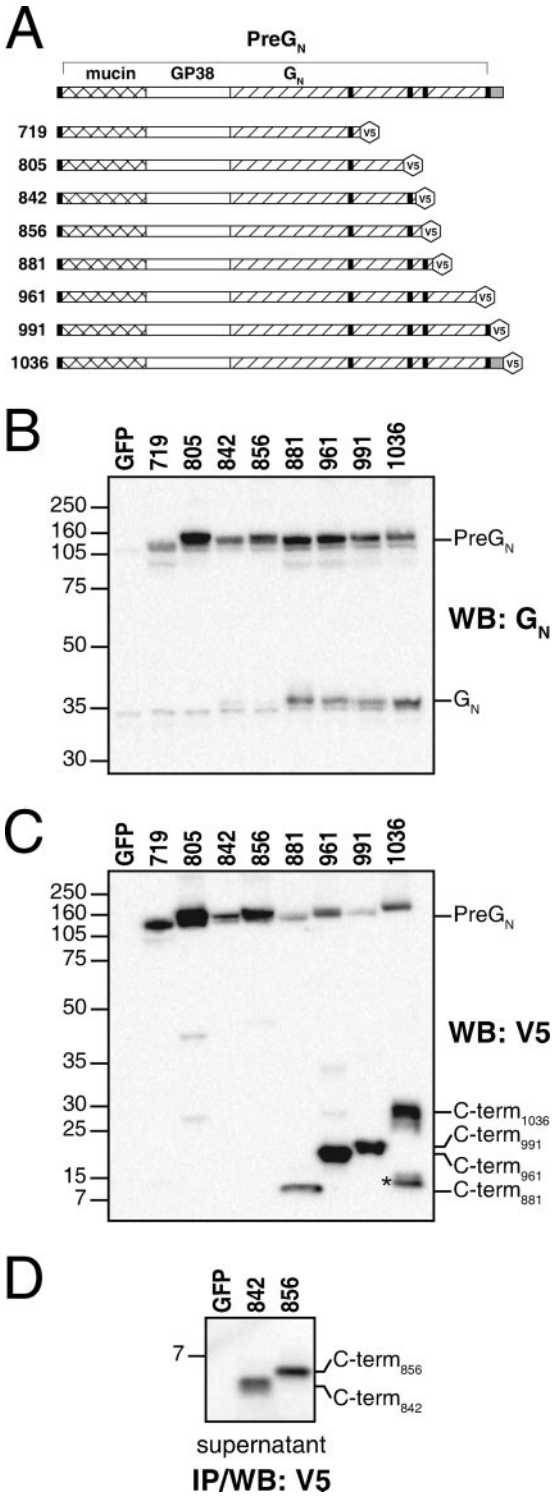

FIG. 5. PreG$_N$ truncation mutants. (A) A schematic of the PreG$_N$V5 truncation constructs is shown, with the predicted transmembrane domains indicated by black bars. The terminal amino acid for each construct (relative to the IbAr10200 M polyprotein) is indicated at the left, and each construct possessed a C-terminal V5-His$_6$ epitope cassette. 293T/17 cells were transfected with the indicated constructs or with a plasmid expressing GFP, and then cell lysates were prepared at 18 to 22 h posttransfection. The samples were separated by SDS-PAGE using 10% Bis-Tris NuPAGE gels and MOPS-based running buffer. Proteins in the cell lysates were immunoblotted with an anti-G$_N$ ectodomain polyclonal antiserum (B) or a monoclonal antibody directed against the V5 epitope (C). An asterisk indicates a putative product of PreG$_N$-PreG$_C$ cleavage in the PreG$_N$V5(1036) construct. (D) For cells transfected with PreG$_N$V5(842) and PreG$_N$V5 (856), proteins were also immunoprecipitated from the culture medium above these cells using a polyclonal antiserum directed against the V5 epitope. Afterwards, the precipitated proteins were separated by SDS-PAGE using 10% Bis-Tris NuPAGE gels and MES-based running buffer, followed by immunoblotting with a monoclonal antibody directed against the V5 epitope. The locations of PreG$_N$ and the C-terminal fragments (C-term$_{xxx}$) are indicated ("xxx" refers to the terminal amino acid of the PreG$_N$V5 truncation construct from which each fragment is derived).

protein's membrane topology. These constructs were then expressed in 293T/17 cells, separated by SDS-PAGE, and immunoblotted with the G$_N$- and V5-specific antibodies. As shown in Fig. 6B (top panel), G$_N$ generated from mutants of the first cytoplasmic loop migrated faster than G$_N$ derived from PreG$_N$V5(961), whereas G$_N$ molecules derived from the lumenal and second cytoplasmic loop deletions (Fig. 6C and D, top panels) were unaffected in comparison to PreG$_N$V5(961). Conversely, when these same constructs were immunoblotted for the V5 epitope tag at their C termini, only deletion mutants within the first cytoplasmic loop generated full-length 20-kDa C-terminal fragments (Fig. 6B, bottom panel), whereas all other deletion mutants gave rise to smaller C-terminal fragments (Fig. 6C and D, bottom panels). Despite having deletions of similar lengths in the first and second cytoplasmic loops, the migration of G$_N$ and the C-terminal fragment was not uniform among the respective panels of mutants (Fig. 6B, top panel, and D, bottom panel). Although subtle differences in the predicted masses of these proteins exist, it is more likely that these migration discrepancies are due to differences in amino acid composition or loss of posttranslational modification sites among these proteins. Nevertheless, these data indicate that the entire first cytoplasmic loop is contained within G$_N$, whereas the lumenal and second cytoplasmic loops are within the C-terminal fragment. Furthermore, since none of the deletions blocked PreG$_N$ C-terminal cleavage, the cleavage site responsible for the fragment is probably not contained within any of the loops of PreG$_N$. Rather, these results point to a cleavage event occurring within or very near to the second predicted transmembrane domain of PreG$_N$ (amino acids 820 to 842).

The CCHFV M segment encodes an NS$_M$ protein. Although the preceding set of experiments clearly demonstrated the C-terminal cleavage of PreG$_N$, the possibility remained that this fragment might in some way be an artifact of these constructs and of the expression system used. Furthermore, to confirm the hypothesis that this fragment represents a true NS$_M$ protein for CCHFV, this species would have to be detected as a product of a complete M polyprotein. To address these issues, a polyclonal antipeptide antiserum, specific to a sequence within the second cytoplasmic domain of PreG$_N$ (amino acids 926 to 939), was developed that would allow for immunoblotting of the putative NS$_M$ domain in the context of both PreG$_N$ and full-length M polyprotein constructs.

This NS$_M$ antiserum was used to probe an immunoblot of

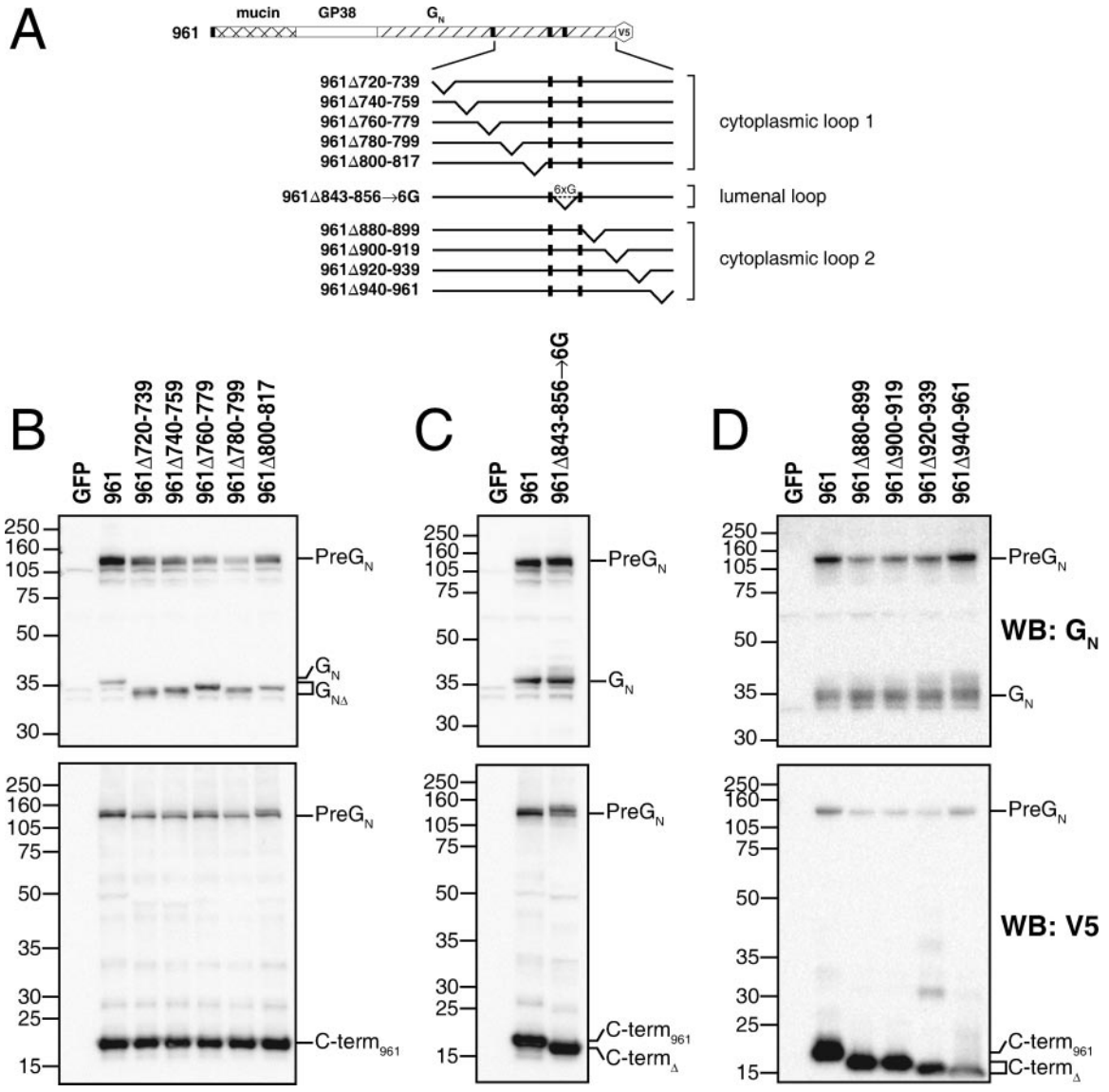

FIG. 6. PreG$_N$ internal deletion mutants. (A) A schematic of the PreG$_N$V5 internal deletion constructs is shown, with the predicted transmembrane domains indicated by black bars. Using the PreG$_N$V5(961) construct as a template, 18 to 22 amino acid deletions were made in cytoplasmic loops 1 and 2 as indicated. The lumenal loop was also deleted but then replaced with six glycines in order to maintain membrane topology of the protein. 293T/17 cells were transfected with the indicated constructs and then cell lysates were prepared at 18 to 22 h posttransfection. The samples were separated by SDS-PAGE using 10% Bis-Tris NuPAGE gels and MOPS-based running buffer. Proteins in the cell lysates were immunoblotted with anti-G$_N$ ectodomain polyclonal antiserum (B to D, top panels) or a monoclonal antibody directed against the V5 epitope (B to D, bottom panels). The locations of PreG$_N$, G$_N$, and the C-terminal fragment of PreG$_N$V5(961) are indicated. G$_N$ and C-terminal fragment species having internal deletions are indicated by G$_{N\Delta}$ and C-term$_{961\Delta}$, respectively.

293T/17 lysates expressing M[G$_C$V5], PreG$_N$V5(961), and PreG$_N$V5(1036). Using this antiserum, an approximately 15-kDa species was detected in the M[G$_C$V5] and PreG$_N$V5(1036) lysates (Fig. 7A). This species is a likely candidate for the NS$_M$ protein, as a polypeptide including all of the lumenal loop, the third transmembrane domain, and the entire second cytoplasmic loop (amino acids 843 to 968 [Fig. 1]) has a predicted molecular mass of 14 kDa. In the PreG$_N$V5(961) lysate, the NS$_M$ antiserum reacted with a 20-kDa species and, in the PreG$_N$V5(1036) lysate, a band of about 30 kDa was also detected. Based on their sizes, we concluded that these proteins were likely the PreG$_N$ C-terminal fragments previously detected by immunoblotting with the anti-V5 antibody (Fig. 5C). The increased mass of the species derived from PreG$_N$V5(961) can be explained by the presence of the V5-His$_6$ cassette encoded by the expression vector, which adds approximately 3.6 kDa to the mass of the protein. The probable C-terminal signal peptidase processing of the PreG$_N$V5(1036) C-terminal fragment likely allows for proper N- and C-terminal cleavage of the NS$_M$ such that it migrates identically to NS$_M$ derived from a complete M polyprotein. However, the presence of the 30-kDa C-terminal fragment suggests that these processing events may not occur as efficiently as in the native M polyprotein.

To demonstrate the presence of an NS$_M$ protein in the

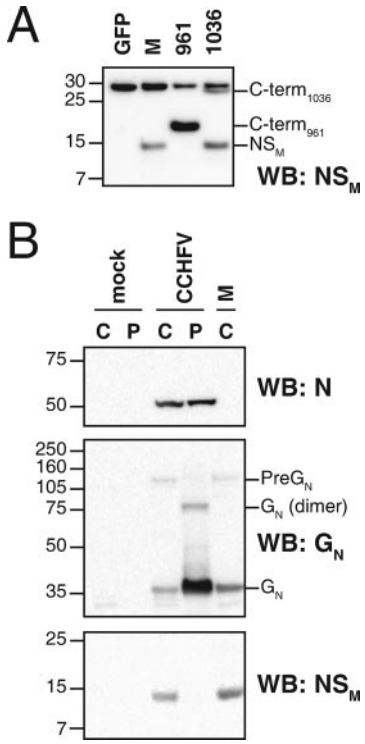

FIG. 7. Identification of an NS_M protein by transient expression and virus infection. (A) 293T/17 cells were transfected with pcDNA3.1 CCHFV glycoprotein expression constructs M[G_CV5], PreG_NV5(961), and PreG_NV5(1036). The 30-kDa band present in all lanes is background, as it was also present in the GFP negative control. (B) 293T/17 cells were infected with CCHFV strain IbAr10200 at an MOI of 5, and cell lysates were prepared at approximately 24 h postinfection. In parallel, cells were also mock infected or transfected with a pCAGGS plasmid expressing the IbAr10200 M segment. Infected and mock culture supernatants were clarified and overlaid on a 20% sucrose–PBS cushion, and virions were semipurified by ultracentrifugation. C, cell lysate; P, virion pellet. The samples for panels A and B were separated by SDS-PAGE using 10% Bis-Tris NuPAGE gels and either MES-based (NS_M) or MOPS-based (N, G_N) running buffers. Proteins in cell and virion lysates were immunoblotted with anti-NS_M cytoplasmic loop polyclonal antiserum (A and B, top panels), anti-N monoclonal antibody 9D5-1-1A (B, top panel), or anti-G_N ectodomain polyclonal antiserum (B, middle panel).

context of CCHFV infection, 293T/17 cells were infected with CCHFV strain IbAr10200 and then cellular lysates were prepared at 24 h postinfection. Additionally, virions released into the culture supernatant were semipurified by ultracentrifugation through a 20% sucrose cushion. When these lysates were separated by SDS-PAGE and immunoblotted using an anti-N monoclonal antibody (Fig. 7B, top panel), the nucleoprotein was detected specifically in the CCHFV-infected lysate and in the virion pellet. Similarly, G_N was present in infected lysates and in virion pellets, as well as in cells transiently expressing the IbAr10200 M segment. PreG_N was detected only in the cell lysates and not in the virion pellet, confirming that the virion pellet was relatively free of cell-associated viral proteins such as the glycoprotein precursors. Interestingly, an approximately 80-kDa band was detected in addition to monomeric G_N in the virion pellet. We assumed that this larger species was an oligomeric form of G_N, as suggested by a previous study (31).

When these lysates were immunoblotted using the NS_M antiserum, NS_M was detected specifically in CCHFV-infected cell lysates. The virus-derived NS_M migrated at the same molecular weight as plasmid-derived NS_M. No NS_M band was detected in the virion lysates, suggesting that this protein is nonstructural. However, this result does not exclude the possibility that NS_M is incorporated into virions in such low abundance that it is undetectable using this immunoblotting system. In summary, these data provide the first direct evidence for a CCHFV-encoded NS_M protein as a product of C-terminal proteolytic cleavage of PreG_N.

DISCUSSION

In addition to the G_N and G_C glycoproteins, the M RNA genome segment of viruses in some genera within the *Bunyaviridae* family encodes a nonstructural (NS_M) protein by a variety of different strategies. The plant-infecting viruses of the *Tospovirus* genus employ an ambisense coding strategy to encode an NS_M protein in the M segment viral RNA (21, 25), while the phleboviruses Rift Valley fever virus (RVFV), Punta Toro virus, and Toscana virus encode NS_M proteins in the same open reading frame as the viral glycoproteins (7, 8, 20). The NS_M proteins of orthobunyaviruses are encoded between G_N and G_C and are liberated by endoproteolysis of the M segment-encoded polyprotein (10, 14). With regards to function, the NS_M protein of the tospovirus Tomato spotted wilt virus acts as a viral movement protein early during infection, enabling viral nucleocapsids to be transported through plasmodesmata prior to assembly of viral particles (22, 36, 38). For the phleboviruses and orthobunyaviruses, however, relatively little is known about the function of their NS_M proteins. The RVFV NS_M1 protein can be coimmunoprecipitated with the G_C glycoprotein, though NS_M-deficient RVFV replicates in cultured mammalian cells with no apparent growth defects (19, 43). For *Orthobunyavirus* genus members, the NS_M proteins are known to traffic to the Golgi compartment, where they may interact with the glycoproteins and nucleoprotein (34). A Maguari virus mutant lacking the C-terminal two-thirds of the NS_M was still viable (30). However, for Bunyamwera virus (BUNV), it was impossible to rescue viruses lacking the entire NS_M or having deletions within the N-terminal regions, suggesting a role for the NS_M in viral assembly (34). No NS_M proteins have been identified for members of the *Hantavirus* and *Nairovirus* genera.

The M polyproteins of nairoviruses possess four predicted transmembrane domains in the region between the ectodomains of the G_N and G_C glycoproteins (Fig. 1). We introduced an N-linked glycosylation site in the lumenal loop that is predicted to exist between the second and third putative transmembrane segments. The fact that this site was glycosylated, in addition to a recent report (13) showing that an N-linked glycosylation site within the G_N ectodomain was utilized, but that a site within the first cytoplasmic loop was not, confirms the topology of this domain, making it identical to that found in the M polyproteins of orthobunyaviruses (34). In addition to a shared topology, we found that this domain is also subject to endoproteolysis, releasing a previously unidentified integral membrane protein whose size is similar to that of the NS_M proteins of the orthobunyaviruses (10, 17).

If the integral membrane protein liberated from the C-terminal region of $PreG_N$ constituted an NS_M protein that was relevant for CCHFV biology, we predict that it would exhibit several characteristics. First, it should be generated through proteolytic cleavage at a defined site, utilizing a protease(s) common to its mammalian and arthropod hosts. Second, an NS_M protein should have a reasonable half-life and perhaps be targeted to the Golgi in a manner analogous to the NS_M protein of the orthobunyaviruses (24, 28, 34). Third, an NS_M protein would likely be absent from virus particles or exist in very low abundance, as there is no evidence from previous studies with semipurified virions to suggest the presence of additional proteins (31, 32, 39).

We found that the novel protein described here fulfilled all three of these criteria, and we therefore conclude that it constitutes an NS_M protein. We identified NS_M in cells infected with CCHFV but could not detect NS_M in partially purified virus preparations. Further, the NS_M protein was produced in a number of mammalian cell lines known to support CCHFV replication, and an extensive panel of $PreG_N$ mutants all suggested that cleavage occurs at a common site. It will be interesting to test if this event also occurs in cell lines derived from ticks, the primary vector for CCHFV. Pulse-chase analysis confirmed that $PreG_N$ C-terminal cleavage occurred efficiently, shortly after its synthesis or cotranslationally, and prior to N-terminal cleavage of the G_N ectodomain.

Utilization of a glycosylation site introduced within the lumenal loop of NS_M confirmed the topology of this domain relative to the membrane. The partial Endo H resistance of the C-terminal fragment in this mutant provided evidence that at least a fraction of the NS_M protein pool traffics to the Golgi compartment, in agreement with data obtained with the NS_M protein of BUNV (24, 28, 34). However, further studies are warranted to examine the trafficking of the CCHFV NS_M when expressed alone or in the context of a complete M segment. If the NS_M possesses its own Golgi targeting signal, then it may contribute to targeting of G_N and G_C to the Golgi or retention therein. Although the NS_M of BUNV could not rescue Golgi localization of G_C (24), when NS_M was deleted from the M polyprotein, the acquisition of Endo H-resistant glycans on G_C was much less efficient, suggesting that NS_M may play a role in maturation of BUNV glycoproteins (35). In this study, deletion of the entire NS_M cytoplasmic domain from $PreG_N$ did not impair SKI-1 cleavage of the G_N ectodomain, but further truncation of $PreG_N$ prevented efficient processing by SKI-1 [Fig. 5, compare $PreG_N$V5(719–856) with 881]. These data suggest that the lumenal loop and third transmembrane domain contained within the NS_M may play a critical role in G_N maturation. Additional studies will be required to test this hypothesis in the context of the M polyprotein.

Perhaps because of its multiple membrane-spanning domains, we have been unable to purify NS_M in sufficient quantity or purity to identify its N-terminal residue. However, using a panel of $PreG_N$ truncation and internal deletion mutants, G_N was defined to include the entire first cytoplasmic loop of $PreG_N$, whereas NS_M was determined to include the lumenal domain and second cytoplasmic loop. Thus, the second predicted transmembrane helix (TM 2) following the G_N ectodomain (amino acids 820 to 842) appears to be a likely candidate for the $PreG_N$-NS_M cleavage site. Interestingly, alignment of the five predicted transmembrane domains of CCHFV with their cognate domains in the Dugbe virus polyprotein showed that TM 2 shared 56% identity between these viruses, whereas the other transmembrane domains were much less conserved (18 to 34% identity). The C-terminal portion of TM 2, which immediately precedes the lumenal domain of NS_M, contains the sequence SxSPVQSAP. Its perfect conservation in CCHFV isolates suggests that it may be a possible cleavage motif. Most of these residues are also conserved within the second transmembrane domain of the M polyprotein of Dugbe virus, suggesting a more generalized role for this domain in the processing of nairovirus M polyproteins. Within this motif, there are a number of serine and proline residues, which are known to disfavor helix formation in lipid membranes (26). The transmembrane helix substrates of intramembrane cleaving proteases (I-CLiPs), such as site 2 protease, Rhomboid, and signal peptide peptidase, often possess helix-breaking residues, which may loosen the helix sufficiently for these I-CLiPs to gain access to the polypeptide backbone (42). Together, these data suggest a role for I-CLiPs in the processing of CCHFV $PreG_N$, and efforts are currently under way to address this hypothesis.

Ideally, the function of the NS_M protein would best be addressed in the context of infections with recombinant CCHFV lacking the NS_M or possessing mutations within it, as has been recently done for BUNV (34), Maguari virus (30), and RVFV (19, 43). Although a reverse genetics system exists for CCHFV (15), it requires superinfection with wild-type CCHFV to drive expression of plasmid-based minigenomes. Refinement of this system to allow rescue of virus solely from plasmids would greatly benefit the study of CCHFV proteins in vitro and in vivo. In the meantime, it may be possible to engineer mutant NS_M proteins and to supply them during wild-type CCHFV infection in hopes of mediating a transdominant effect against the virus.

In summary, this report provides the first direct evidence of an NS_M protein for a *Nairovirus*. Further study of the CCHFV-encoded NS_M and the proteases involved in its generation may lead to better understanding of CCHFV assembly events, development of attenuated CCHFV vaccines, or inhibitors of CCHFV replication.

ACKNOWLEDGMENTS

L.A. thanks Aura Garrison, Wendy Grace, Kristin Spik, and the members of the Schmaljohn and Paragas laboratories for training and excellent technical assistance while using BSL-3+ facilities at USAMRIID. Donald Pijak, Val Hardy, and other members of the Doms laboratory provided invaluable support throughout this work. We also thank Stuart Nichol, Martin Vincent, and Eric Bergeron at the CDC for providing reagents and helpful discussions.

This work was funded by Department of Defense Peer Reviewed Medical Research Program grant PRMRP PR033269. L.A. and A.B.-C. were supported in part by NIH T32 AI055400.

REFERENCES

1. **Ahmed, A. A., J. M. McFalls, C. Hoffmann, C. M. Filone, S. M. Stewart, J. Paragas, S. Khodjaev, D. Shermukhamedova, C. S. Schmaljohn, R. W. Doms, and A. Bertolotti-Ciarlet.** 2005. Presence of broadly reactive and group-specific neutralizing epitopes on newly described isolates of Crimean-Congo hemorrhagic fever virus. J. Gen. Virol. **86:**3327–3336.
2. **Alexander, W. A., B. Moss, and T. R. Fuerst.** 1992. Regulated expression of foreign genes in vaccinia virus under the control of bacteriophage T7 RNA polymerase and the *Escherichia coli lac* repressor. J. Virol. **66:**2934–2942.
3. **Bertolotti-Ciarlet, A., J. Smith, K. Strecker, J. Paragas, L. A. Altamura, J. M. McFalls, N. Frias-Staheli, A. Garcia-Sastre, C. S. Schmaljohn, and**

R. W. Doms. 2005. Cellular localization and antigenic characterization of Crimean-Congo hemorrhagic fever virus glycoproteins. J. Virol. **79:**6152–6161.
4. **Cash, P.** 1985. Polypeptide synthesis of Dugbe virus, a member of the Nairovirus genus of the Bunyaviridae. J. Gen. Virol. **66:**141–148.
5. **Clerx, J. P., and D. H. Bishop.** 1981. Qalyub virus, a member of the newly proposed Nairovirus genus (Bunyavividae). Virology **108:**361–372.
6. **Clerx, J. P., J. Casals, and D. H. Bishop.** 1981. Structural characteristics of nairoviruses (genus Nairovirus, Bunyaviridae). J. Gen. Virol. **55:**165–178.
7. **Collett, M. S., A. F. Purchio, K. Keegan, S. Frazier, W. Hays, D. K. Anderson, M. D. Parker, C. Schmaljohn, J. Schmidt, and J. M. Dalrymple.** 1985. Complete nucleotide sequence of the M RNA segment of Rift Valley fever virus. Virology **144:**228–245.
8. **Di Bonito, P., S. Mochi, M. C. Gro, D. Fortini, and C. Giorgi.** 1997. Organization of the M genomic segment of Toscana phlebovirus. J. Gen. Virol. **78:**77–81.
9. **Donets, M. A., M. P. Chumakov, M. B. Korolev, and S. G. Rubin.** 1977. Physicochemical characteristics, morphology and morphogenesis of virions of the causative agent of Crimean hemorrhagic fever. Intervirology **8:**294–308.
10. **Elliott, R. M.** 1985. Identification of nonstructural proteins encoded by viruses of the Bunyamwera serogroup (family Bunyaviridae). Virology **143:**119–126.
11. **Ellis, D. S., T. Southee, G. Lloyd, G. S. Platt, N. Jones, S. Stamford, E. T. Bowen, and D. I. Simpson.** 1981. Congo/Crimean haemorrhagic fever virus from Iraq 1979. I. Morphology in BHK21 cells. Arch. Virol. **70:**189–198.
12. **Ergonul, O.** 2006. Crimean-Congo haemorrhagic fever. Lancet Infect. Dis. **6:**203–214.
13. **Erickson, B. R., V. Deyde, A. J. Sanchez, M. J. Vincent, and S. T. Nichol.** 2007. N-linked glycosylation of Gn (but not Gc) is important for Crimean Congo hemorrhagic fever virus glycoprotein localization and transport. Virology **361:**348–355.
14. **Fazakerley, J. K., F. Gonzalez-Scarano, J. Strickler, B. Dietzschold, F. Karush, and N. Nathanson.** 1988. Organization of the middle RNA segment of snowshoe hare Bunyavirus. Virology **167:**422–432.
15. **Flick, R., K. Flick, H. Feldmann, and F. Elgh.** 2003. Reverse genetics for Crimean-Congo hemorrhagic fever virus. J. Virol. **77:**5997–6006.
16. **Fortna, R. R., A. S. Crystal, V. A. Morais, D. S. Pijak, V. M. Lee, and R. W. Doms.** 2004. Membrane topology and nicastrin-enhanced endoproteolysis of APH-1, a component of the gamma-secretase complex. J. Biol. Chem. **279:**3685–3693.
17. **Fuller, F., and D. H. Bishop.** 1982. Identification of virus-coded nonstructural polypeptides in bunyavirus-infected cells. J. Virol. **41:**643–648.
18. **Garry, C. E., and R. F. Garry.** 2004. Proteomics computational analyses suggest that the carboxyl terminal glycoproteins of Bunyaviruses are class II viral fusion protein (beta-penetrenes). Theor. Biol. Med. Model. **1:**10.
19. **Gerrard, S. R., B. H. Bird, C. G. Albarino, and S. T. Nichol.** 2007. The NSm proteins of Rift Valley fever virus are dispensable for maturation, replication and infection. Virology **359:**459–465.
20. **Ihara, T., J. Smith, J. M. Dalrymple, and D. H. Bishop.** 1985. Complete sequences of the glycoproteins and M RNA of Punta Toro phlebovirus compared to those of Rift Valley fever virus. Virology **144:**246–259.
21. **Kormelink, R., P. de Haan, C. Meurs, D. Peters, and R. Goldbach.** 1993. The nucleotide sequence of the M RNA segment of tomato spotted wilt virus, a bunyavirus with two ambisense RNA segments. J. Gen. Virol. **74:**790.
22. **Kormelink, R., M. Storms, J. Van Lent, D. Peters, and R. Goldbach.** 1994. Expression and subcellular location of the NSM protein of tomato spotted wilt virus (TSWV), a putative viral movement protein. Virology **200:**56–65.
23. **Korolev, M. B., M. A. Donets, S. G. Rubin, and M. P. Chumakov.** 1976. Morphology and morphogenesis of Crimean hemorrhagic fever virus. Arch. Virol. **50:**169–172.
24. **Lappin, D. F., G. W. Nakitare, J. W. Palfreyman, and R. M. Elliott.** 1994. Localization of Bunyamwera bunyavirus G1 glycoprotein to the Golgi requires association with G2 but not with NSm. J. Gen. Virol. **75:**3441–3451.
25. **Law, M. D., J. Speck, and J. W. Moyer.** 1992. The M RNA of impatiens necrotic spot Tospovirus (Bunyaviridae) has an ambisense genomic organization. Virology **188:**732–741.
26. **Li, S. C., and C. M. Deber.** 1994. A measure of helical propensity for amino acids in membrane environments. Nat. Struct. Biol. **1:**368–373.
27. **Marriott, A. C., A. A. el-Ghorr, and P. A. Nuttall.** 1992. Dugbe Nairovirus M RNA: nucleotide sequence and coding strategy. Virology **190:**606–615.
28. **Nakitare, G. W., and R. M. Elliott.** 1993. Expression of the Bunyamwera virus M genome segment and intracellular localization of NSm. Virology **195:**511–520.
29. **Nilsson, I. M., and G. von Heijne.** 1993. Determination of the distance between the oligosaccharyltransferase active site and the endoplasmic reticulum membrane. J. Biol. Chem. **268:**5798–5801.
30. **Pollitt, E., J. Zhao, P. Muscat, and R. M. Elliott.** 2006. Characterization of Maguari orthobunyavirus mutants suggests the nonstructural protein NSm is not essential for growth in tissue culture. Virology **348:**224–232.
31. **Sanchez, A. J., M. J. Vincent, B. R. Erickson, and S. T. Nichol.** 2006. Crimean-Congo hemorrhagic fever virus glycoprotein precursor is cleaved by furin-like and SKI-1 proteases to generate a novel 38-kilodalton glycoprotein. J. Virol. **80:**514–525.
32. **Sanchez, A. J., M. J. Vincent, and S. T. Nichol.** 2002. Characterization of the glycoproteins of Crimean-Congo hemorrhagic fever virus. J. Virol. **76:**7263–7275.
33. **Schmaljohn, C. S., and J. W. Hooper.** 2001. *Bunyaviridae*: the viruses and their replication, p. 1581–1602. *In* D. M. Knipe and P. M. Howley (ed.), Fields virology, 2nd ed. Lippincott Williams & Wilkins, Philadelphia, PA.
34. **Shi, X., A. Kohl, V. H. Leonard, P. Li, A. McLees, and R. M. Elliott.** 2006. Requirement of the N-terminal region of orthobunyavirus nonstructural protein NSm for virus assembly and morphogenesis. J. Virol. **80:**8089–8099.
35. **Shi, X., D. F. Lappin, and R. M. Elliott.** 2004. Mapping the Golgi targeting and retention signal of Bunyamwera virus glycoproteins. J. Virol. **78:**10793–10802.
36. **Soellick, T., J. F. Uhrig, G. L. Bucher, J. W. Kellmann, and P. H. Schreier.** 2000. The movement protein NSm of tomato spotted wilt tospovirus (TSWV): RNA binding, interaction with the TSWV N protein, and identification of interacting plant proteins. Proc. Natl. Acad. Sci. USA **97:**2373–2378.
37. **Sonnhammer, E. L. L., G. von Heijne, and A. Krogh.** 1998. A hidden Markov model for predicting transmembrane helices in protein sequences, p. 175–182. *In* J. Glasgow, T. Littlejohn, F. Major, R. Lathrop, D. Sankoff, and C. Sensen (ed.), Proceedings of the Sixth International Conference on Intelligent Systems for Molecular Biology. AAAI Press, Menlo Park, CA.
38. **Storms, M. M., R. Kormelink, D. Peters, J. W. Van Lent, and R. W. Goldbach.** 1995. The nonstructural NSm protein of tomato spotted wilt virus induces tubular structures in plant and insect cells. Virology **214:**485–493.
39. **Vincent, M. J., A. J. Sanchez, B. R. Erickson, A. Basak, M. Chretien, N. G. Seidah, and S. T. Nichol.** 2003. Crimean-Congo hemorrhagic fever virus glycoprotein proteolytic processing by subtilase SKI-1. J. Virol. **77:**8640–8649.
40. **Watret, G. E., and R. M. Elliott.** 1985. The proteins and RNAs specified by Clo Mor virus, a Scottish nairovirus. J. Gen. Virol. **66:**2513–2516.
41. **Watret, G. E., C. R. Pringle, and R. M. Elliott.** 1985. Synthesis of bunyavirus-specific proteins in a continuous cell line (XTC-2) derived from Xenopus laevis. J. Gen. Virol. **66:**473–482.
42. **Wolfe, M. S., and R. Kopan.** 2004. Intramembrane proteolysis: theme and variations. Science **305:**1119–1123.
43. **Won, S., T. Ikegami, C. J. Peters, and S. Makino.** 2006. NSm and 78-kilodalton proteins of Rift Valley fever virus are nonessential for viral replication in cell culture. J. Virol. **80:**8274–8278.

Cell Host & Microbe
Article

Ovarian Tumor Domain-Containing Viral Proteases Evade Ubiquitin- and ISG15-Dependent Innate Immune Responses

Natalia Frias-Staheli,[1,12] Nadia V. Giannakopoulos,[4,12] Marjolein Kikkert,[6] Shannon L. Taylor,[7] Anne Bridgen,[8] Jason Paragas,[9] Juergen A. Richt,[10] Raymond R. Rowland,[11] Connie S. Schmaljohn,[7] Deborah J. Lenschow,[4,5] Eric J. Snijder,[6] Adolfo García-Sastre,[1,2,3,*] and Herbert Whiting Virgin IV[4,*]
[1]Department of Microbiology
[2]Department of Medicine, Division of Infectious Diseases
[3]Emerging Pathogens Institute
Mount Sinai School of Medicine, New York, NY 10029, USA
[4]Department of Pathology and Immunology, Department of Molecular Microbiology
[5]Department of Medicine
Washington University School of Medicine, St. Louis, MO 63110, USA
[6]Molecular Virology Laboratory, Department of Medical Microbiology, Center of Infectious Diseases,
Leiden University Medical Center, LUMC, P.O. Box 9600, 2300 RC Leiden, The Netherlands
[7]United States Army Medical Research Institute for Infectious Diseases, Fort Detrick, MD 21702, USA
[8]Department of Biomedical Sciences, University of Ulster, Cromore Road, Coleraine BT52 1SA, UK
[9]Emerging Viral Pathogens Section, National Institute of Allergy and Infectious Diseases,
National Institutes of Health, Bethesda, MD 20892, USA
[10]National Animal Disease Center-ARS-USDA, Ames, IA 50010, USA
[11]Diagnostic Medicine and Pathobiology, Kansas State University, Manhattan, KS 66506, USA
[12]These authors contributed equally to this work.
*Correspondence: adolfo.garcia-sastre@mssm.edu (A.G.-S.), virgin@wustl.edu (H.W.V.)
DOI 10.1016/j.chom.2007.09.014

SUMMARY

Ubiquitin (Ub) and interferon-stimulated gene product 15 (ISG15) reversibly conjugate to proteins and mediate important innate antiviral responses. The ovarian tumor (OTU) domain represents a superfamily of predicted proteases found in eukaryotic, bacterial, and viral proteins, some of which have Ub-deconjugating activity. We show that the OTU domain-containing proteases from nairoviruses and arteriviruses, two unrelated groups of RNA viruses, hydrolyze Ub and ISG15 from cellular target proteins. This broad activity contrasts with the target specificity of known mammalian OTU domain-containing proteins. Expression of a viral OTU domain-containing protein antagonizes the antiviral effects of ISG15 and enhances susceptibility to Sindbis virus infection in vivo. We also show that viral OTU domain-containing proteases inhibit NF-κB-dependent signaling. Thus, the deconjugating activity of viral OTU proteases represents a unique viral strategy to inhibit Ub- and ISG15-dependent antiviral pathways.

INTRODUCTION

Viruses have evolved a panoply of different mechanisms to subvert cellular processes to their own advantage. In particular, viruses must overcome the potent antiviral and inflammatory effects of innate immune cytokines such as type I interferon (IFNαβ) and tumor necrosis factor alpha (TNFα). The induction and activity of these antiviral cytokines is controlled by, among other factors, Ub and Ub-like (UBL) molecules (Kirkin and Dikic, 2007). The activation of the transcriptional regulator nuclear factor-κB (NF-κB) by TNFα was one of the first immune regulatory pathways found to be dependent on protein ubiquitination (Karin and Ben-Neriah, 2000). NF-κB is sequestered in the cytoplasm of unstimulated cells through binding to IκB. TNFα binding to its receptor induces IκB phosphorylation followed by K^{48}-linked poly-ubiquitination targeting IκB for proteasomal degradation. This releases NF-κB dimers for translocation to the nucleus, where they regulate transcription. NF-κB-induced genes include type I IFN and other cytokines, hence this Ub-controlled pathway plays a vital role in innate and adaptive immunity, as well as in inflammation (Tergaonkar, 2006). In addition to ubiquitination of IκB, K^{63}- and K^{48}-linked ubiquitination regulates other molecules involved in this signaling pathway (Chen, 2005).

ISG15 is an interferon-induced UBL molecule with important antiviral activity against Sindbis, herpes simplex, influenza A, and influenza B viruses (Lenschow et al., 2007). ISG15, like Ub, is covalently conjugated to target proteins via a C-terminal LRLRGG sequence (Haas et al., 1987; Loeb and Haas, 1992; Narasimhan et al., 1996). Although conjugation is critical for the antiviral activity of ISG15 (Lenschow et al., 2005, 2007), the mechanism by which ISG15 mediates its antiviral function is not completely understood.

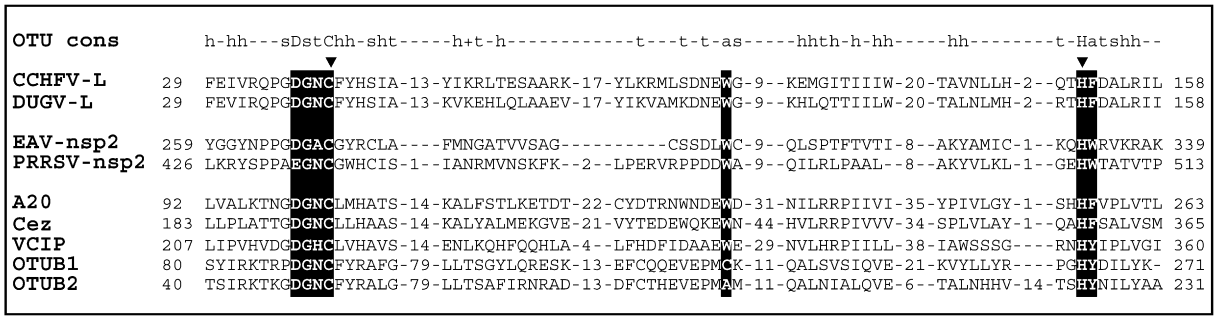

Figure 1. The OTU Domain Sequence Is Conserved across Viral and Mammalian Proteins

Multiple alignment of the OTU domains present in the proteins used in this study. In the consensus (Makarova et al., 2000), "h" indicates hydrophobic residues (A, C, F, L, I, M, V, W, Y, T, S, G), "s" indicates small residues (A, C, S, T, D, V, G, P), "+" indicates positively charged residues (R, K), "a" indicates aromatic residues (W, Y, F, H), and "t" indicates residues with high β-turn-forming propensity (A, C, S, T, D, E, N, V, G, P). Highly conserved residues are shaded in black. Numbers at the beginning and end of each sequence indicate the positions of the first and last aligned residue in the respective protein sequences; the numbers between aligned blocks indicate the numbers of residues that are not shown. CCHFV, Crimean Congo hemorrhagic fever virus; DUGV, Dugbe virus; EAV, equine arteritis virus; PRRSV, porcine respiratory and reproductive syndrome virus; VCIP, VCIP135; Cez, Cezanne; OTUB1 and OTUB2, Otubains 1 and 2, respectively.

Ub and ISG15 are synthesized as inactive precursors with C-terminal extensions that undergo cleavage to reveal the motif required for conjugation. Coordinated activities of an enzymatic cascade comprising an activating enzyme (E1), a conjugating enzyme (E2) and a ligase (E3) result in the conjugation of Ub or ISG15 to the ε-amino group of a lysine residue present in the target protein. Both Ub and ISG15 conjugation can be reversed by the activity of deconjugating enzymes. Deubiquitinating (DUB) proteolytic enzymes are also involved in processing of Ub precursors. Five classes of DUBs have been described (Nijman et al., 2005); one of the most recently identified is the ovarian tumor (OTU) domain family. This family comprises a group of putative cysteine proteases, homologous to the OTU protein in *Drosophila*, and includes more than a hundred proteins from eukaryotes, bacteria, and viruses (Makarova et al., 2000). Several OTU domain-containing mammalian proteins, such as Cezanne (Evans et al., 2003), Otubain 1 and 2 (Balakirev et al., 2003), and A20 (Evans et al., 2004) have been identified as proteases that participate in substrate-specific deubiquitinating processes. For example, A20 is an important downregulator of TNFα signaling via its deubiquitination of TRAF6 (Boone et al., 2004) and its dual function of poly-Ub^{63} deconjugation followed by poly-Ub^{48} modification of RIP (Wertz et al., 2004). These activities are mediated by its N-terminal OTU domain and its C-terminal zinc finger domain, respectively. However, the substrate specificity and physiologic role of most OTU domain-containing proteins remains unknown.

As protein ubiquitination and ISGylation are both important for innate immunity, rely on terminal LRLRGG sequences, and share a common mechanism of conjugation, we tested the hypothesis that viral OTU domain-containing proteases regulate Ub- and ISG15-dependent innate immunity via deconjugating protease activity. We found that two unrelated families of RNA viruses express OTU domain-containing proteases with the capacity to decrease Ub and ISG15 conjugation. Nairoviruses are negative-sense, segmented, RNA viruses of the *Bunyaviridae* family. Their large (L) protein contains an OTU domain and an RNA polymerase domain, placing this protein in the growing category of multifunctional viral proteins. Crimean Congo hemorrhagic fever virus (CCHFV) is a human nairovirus that causes hemorrhagic fever with up to 30% mortality (Whitehouse, 2004). Arteriviruses, including equine arteritis virus (EAV) and porcine respiratory and reproductive syndrome virus (PRRSV), are the causative agents of important diseases in horses and pigs. They are positive-sense, nonsegmented RNA viruses that contain an OTU domain within their nonstructural protein 2 (nsp2), which is also involved in viral replicase polyprotein processing (Snijder et al., 1995). We found that these viral OTU domains, in contrast to known mammalian OTU proteases, display a broad deconjugating activity toward ubiquitinated and ISGylated products and consequently inhibit innate immunity pathways that are dependent on Ub and ISG15. Thus, the deconjugating activity of viral OTU domains represents a unique strategy used by nairoviruses and arteriviruses to evade the host antiviral response, probably by targeting a common biochemical structure in Ub and the UBL protein ISG15.

RESULTS

OTU Domains in Viral and Mammalian Proteins

Sequencing of the L gene of the highly pathogenic human virus CCHFV (NFS and AGS, data not shown) (Honig et al., 2004; Kinsella et al., 2004) led to the identification of an OTU domain in the N-terminal region of the viral protein (Figure 1). This domain was also present in the L proteins of the nairoviruses Dugbe virus (DUGV) and Nairobi sheep disease virus (Honig et al., 2004) but has not been found in the L proteins of any other genus in the *Bunyaviridae*

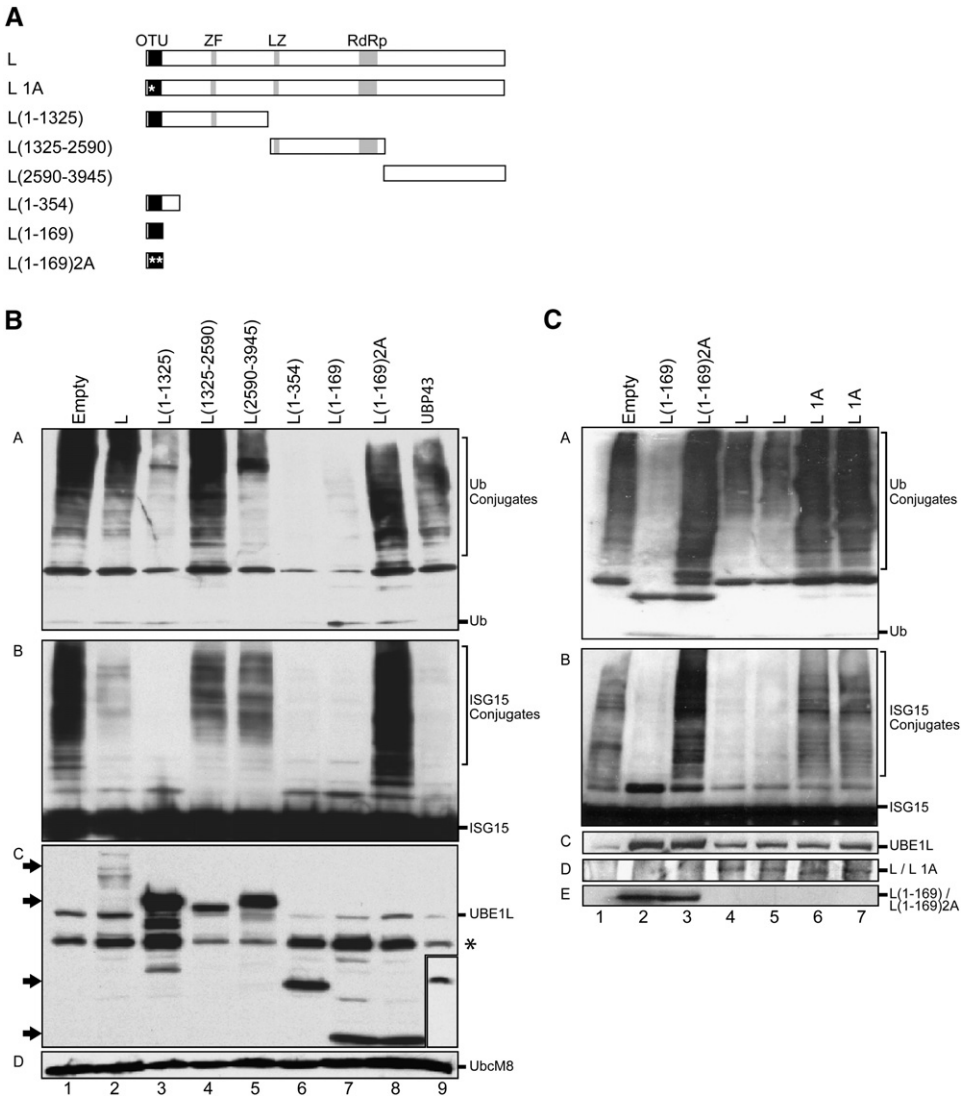

Figure 2. Levels of Ubiquitinated and ISGylated Proteins in Cells Expressing CCHFV-L and CCHFV-L Mutants

(A) Schematic representation of the CCHFV-L constructs utilized in these studies. Predicted protein domains within the protein: OTU domain; ZF, zinc finger; LZ, leucine zipper; RdRp, RNA-dependent RNA polymerase conserved motifs. White stars represent mutations in the OTU domain: 1A (C40A) or 2A (C40A and H151A). All constructs were HA tagged.

(B) 293T cells were transfected with either HA-Ub (panel A) or His-ISG15, HA-mUBE1L, and Flag-UbcM8 (panels B–D) along with HA-tagged CCHFV-L constructs, Flag-UBP43, or empty plasmid. Total protein ubiquitination was visualized by immunoblotting with anti-HA (panel A), and protein ISGylation was visualized by anti-ISG15 immunoblot (panel B). ISG15-transfected samples were also probed with anti-HA or anti-Flag (panels C and D) for detection of the CCHFV-L constructs (left arrows), mUbE1L, UBP43 (inset), and UbcM8. Asterisk indicates a nonspecific band.

(C) L and L 1A were analyzed for their effect on total ubiquitination (panel A) or ISGylation (panel B) as described in (B). Expression of HA-tagged UBE1L (panel C), L and L 1A (panel D), and L(1–169) and L(1–169)2A (panel E) is shown.

family. An alignment of the OTU domains present in nairoviruses, arteriviruses, and mammalian proteins A20, Cezanne, VCIP135, Otubain 1, and Otubain 2 revealed limited identity; however, a strong conservation of D^{37}, G^{38}, N^{39}, C^{40}, W^{71}, H^{151}, and an aromatic amino acid at position 152 (numbering based on the CCHFV-L sequence) was observed (Figure 1, black boxes). Among these amino acids, C^{40} and H^{151} (Figure 1, black arrows) were predicted to be the catalytic residues present in the putative protease active site (Balakirev et al., 2003; Makarova et al., 2000; Nanao et al., 2004; Snijder et al., 1995).

Impact of CCHFV-L Expression on Protein Ubiquitination and ISGylation

Given that host OTU domain proteins have deubiquitinating activity (Nijman et al., 2005), we tested the hypothesis that the L protein of CCHFV (CCHFV-L) has deubiquitinating and deISGylating activity (Figure 2). Transfection of

cells with plasmids expressing CCHFV-L slightly decreased the overall expression of Ub-conjugated proteins (Figure 2B, lanes 1 and 2, panel A; Figure 2C, lanes 1, 4, and 5, panel A). To test the effect of CCHFV-L expression on protein ISGylation, ISG15 conjugates were generated by transfecting plasmids expressing ISG15 and its specific E1 (UBE1L) (Yuan and Krug, 2001) and E2 (UbcM8) (Kim et al., 2004; Zhao et al., 2004) enzymes, since endogenous levels of ISGylated proteins are low in the absence of IFN stimulation. Cotransfection of CCHFV-L resulted in a clear decrease in the level of ISGylated proteins (Figure 2B, lanes 1 and 2, panel B; Figure 2C, lanes 1, 4, and 5, panel B). This decrease was also observed when CCHFV-L was untagged (data not shown). The decrease in total ISGylation was comparable to the effect of UBP43, a known ISG15 deconjugating enzyme (Figure 2B, lane 9, panel B). Expression of CCHFV-L did not affect levels of expression of UBE1L or UbcM8 (Figure 2B, lane 2, panels C and D; Figure 2C, lanes 4 and 5, panel C), consistent with CCHFV-L acting via inhibition of ubiquitination and ISGylation reactions or by directly deubiquitinating or deISGylating proteins.

The OTU Domain of CCHFV-L Decreases the Levels of Ubiquitinated and ISGylated Proteins

To determine the region of the L protein responsible for decreasing ubiquitinated and ISGylated proteins, plasmids expressing three portions of the L protein were constructed (Figure 2A). Expression of the OTU domain-containing N-terminal portion, L(1–1325), resulted in the greatest decrease of Ub and ISG15 conjugates (Figure 2B, lane 3, panels A and B). To further map this region, truncation mutants of the L protein expressing only the first 354, L(1–354), or 169 amino acids, L(1–169), were tested. The results indicated that the region responsible for the decreased levels of Ub and ISG15 conjugates mapped to the OTU domain, L-(1–169) (Figure 2B, lanes 6 and 7, panels A and B; Figure 2C, lane 2, panels A and B).

The Predicted Protease Active Site of the CCHFV-L OTU Domain Is Required for Reducing Ub and ISG15 Conjugates

To test whether the amino acids C^{40} and H^{151} (Figure 1, black arrows) were critical for the observed reduction in ubiquitinated and ISGylated proteins by the CCHFV-L OTU domain, we expressed a full-length L protein with a C^{40} to A^{40} mutation (L 1A) and a mutant L(1–169) protein in which both amino acids were replaced by alanines [L(1–169)2A] (Figure 2A). Expression of L 1A and L(1–169)2A proteins did not decrease levels of ubiquitinated or ISGylated proteins (Figure 2B, lane 8, panels A and B; Figure 2C, lanes 3, 6, and 7, panels A and B), strongly suggesting that the OTU domain contains a cysteine protease activity that mediates the decrease in ubiquitinated and ISGylated proteins.

The OTU Domain of CCHFV-L Is a Deconjugating Enzyme with Specificity for Poly-Ub Conjugates and ISG15

To determine whether the CCHFV-L OTU domain directly deconjugates Ub and ISG15 from target proteins, we expressed and purified L(1–169) and a catalytic C^{40} to A^{40} mutant, L(1–169)1A, for in vitro deconjugation assays (Figure 3A). Recombinant L(1–169) cleaved both K^{48}- and K^{63}-linked poly-Ub chains into monomers (Figure 3B, lanes 2 to 5), similarly to isopeptidase T, a known DUB enzyme (Figure 3B, lane 10). This activity was markedly decreased by mutating the amino acid C^{40} (Figure 3B, lanes 6 to 9), indicating that this residue is required for optimal protease activity. The small amount of deconjugation observed with L(1–169)1A is not unexpected, as mutation of Cezanne's catalytic cysteine yielded similar data where most, but not all, catalytic activity was impaired (Evans et al., 2003). This result shows that the OTU domain of CCHFV-L has bona fide DUB activity in the absence of other cellular proteins.

We next determined whether L(1–169) can deconjugate ISGylated proteins. For this, we generated cell lysates from IFNβ-treated *Ubp43*$^{-/-}$ murine embryonic fibroblasts (MEFs) that are rich in ISG15 conjugates (Malakhov et al., 2003). Incubation of these lysates with recombinant L(1–169) protein, but not L(1–169)1A, appreciably decreased ISGylated proteins (Figure 3C, top panel) in a L(1–169) concentration-dependent manner. This result suggests that the CCHFV OTU domain has C^{40}-dependent ISG15 deconjugating activity but does not exclude the possibility that the protease activity of the viral OTU domain was activating another deISGylating enzyme present in cell lysates. To address this possibility, we enriched 6xHisISG15 conjugates using affinity chromatography. Incubation of ISG15 conjugates with increasing amounts of L(1–169) resulted in ISG15 deconjugation (Figure 3C, lanes 2 to 5, bottom panel). No deconjugation was detected with the mutant L(1–169)1A protein (Figure 3C, lanes 6 to 9, bottom panel). In addition, L(1–169) processed a pro-ISG15 protein into its mature form (Figure 3E, lane 2, panel A). These data suggest that the CCHFV-L OTU domain directly deconjugates ISGylated proteins through its predicted cysteine protease activity.

To gain further insights on the specificity of the OTU domain, we assessed the ability of L(1–169) and L(1–169)1A to hydrolyze poly-SUMO-2 (Figure 3D, top panel) and poly-SUMO-3 chains (Figure 3D, bottom panel), pro-SUMO-1 (Figure 3E, panel C), and pro-Nedd8 (Figure 3E, panel B). While the catalytic domain of SENP2 ($SENP2_{CD}$), a SUMO-specific protease, could hydrolyze SUMO chains to monomers (Figure 3D, lane 10) and process pro-SUMO-1 (Figure 3E, lane 5, panel C), neither L(1–169) nor L(1–169)1A was able to cleave SUMO chains or a pro-SUMO-1 precursor. However, similar to its ability to process pro-ISG15 (Figure 3E, lane 2, panel A), L(1–169) hydrolyzed pro-Nedd8 into a mature form (Figure 3E, lane 2, panel B). In summary, the OTU domain of CCHFV-L hydrolyzes Ub and ISG15, but not SUMO-2 or SUMO-3,

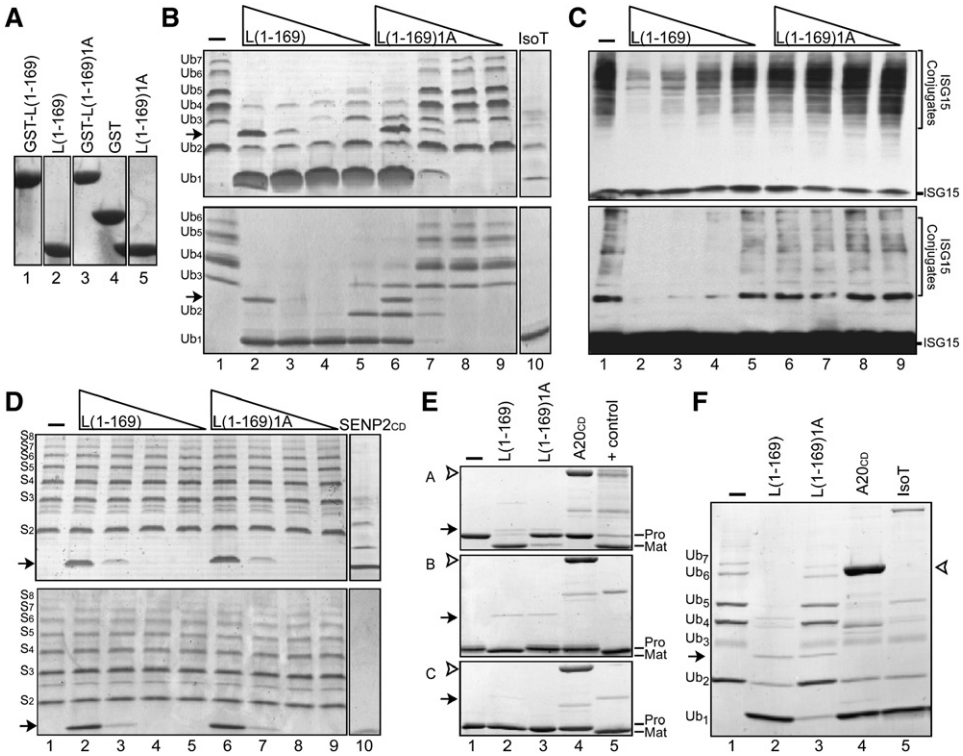

Figure 3. In Vitro Ub and ISG15 Deconjugation Activities of the CCHFV-L OTU Domain

(A) Coomassie-stained gel of GST-L(1–169), L(1–169), GST-L(1–169)1A, and L(1–169)1A recombinant proteins. L(1–169) and L(1–169)1A proteins were used for the in vitro experiments.

(B) K^{48} (top panel)- or K^{63} (bottom panel)-linked poly-Ub chains were incubated with reaction buffer (lane 1) or 10-fold dilutions of L(1–169) or L(1–169)1A recombinant proteins, subjected to SDS-PAGE and visualized by Coomassie staining. Isopeptidase T (IsoT) was used as a positive control. Black arrows indicate L(1–169) and L(1–169)1A proteins.

(C) Lysates of *Ubp43*$^{-/-}$ MEFs (top panel) or ISG15 conjugates purified from ISG15, HA-mUBE1L, and Flag-UbcM8 transfected 293T cells (bottom panel) were incubated with reaction buffer (lane 1) or 10-fold dilutions of L(1–169) or L(1–169)1A protein. ISG15 conjugates were visualized by anti-ISG15 immunoblot.

(D) SUMO-2 (top panel) or SUMO-3 (bottom panel) chains were incubated with reaction buffer (lane 1) or 10-fold dilutions of L(1–169) or L(1–169)1A and visualized by Coomassie staining. His_6-$SENP2_{CD}$ was used as a positive control. Black arrows indicate L(1–169) and L(1–169)1A proteins. S_{2-8} indicates number of SUMO-2 or SUMO-3 molecules.

(E and F) ProISG15 (panel A), proNedd8 (panel B), proSUMO-1 (panel C) or K^{48}-linked Ub (F) chains were incubated with reaction buffer, L(1–169), L(1–169)1A, or A20 catalytic domain ($A20_{CD}$) and visualized by Coomassie staining. Positive controls indicate incubation with UBP43 (panel A), NEDP1 (panel B), $SENP2_{CD}$ (panel C), or IsoT (F). Black arrows indicate L(1–169) and L(1–169)1A proteins, and white arrowhead indicates $A20_{CD}$. "Pro" indicates the pro-UBL molecule form, and "Mat" indicates the mature protein.

from conjugates in vitro, suggesting that viral OTU domains have the unique ability to recognize Ub and specific UBL molecules.

Additional Viral OTU Domains Mediate Deubiquitination and DeISGylation

In addition to CCHFV, viral OTU domains are found in the L proteins of other nairoviruses and in the nsp2 proteins of arteriviruses such as EAV and PRRSV (Figure 1). The arterivirus nsp2 cysteine protease cleaves the nsp2/nsp3 site within the large viral polyprotein during replicase maturation. In the case of EAV, this process is known to be mediated by the 166 N-terminal residues of nsp2, which contains the OTU domain (Snijder et al., 1995). In our study, a slightly larger N-terminal EAV-nsp2 domain (175 amino acids; nsp2N) was used in addition to the full-length protein. The OTU domain of the L protein of DUGV, a nairovirus related to CCHFV, as well as EAV-nsp2, EAV-nsp2N, and PRRSV-nsp2, decreased Ub and ISG15 conjugates when expressed in 293T cells (Figure 4A, lanes 3–6), indicating that deconjugation may be an immune evasion strategy shared by diverse viral families.

Previous studies have demonstrated that the OTU domain-containing mammalian proteins Otubain 1, Otubain 2, Cezanne, VCIP135, and A20 cleave poly-Ub chains in vitro (Balakirev et al., 2003; Evans et al., 2003, 2004; Wang et al., 2004). In contrast, only overexpression of Otubain 1 and Cezanne moderately decreased cellular global Ub conjugate levels, while expression of A20 or Otubain 2 had no effect on total levels of ubiquitinated proteins (Balakirev et al., 2003; Evans et al., 2003, 2004). To date, there have been no published studies investigating the effects of these proteins on ISG15 conjugates. We therefore tested Otubain 1, Otubain 2, Cezanne, VCIP135, and A20 for their

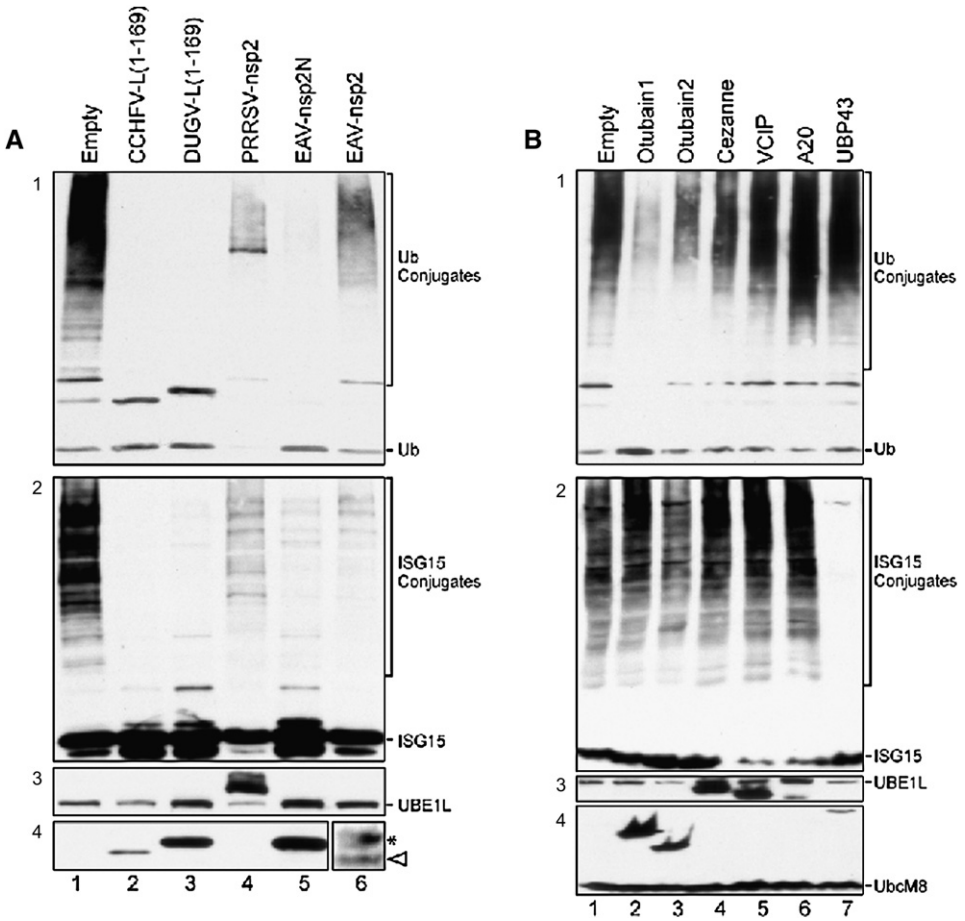

Figure 4. Ub and ISG15 Deconjugation Activity of OTU Domain-Containing Polypeptides of Viral and Mammalian Origin

(A) CCHFV-L(1–169), DUGV-L(1–169), PPRSV-nsp2, EAV-nsp2N, or EAV-nsp2 were cotransfected into 293T cells with either HA-Ub (panel 1) or ISG15, HA-mUBE1L, Flag-UbcM8, and Herc5 plasmids (panels 2 and 3). Samples were immunoblotted for HA (panel 1) or ISG15 (panel 2). ISG15-transfected samples were also probed with anti-HA (panel 3) or anti-Flag plus anti-HA (panel 4) to show expression of HA-mUBE1L, PPRSV-nsp2, CCHFV-L(1–169), DUGV-L(1–169), EAV-nsp2N, or EAV-nsp2 (inset, open triangle). Asterisk indicates a nonspecific band.

(B) Otubain 1, Otubain 2, Cezanne, VCIP135, A20, or UBP43 were analyzed for their effect on total ubiquitination (panel 1) or ISGylation (panels 2–4) as described in (A). Expression of HA-tagged Cezanne and VCIP135 (panel 3) and Flag-tagged Otubain 1 and 2 and UBP43 (panel 4) is shown.

ability to decrease overall protein ubiquitination and ISGylation in transfected cells (Figure 4B). Expression of Otubain 1 resulted in a significant decrease in Ub conjugate levels, while Otubain 2 and Cezanne had a lesser effect (Figure 4B, lanes 2–4, panel 1). Consistent with their specificity for particular ubiquitinated substrates, expression of VCIP135 and A20 did not result in a decrease in overall ubiquitination. None of the OTU-containing mammalian proteins tested decreased global levels of ISG15 conjugates (Figure 4B, lanes 2–6, panel 2). Similar results were obtained when truncation mutants expressing the OTU domains of Otubain 1, Otubain 2, Cezanne, and A20 were tested (data not shown). In addition, the OTU-containing catalytic domain of A20 ($A20_{CD}$) was unable to process either ISG15 or Nedd8 (Figure 3E, lane 4, panels A and B), even though it cleaved K^{48}-linked Ub chains (Figure 3F, lane 4). By contrast, overexpression of the mammalian deISGylating enzyme UBP43 decreased overall levels of ISG15 conjugates but not Ub conjugates (Figure 4B, lane 7). Thus, viral OTU proteases appear to be unique in their ability to target both ISG15 and Ub conjugates.

Transgenic Mice Expressing CCHFV-L(1–1325) Have Increased Susceptibility to Sindbis Virus Infection

To assess the effect of expressing an OTU domain during viral infection, we generated transgenic mice expressing the CCHFV-L(1–1325) OTU domain-containing protein, which exhibits DUB and deISGylating activities (Figure 2B, lane 3). We obtained germline transgene transmission in three lines designated 1836, 1854, and 2929, and we evaluated L(1–1325) expression in both MEFs and brain lysates from these transgenic lines. MEF cells and brain tissue from 1836 transgenic mice contained detectable L(1–1325) protein, while protein expression from the 1854 and 2929 lines was either undetectable or very low (Figures 5A and 5B). We next evaluated the

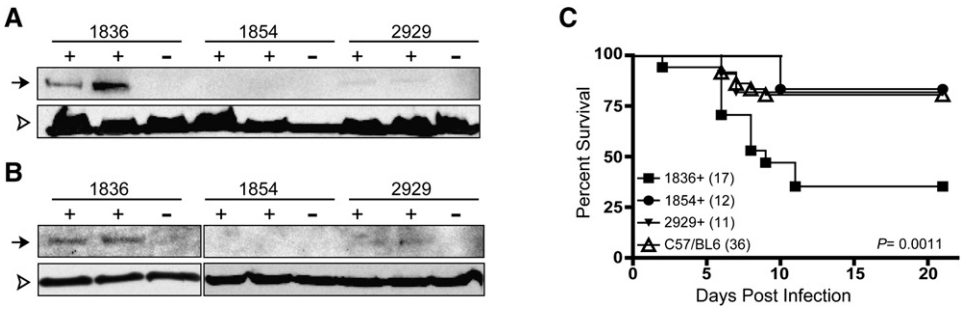

Figure 5. Expression of L(1–1325) Transgene Correlates with Increased Susceptibility to Sindbis Virus Infection

(A and B) Expression of L(1–1325) transgene and actin in MEFs (A) and brain lysates (B). + indicates a transgene-positive mouse, and − indicates a C57/BL6 mouse. The arrows indicate L(1–1325) protein and open triangles denote actin.

(C) Survival of L(1–1325) transgenic mice following infection with Sindbis virus AR86. Transgene-negative littermates from 1836, 1854, and 2929 served as C57/BL6 controls. Numbers of mice in each group are indicated in parenthesis. Comparison by statistical analysis was made between 1836+ and C57/BL6 ($p = 0.0011$).

sensitivity of L(1–1325) transgenic mice to infection with the virulent Sindbis virus strain AR86, an alphavirus that causes lethal encephalitis in young mice and is sensitive to ISG15-mediated antiviral effects (Lenschow et al., 2005). Susceptibility to Sindbis virus infection tracked with expression of the L(1–1325) protein (Figure 5C). Thirty-five percent of mice from the 1836 transgenic line survived infection compared to ≥80% survival in C57/BL6 littermate controls or transgenic mice expressing low or undetectable levels of transgene-encoded protein. The decreased survival of line 1836 transgenic mice following AR86 infection suggests that CCHFV-L OTU enhances susceptibility to viral disease in vivo.

The OTU Domain of CCHFV Overcomes ISG15-Mediated Protection from Sindbis Virus-Induced Lethality

The increased pathogenicity of Sindbis virus observed in L(1–1325)-expressing mice suggested that the CCHFV-L OTU domain might counteract the antiviral activities of ISG15 in vivo. It was previously shown that expression of ISG15 from the chimeric Sindbis virus dsTE12Q protects adult *IFNαβR*$^{-/-}$ mice from Sindbis virus-induced lethality (Lenschow et al., 2005). To determine whether expression of the CCHFV-L OTU domain would antagonize this protective effect of ISG15, we engineered four recombinant chimeric Sindbis viruses (Figure 6A). Two viruses expressed ISG15 followed by an IRES element to drive translation of either L(1–169) (169GG) or enzymatically inactive L(1–169)2A (MTGG). We also generated control viruses that expressed either L(1–169) (169) or L(1–169)2A (MT) in the absence of ISG15.

The recombinant viruses expressed the OTU domains and ISG15 as expected (Figures S1A and S1B in the Supplemental Data available with this article online) as well as similar levels of Sindbis virus proteins in infected cells (Figure S1C). All four viruses grew with similar kinetics to similar final titers under single-step growth conditions in BHK-21 cells (Figure S2). This is expected, as to date ISG15 has only demonstrated antiviral activity in vivo.

We assessed the ability of the L(1–169) protein expressed from within the Sindbis virus genome to deISGylate and deubiquitinate proteins by infecting BHK-21 cells (Figure 6B). Infection with 169GG or 169, but not MTGG or MT, reduced the amount of Ub conjugates detected in cells (Figure 6B, right panel), indicating that the viral OTU domain functions as a DUB enzyme when expressed from a Sindbis virus. Following transfection with ISG15 and its E1, E2, and E3 enzymes, ISGylated proteins can be detected in BHK-21 cells (Figure 6B, lane 1, middle panel). Infection with 169GG or 169 greatly reduced ISG15 conjugates, confirming that OTU expression results in deconjugation of ISGylated proteins. When cells were transfected with the E1, E2, and E3 enzymes but not ISG15, ISG15 conjugates were observed only following MTGG infection (Figure 6B, left panel). This shows that ISG15 expressed from dsTE12Q is capable of ISGylating proteins in the presence of the relevant conjugating enzymes but that this is only seen in the presence of a catalytically inactive form of the coexpressed L(1–169) protein (Figure 6B, lane 3, left panel).

We then determined whether OTU expression could counter ISG15's in vivo antiviral effect. In order to exclude effects due to IFNαβ-stimulated genes other than ISG15, we infected *IFNαβR*$^{-/-}$ mice (Figure 6C). Seventy percent of mice infected with a virus expressing ISG15 and the mutant OTU domain (MTGG) survived, consistent with previous observations that expression of ISG15 protects mice from lethality following Sindbis virus infection (Lenschow et al., 2005). In contrast, only 20% of mice infected with a virus expressing ISG15 and a functional OTU domain (169GG) survived infection ($p = 0.0015$). These data also correlate with our in vitro data demonstrating that L(1–169), but not L(1–169)2A, can deISGylate proteins following infection (Figure 6B). Mice infected with 169 or MT died with similar kinetics, demonstrating that the expression of L(1–169) did not increase the virulence of dsTE12Q in the absence of the IFN-mediated antiviral response. The slight increase in survival between 169GG and 169 ($p < 0.0001$) or MT ($p = 0.0032$) suggests that

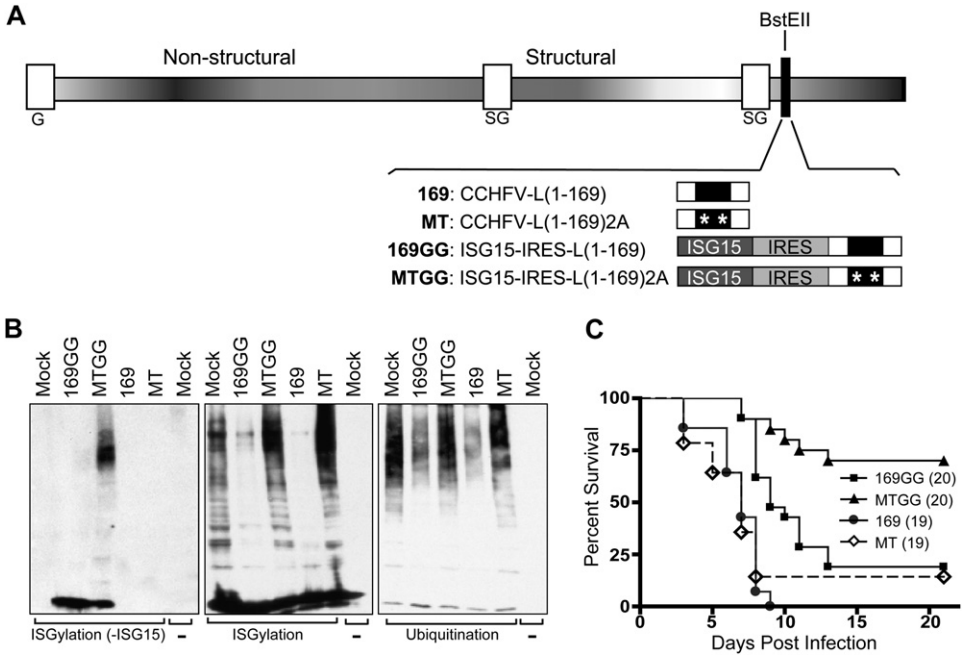

Figure 6. Sindbis Viruses Expressing the CCHFV-L OTU Domain Deconjugate Ub and ISG15 and Inhibit ISG15-Mediated Antiviral Effects in Mice

(A) Schematic diagram representing the CCHFV OTU domain-expressing Sindbis viruses utilized in these studies. G, genomic promoter; SG, subgenomic promoter.

(B) BHK-21 cells were transfected with UBE1L, UbcM8, and Herc5 (left panel), UBE1L, UbcM8, Herc5, and ISG15 (middle panel), or HA-Ub (right panel) and subsequently infected with recombinant Sindbis viruses as indicated. Cells lysates were immunoblotted with anti-ISG15 (left and middle panels) or anti-HA (right panel) antibodies. – indicates untransfected cells.

(C) *IFNαβR*$^{-/-}$ mice were infected with recombinant Sindbis viruses as indicated and monitored for survival. Data are pooled from four independent experiments, and numbers of mice in each group are indicated in parenthesis. Differences in survival were analyzed by the log-rank test: 169GG and 169 ($p < 0.0001$), 169GG and MT ($p = 0.0032$), 169GG and MTGG ($p = 0.0015$), MTGG and 169 ($p < 0.0001$), and MTGG and MT ($p < 0.0001$).

expression of the CCHFV OTU domain cannot completely antagonize the effects of ISG15 in this system. Nevertheless, these data show that expression of a catalytically active viral OTU domain can antagonize the antiviral effects of ISG15 in vivo.

Negative Regulation of the NF-κB Pathway by Viral OTU Domains

While the data above indicate that a viral OTU domain protease can counter the antiviral activities of ISG15, they do not address the possibility that the DUB activity of these proteins might also play a role in immune evasion. To address this hypothesis, we evaluated the effects of the CCHFV-L and EAV-nsp2 OTU domains on the NF-κB signaling pathway. Expression of the OTU domains of CCHFV-L and of EAV-nsp2 decreased in a dose-dependent manner the activation of an NF-κB-responsive promoter (Fujita et al., 1992) after TNFα treatment. This inhibition was similar to that mediated by A20, an OTU domain-containing inhibitor of the NF-κB pathway (Figure 7A). Inhibition was about 10-fold greater in the presence of the L(1–169) domain than the L(1–169)2A mutant, indicating a role for the OTU domain protease activity. These results were further confirmed by the ability of CCHFV-L(1–169) to inhibit NF-κB activation as measured by the inhibition of endogenous p65 nuclear translocation upon TNFα treatment (Figures 7B and 7C). The slight inhibition of NF-κB activation by the L(1–169)2A protein could be caused by some residual binding of this mutant to ubiquitinated substrates or by the presence of some other regulatory motifs within this protein. Nevertheless, the p65 nuclear translocation inhibition by the L(1–169) protein was significantly higher when compared to its mutant counterpart ($p = 0.0044$). Overall, these results demonstrate the ability of viral OTU domains to affect immune pathways that are regulated by ubiquitination.

DISCUSSION

Here we show that viral OTU domain-containing proteins are proteases that hydrolyze Ub and ISG15 from conjugated proteins. This dual deconjugating activity provide an elegant example of the economy of viral evolution, since both Ub and ISG15 rely on a conserved conjugation motif. Furthermore, the protease activity by the viral OTU domains has the physiologic capacity to evade two different cytokine pathways, IFNαβ and TNFα, that are fundamentally important for antiviral immunity.

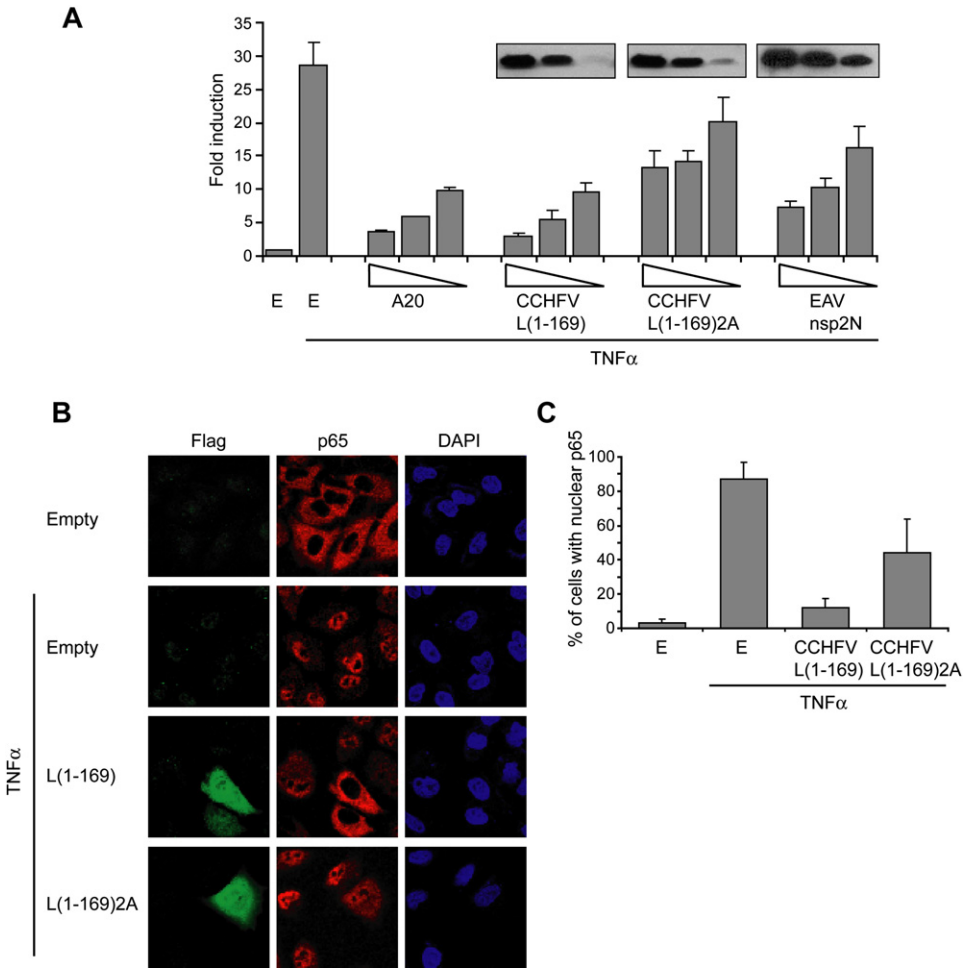

Figure 7. CCHFV-L and EAV-nsp2 OTU Domains Inhibit TNFα-Mediated NF-κB Activation

(A) NF-κB reporter assay in 293T cells transfected with OTU domains and treated with TNFα. Results shown are an average of three independent experiments. The western blot indicates expression of viral OTU proteins as detected with anti-HA [CCHFV-L(1–169) and CCHFV-L(1–169)2A] or anti-Flag antibodies (EAV-nsp2N). E, empty plasmid.

(B) A549 cells were transfected with indicated plasmids, stimulated with TNFα, and stained for p65 (red) and L(1–169) or L(1–169)2A (green). Nuclei were stained with DAPI (blue). The result shown is a representative of three independent experiments.

(C) L(1–169) or L(1–169)2A transfected cells in (B) were scored according to subcellular distribution of p65. Differences in p65 nuclear accumulation in TNFα-treated cells were analyzed by Student's t test: E and L(1–169) ($p < 0.0001$), E and L(1–169)2A ($p = 0.0007$), and L(1–169) and L(1–169)2A ($p = 0.0045$). E, empty plasmid. The result shown is a representative of three independent experiments.

Data in (A) and (C) are presented as mean ± SD (n = 3).

Viral DUB and DeISGylating Enzymes: A Unique Strategy for Immune Evasion?

Biochemical and genetic evidence supports the concept that protein ubiquitination plays a critical role in the induction of both the innate and the adaptive cellular immune system (Liu et al., 2005). For example, in addition to NF-κB signaling, Ub regulates several aspects of antiviral immunity, such as MHC class I and II antigen presentation (Loureiro and Ploegh, 2006; Shin et al., 2006), TLR/IL1 signaling (Chen, 2005), and induction of type I IFN by the cellular viral sensor RIGI (Gack et al., 2007). Inhibition of protein ubiquitination might also affect other cellular processes that can be subverted by viruses for their own advantage, such as the proteasome-mediated protein degradation system, multiple signal transduction events, or cell cycle progression. Given the effects that we observed on NF-κB signaling, it seems likely that viral OTU domain-containing proteases may be able to target these and other Ub-dependent pathways.

While the biochemical effects of ISGylation have been studied far less extensively than those of Ub, ISG15 is an important antiviral protein (Lenschow et al., 2005, 2007; Okumura et al., 2006). Thus, it is not surprising that viruses may use multiple strategies to counter the antiviral effects of ISG15. The work presented here provides a viral strategy for decreasing expression of bona fide ISG15 conjugates in cells. The first such strategy reported is the direct association of the NS1 protein of influenza B virus with ISG15. This association inhibits protein ISGylation by blocking the ISG15-UBE1L interaction (Yuan et al., 2002; Yuan

and Krug, 2001), while the viral OTU domain proteases analyzed here accomplish a similar effect via deconjugation.

The Ub and ISG15 deconjugation activities by the viral OTU domains contrast with the specific Ub deconjugation activity by the OTU domain-containing cellular proteins tested in this study. We speculate that other viral proteases, perhaps including some that do not have OTU domains, will be found to target both Ub- and ISG15-dependent processes. To date, viral DUB activities and in vitro cleavage of ISG15 fusion proteins have been demonstrated for the adenoviral protease adenain (Balakirev et al., 2002) and the papain-like proteases from the severe acute respiratory syndrome coronavirus (SARS-CoV) (Barretto et al., 2005; Lindner et al., 2005; Ratia et al., 2006).

OTU Domain Specificity and Deconjugating Activity, a Target for Antiviral Drug Development?

We found that the CCHFV-L OTU domain processed Ub and ISG15 conjugates and pro-ISG15 and pro-Nedd8 in vitro but did not have activity against any SUMO isoforms. Ub, ISG15, and Nedd8 differ from SUMO in their exposed C-terminal motifs: LRLRGG for Ub and ISG15 and LALRGG for Nedd8 versus QQQTGG for SUMO-2 and SUMO-3. This raises the interesting possibility that sequences similar to the LRLRGG motif may play an important role in substrate recognition and specific cleavage by CCHFV-L OTU and perhaps other viral proteases. Interestingly, the nsp2 of arteriviruses cleaves the nsp2/3 junction at FRLIGG (EAV) or GRLLGG (PRSSV) (Allende et al., 1999; Snijder et al., 1996; Ziebuhr et al., 2000), sequences similar to the LRLRGG motif. Thus, arterivirus OTU proteases have dual functions: performing essential viral polyprotein processing and targeting host substrates to modulate the antiviral response. This is analogous to the hepatitis C virus NS3-4A protease, which is involved both in viral polyprotein processing and in cleaving the cellular antiviral proteins TRIF and IPS-1 (Li et al., 2005; Lin et al., 2006).

The characterization of the CCHFV-L OTU domain and the development of in vitro assays for its enzymatic activities as described in this study will make it feasible to screen for potential inhibitors specific for CCHFV-L and other OTU domain-containing viral proteins. High-throughput screening of chemical compound libraries has proven to be a valuable tool in the identification of small-molecule inhibitors of other viral proteases such as HCV-NS3-4A (Sudo et al., 2005) and SARS-3CLpro (Blanchard et al., 2004). Since the viral OTU domains have a unique capacity to target both Ub and ISG15 conjugates, the design of specific inhibitors might be possible. For this reason, structural studies will be of great value to understand both the molecular basis of the unique biochemical activities of these viral proteins and the potential for development of antiviral compounds.

Physiologic Importance of Viral OTU Domain Protease DUB and DeISGylating Activities

Our demonstration that viral OTU domain-containing proteases can decrease both Ub and ISG15 conjugates in cells does not alone constitute proof that protease activity directed toward these substrates plays a role in viral infection. We were limited in performing the obvious experiment of assessing the role of viral OTU domain protease activity during infection by two things. First, CCHFV is a biosafety level 4 pathogen lacking a good animal model and whose molecular biology is not well enough developed to allow generation of mutant viruses. Second, the viral OTU domain proteases evaluated here either have, or are likely to have, important effects on processing of viral polyproteins (see above). Given this, we felt that it would be difficult to prove that these proteases have effects during infection that are solely attributable to their DUB and deISGylating activities. However, in transgenic mice, recombinant chimeric Sindbis viruses, and transfected cells, we found that viral OTU domain-containing proteases have significant effects on Ub- and ISG15-dependent host processes of known importance for innate immunity. We therefore conclude that these proteins have bona fide immune evasion properties. It will be interesting to further investigate the activities of these and other viral proteases that target Ub- and ISG15-dependent processes during viral infection.

EXPERIMENTAL PROCEDURES

Expression Plasmids

Plasmids pCAGGS-6HismISG15, pCAGGS-hUBE1L-HA, pFLAGCMV2-UbcM8, and pcDNA3.1-UbcM8 were provided by Dong-Er Zhang (Scripps Research Institute, La Jolla, CA) (Giannakopoulos et al., 2005). Herc5 was provided by Motoaki Ohtsubo (Kurume University, Fukuoka-ken, Japan). pcDNA 3.1^{+}-HA-Ub was provided by Dr. Domenico Tortorella (Mount Sinai School of Medicine, NY) (Treier et al., 1994). Peak10-Flag-A20 plasmid was provided by Dr. Adrian Ting (Mount Sinai School of Medicine). The construction of all other plasmids is described in the Supplemental Experimental Procedures.

Antibodies

Antibodies against Flag (M2 and rabbit polyclonal, Sigma, St. Louis, MO), HA (HA.7 [Sigma] HA.11 [Covance Research, Berkeley, CA]), Ub (P4D1, Cell Signaling, Danvers, MA,) NF-κB p65 (F-6, Santa Cruz Biotech, Santa Cruz, CA), and actin (AC-74, Sigma) were used following manufacturer's protocol. Anti-mouse ISG15 monoclonal (3C2 and 2D12) and polyclonal antibodies (Lenschow et al., 2005) and antiserum recognizing EAV-nsp2 (Snijder et al., 1994) have been previously described.

Purification of CCHFV L(1–169) from *E. coli*

BL-21 cells (Stratagene, La Jolla, CA) were transformed with pGEX-L(1–169) or pGEX-L(1–169)1A CCHFV, cultured to an OD_{600} of 0.6 in 2xYT medium and induced for 6 hr at 30°C with 0.1 mM IPTG. Bacteria were resuspended in lysis buffer (50 mM Tris-HCl, 5 mM EDTA, 1 mM DTT, 200 mM NaCl, and 0.1% NP-40), and purification of the GST fusion proteins was performed using GSH Sepharose resin (Amersham) according to the manufacturer's protocol. GST was cleaved using PreScission Protease (Pharmacia, Uppsala, Sweden) in cleavage buffer (50 mM Tris-HCl [pH 7.6], 150 mM NaCl, 1 mM EDTA, and 1 mM DTT).

Assays for DeISGylation in Cultured Cells

Initially, 293T cells cultured in 12-well dishes were cotransfected with 0.4 μg of pCAGGS-6HismISG15, 0.4 μg of pCAGGS-hUBE1L-HA, and 0.2 μg of pFLAGCMV2-UbcM8 along with OTU domain expression plasmids or empty pCAGGS plasmid using Lipofectamine 2000. In

subsequent experiments testing eukaryotic and viral OTU constructs, 293T cells in 12-well dishes were cotransfected with OTU domain expression plasmids and 0.5 μg pCAGGS-6His mISG15, 0.5 μg pCAGGS-mUBE1L-HA, 0.5 μg of plasmid encoding Herc5, and 0.2 μg pFLAGCMV2 UbcM8 or pCDNA3.1-UbcM8. Twenty-four hours posttransfection, cells were lysed in Laemmli sample buffer, boiled, and analyzed by immunoblot using anti-ISG15 mAb 3C2 as previously described (Lenschow et al., 2005). Each transfection experiment was performed a minimum of three times.

Assay for Deubiquitination in Cultured Cells

293T cells cultured in 12-well dishes were cotransfected with 0.5 μg of pcDNA3.1-HA-Ub and various OTU domain expression plasmids or empty pCAGGS plasmid using Lipofectamine 2000. Twenty-four hours posttransfection, the cells were lysed in Laemmli sample, boiled, and immunoblotted with anti-HA antibody. Each transfection experiment was performed a minimum of three times.

Generation of ISG15 Conjugates

Fourteen 10 cm dishes of 293T cells were transfected with 6 μg pCAGGS-6HismISG15, 3 μg pCAGGS-hUBE1L-HA, and 3 μg pFLAGCMV2-UbcM8. Twenty-four hours later, cells were harvested, resuspended in 20 mM Tris-HCl (pH 8.0) with 300 mM NaCl, and lysed by three cycles of freeze-thaw. Lysates were centrifuged for 15 min at 14,000 rpm. His-tagged ISG15 conjugates were purified over a His-Select Spin Column (SIGMA) following the manufacturer's directions. Column-bound conjugates were washed extensively with washing buffer (20 mM Tris-HCl [pH 8.0], 300 mM NaCl, and 5 mM Imidazole) and eluted with 20 mM Tris-HCl (pH 8.0), 300 mM NaCl, and 250 mM Imidazole. Protein concentration was measured by Bradford assay (Bio-Rad).

In Vitro Deconjugation Assays

K^{48} Ub_{2-7}, K^{63} Ub_{3-7}, SUMO-2_{2-8}, SUMO-3_{2-8}, pro-ISG15, pro-Nedd8, pro-SUMO-1, USP5/Isopeptidase T, NEDP1, UBP43, $A20_{CD}$, and His6-$SENP2_{CD}$ were purchased from Boston Biochem (Cambridge, MA). All reactions were performed in 50 mM Tris-HCl (pH 7.6), 5 mM MgCl2, and 2 mM DTT at 37°C for 2 hr. Serial 10-fold dilutions of L(1–169) or L(1–169)1A (ranging from 2.5 μM to 2.5 nM) were incubated with either 2.5 μg Ub chains or SUMO chains; 2.5 μg pro-ISG15, pro-Nedd8, or pro-SUMO-1; 10 μl *Ubp43*$^{-/-}$ lysate; or 3 μg of 6HisISG15 conjugates. Positive control for deconjugation was incubation with 100 mM USP5 (Ub), $SENP2_{CD}$ (SUMO), NEDP1 (Nedd8), or UBP43 (ISG15). Negative control was incubation of chains or conjugates in assay buffer alone. Reactions were terminated by addition of Laemmli sample buffer and separated by SDS-PAGE electrophoresis on a 4%–20% gradient gel (BioRad). Proteins were visualized by SimplyBlue Safestain (Invitrogen) staining (Ub and SUMO) or by anti-ISG15 western blot.

Viruses

Sindbis viruses were generated from a cDNA clone by in vitro transcription and RNA transfection of BHK-21 cells as previously described (Levine et al., 1996; Lenschow et al., 2005). Recombinant virus stocks were produced and titered on BHK-21 cells as previously described (Lenschow et al., 2005). Sindbis virus AR86 was a kind gift of Dr. Mark Heise (University of North Carolina, Chapel Hill) (Heise et al., 2000).

NF-κB Reporter Gene Assay

293T cells were cotransfected with 3.3-fold dilutions (starting at 100 ng) of A20, CCHFV-L(1–169), CCHFV-L(1–169)2A, EAV-nsp2N, or empty plasmid along with the firefly luciferase gene construct under the control of the NF-κB-binding sites) (Wang et al., 2000) and pRL-TK (*Renilla* luciferase; Promega, WI). The total amount of transfected DNA was kept constant by adding the pCAGGS empty vector. Twenty-four hours posttransfection, the cells were stimulated with TNFα (10 ng/ml) for 6 hr, and luciferase activities were measured using the Dual-Luciferase Reporter (DLR) Assay System (Promega). Final NF-κB luciferase values were normalized with the *Renilla* luciferase values as internal control.

Immunofluorescence

Two hundred nanograms of empty plasmid or Flag-tagged L(1–169) and L(1–169)2A were transfected into A549 cells. Twenty-four hours later, cells were stimulated with 10 ng/ml TNFα for 2 hr. Cells were fixed and permeabilized for 30 min at room temperature with 2.5% formaldehyde and 0.5% Triton X-100, washed extensively with PBS, and stained with anti-p65 and anti-Flag antibodies. Following PBS washes, cells were stained with anti-mouse (p65) or anti-rabbit (Flag) and secondary antibodies, and then mounted in medium containing an antifade reagent. Nuclear localization of p65 was scored in 100 to 400 transfected cells for each experimental condition.

Mouse Studies

IFNαβR$^{-/-}$ mice on the 129/SV/Pas background were initially obtained from M. Aguet, Swiss Institute of Experimental Cancer Research (Epalinges, Switzerland) (Behr et al., 2001; Dunn et al., 2005). CCHFV-L(1–1325) transgenic mice were generated at the WUSM Pathology Microinjection Core by microinjecting a linearized construct derived from pCAGGS-HA-L(1–1325) into B6 oocytes. Oocytes were implanted into pseudopregnant mice, and resulting litters were genotyped using PCR (primer sequences available upon request). Individual embryo MEFs from transgenic lines 1836, 1854, and 2929 were generated as described previously (Weck et al., 1999). Uninfected transgenic brain was homogenized in 1 ml of DMEM with protease inhibitors using 100 μl 1.0 mm diameter zirconia-silica beads in a MagNa Lyser (Roche, Indianapolis, IN). To assess transgene expression, 4 × 10^5 MEFs or 12 μl of brain homogenate were immunoblotted with HA.11 and anti-actin antibodies. Eight- to ten-week-old male *IFNαβR*$^{-/-}$ mice were infected subcutaneously (s.c.) in the left hind footpad with 5 × 10^6 PFU of virus diluted in 50 μl of Hank's balanced salt solution (HBSS). Four- to five-week old L(1–1325) transgenic mice were infected s.c. in the left hind footpad with 5000 PFU of Sindbis virus AR86 diluted in 50 μl of HBSS. Mice were bred and maintained at Washington University School of Medicine in accordance with all federal and university guidelines.

Statistical Analysis

All data were analyzed with Prism software (GraphPad, San Diego, CA). Survival data were analyzed by the log-rank (Mantel-Haenzsel) test, with death as the primary variable. Single-step growth curves were analyzed by one-way analysis of variance (ANOVA).

Supplemental Data

The Supplemental Data include Supplemental Experimental Procedures and two supplemental figures and can be found with this article online at http://www.cellhostandmicrobe.com/cgi/content/full/2/6/404/DC1/.

ACKNOWLEDGMENTS

We thank Richard Cadagan, Caroline Lai, and Lindsay Droit for technical assistance; Dr. Domenico Tortorella for helpful discussions; and Drs. Dong-Er Zhang, Motoaki Ohtsubo, Adrian Ting, and Dianne Griffin for providing reagents. This work was partially supported by DoD grants W81XWH-04-1-0876 and W81XWH-07-2-0028, and by a NIAID-funded Center to Investigate Virus Immunity and Antagonism (CIVIA) U19 AI62623 (to A.G.-S.), and by NIAID grants U54 AI057160 Projects 6 and 10 (to H.W.V.) and U54 AI057158 (to A.G.-S.).

Received: May 4, 2007
Revised: July 23, 2007
Accepted: September 21, 2007
Published: December 12, 2007

REFERENCES

Allende, R., Lewis, T.L., Lu, Z., Rock, D.L., Kutish, G.F., Ali, A., Doster, A.R., and Osorio, F.A. (1999). North American and European porcine reproductive and respiratory syndrome viruses differ in non-structural protein coding regions. J. Gen. Virol. *80*, 307–315.

Balakirev, M.Y., Jaquinod, M., Haas, A.L., and Chroboczek, J. (2002). Deubiquitinating function of adenovirus proteinase. J. Virol. *76*, 6323–6331.

Balakirev, M.Y., Tcherniuk, S.O., Jaquinod, M., and Chroboczek, J. (2003). Otubains: A new family of cysteine proteases in the ubiquitin pathway. EMBO Rep. *4*, 517–522.

Barretto, N., Jukneliene, D., Ratia, K., Chen, Z., Mesecar, A.D., and Baker, S.C. (2005). The papain-like protease of severe acute respiratory syndrome coronavirus has deubiquitinating activity. J. Virol. *79*, 15189–15198.

Behr, M., Schieferdecker, K., Buhr, P., Buter, M., Petsophonsakul, W., Sirirungsi, W., Redmann-Muller, I., Muller, U., Prempracha, N., and Jungwirth, C. (2001). Interferon-stimulated response element (ISRE)-binding protein complex DRAF1 is activated in Sindbis virus (HR)-infected cells. J. Interferon Cytokine Res. *21*, 981–990.

Blanchard, J.E., Elowe, N.H., Huitema, C., Fortin, P.D., Cechetto, J.D., Eltis, L.D., and Brown, E.D. (2004). High-throughput screening identifies inhibitors of the SARS coronavirus main proteinase. Chem. Biol. *11*, 1445–1453.

Boone, D.L., Turer, E.E., Lee, E.G., Ahmad, R.C., Wheeler, M.T., Tsui, C., Hurley, P., Chien, M., Chai, S., Hitotsumatsu, O., et al. (2004). The ubiquitin-modifying enzyme A20 is required for termination of Toll-like receptor responses. Nat. Immunol. *5*, 1052–1060.

Chen, Z.J. (2005). Ubiquitin signalling in the NF-κB pathway. Nat. Cell Biol. *7*, 758–765.

Dunn, G.P., Bruce, A.T., Sheehan, K.C., Shankaran, V., Uppaluri, R., Bui, J.D., Diamond, M.S., Koebel, C.M., Arthur, C., White, J.M., and Schreiber, R.D. (2005). A critical function for type I interferons in cancer immunoediting. Nat. Immunol. *6*, 722–729.

Evans, P.C., Smith, T.S., Lai, M.J., Williams, M.G., Burke, D.F., Heyninck, K., Kreike, M.M., Beyaert, R., Blundell, T.L., and Kilshaw, P.J. (2003). A novel type of deubiquitinating enzyme. J. Biol. Chem. *278*, 23180–23186.

Evans, P.C., Ovaa, H., Hamon, M., Kilshaw, P.J., Hamm, S., Bauer, S., Ploegh, H.L., and Smith, T.S. (2004). Zinc-finger protein A20, a regulator of inflammation and cell survival, has de-ubiquitinating activity. Biochem. J. *378*, 727–734.

Fujita, T., Nolan, G.P., Ghosh, S., and Baltimore, D. (1992). Independent modes of transcriptional activation by the p50 and p65 subunits of NF-κB. Genes Dev. *6*, 775–787.

Gack, M.U., Shin, Y.C., Joo, C.H., Urano, T., Liang, C., Sun, L., Takeuchi, O., Akira, S., Chen, Z., Inoue, S., and Jung, J.U. (2007). TRIM25 RING-finger E3 ubiquitin ligase is essential for RIG-I-mediated antiviral activity. Nature *446*, 916–920.

Giannakopoulos, N.V., Luo, J.K., Papov, V., Zou, W., Lenschow, D.J., Jacobs, B.S., Borden, E.C., Li, J., Virgin, H.W., and Zhang, D.E. (2005). Proteomic identification of proteins conjugated to ISG15 in mouse and human cells. Biochem. Biophys. Res. Commun. *336*, 496–506.

Haas, A.L., Ahrens, P., Bright, P.M., and Ankel, H. (1987). Interferon induces a 15-kilodalton protein exhibiting marked homology to ubiquitin. J. Biol. Chem. *262*, 11315–11323.

Heise, M.T., Simpson, D.A., and Johnston, R.E. (2000). A single amino acid change in nsP1 attenuates neurovirulence of the Sindbis-group alphavirus S.A.AR86. J. Virol. *74*, 4207–4213.

Honig, J.E., Osborne, J.C., and Nichol, S.T. (2004). Crimean-Congo hemorrhagic fever virus genome L RNA segment and encoded protein. Virology *321*, 29–35.

Karin, M., and Ben-Neriah, Y. (2000). Phosphorylation meets ubiquitination: The control of NF-κB activity. Annu. Rev. Immunol. *18*, 621–663.

Kim, K.I., Giannakopoulos, N.V., Virgin, H.W., and Zhang, D.E. (2004). Interferon-inducible ubiquitin E2, Ubc8, is a conjugating enzyme for protein ISGylation. Mol. Cell. Biol. *24*, 9592–9600.

Kinsella, E., Martin, S.G., Grolla, A., Czub, M., Feldmann, H., and Flick, R. (2004). Sequence determination of the Crimean-Congo hemorrhagic fever virus L segment. Virology *321*, 23–28.

Kirkin, V., and Dikic, I. (2007). Role of ubiquitin- and Ubl-binding proteins in cell signaling. Curr. Opin. Cell Biol. *19*, 199–205.

Lenschow, D.J., Giannakopoulos, N.V., Gunn, L.J., Johnston, C., O'Guin, A.K., Schmidt, R.E., Levine, B., and Virgin, H.W., IV. (2005). Identification of interferon-stimulated gene 15 as an antiviral molecule during Sindbis virus infection in vivo. J. Virol. *79*, 13974–13983.

Lenschow, D.J., Lai, C., Frias-Staheli, N., Giannakopoulos, N.V., Lutz, A., Wolff, T., Osiak, A., Levine, B., Schmidt, R.E., Garcia-Sastre, A., et al. (2007). IFN-stimulated gene 15 functions as a critical antiviral molecule against influenza, herpes, and Sindbis viruses. Proc. Natl. Acad. Sci. USA *104*, 1371–1376.

Levine, B., Goldman, J.E., Jiang, H.H., Griffin, D.E., and Hardwick, J.M. (1996). Bc1-2 protects mice against fatal alphavirus encephalitis. Proc. Natl. Acad. Sci. USA *93*, 4810–4815.

Li, K., Foy, E., Ferreon, J.C., Nakamura, M., Ferreon, A.C., Ikeda, M., Ray, S.C., Gale, M., Jr., and Lemon, S.M. (2005). Immune evasion by hepatitis C virus NS3/4A protease-mediated cleavage of the Toll-like receptor 3 adaptor protein TRIF. Proc. Natl. Acad. Sci. USA *102*, 2992–2997.

Lin, R., Lacoste, J., Nakhaei, P., Sun, Q., Yang, L., Paz, S., Wilkinson, P., Julkunen, I., Vitour, D., Meurs, E., and Hiscott, J. (2006). Dissociation of a MAVS/IPS-1/VISA/Cardif-IKKepsilon molecular complex from the mitochondrial outer membrane by hepatitis C virus NS3-4A proteolytic cleavage. J. Virol. *80*, 6072–6083.

Lindner, H.A., Fotouhi-Ardakani, N., Lytvyn, V., Lachance, P., Sulea, T., and Menard, R. (2005). The papain-like protease from the severe acute respiratory syndrome coronavirus is a deubiquitinating enzyme. J. Virol. *79*, 15199–15208.

Liu, Y.C., Penninger, J., and Karin, M. (2005). Immunity by ubiquitylation: A reversible process of modification. Nat. Rev. Immunol. *5*, 941–952.

Loeb, K.R., and Haas, A.L. (1992). The interferon-inducible 15-kDa ubiquitin homolog conjugates to intracellular proteins. J. Biol. Chem. *267*, 7806–7813.

Loureiro, J., and Ploegh, H.L. (2006). Antigen presentation and the ubiquitin-proteasome system in host-pathogen interactions. Adv. Immunol. *92*, 225–305.

Makarova, K.S., Aravind, L., and Koonin, E.V. (2000). A novel superfamily of predicted cysteine proteases from eukaryotes, viruses and Chlamydia pneumoniae. Trends Biochem. Sci. *25*, 50–52.

Malakhov, M.P., Kim, K.I., Malakhova, O.A., Jacobs, B.S., Borden, E.C., and Zhang, D.E. (2003). High-throughput immunoblotting. Ubiquitiin-like protein ISG15 modifies key regulators of signal transduction. J. Biol. Chem. *278*, 16608–16613.

Nanao, M.H., Tcherniuk, S.O., Chroboczek, J., Dideberg, O., Dessen, A., and Balakirev, M.Y. (2004). Crystal structure of human otubain 2. EMBO Rep. *5*, 783–788.

Narasimhan, J., Potter, J.L., and Haas, A.L. (1996). Conjugation of the 15-kDa interferon-induced ubiquitin homolog is distinct from that of ubiquitin. J. Biol. Chem. *271*, 324–330.

Nijman, S.M., Luna-Vargas, M.P., Velds, A., Brummelkamp, T.R., Dirac, A.M., Sixma, T.K., and Bernards, R. (2005). A genomic and functional inventory of deubiquitinating enzymes. Cell *123*, 773–786.

Okumura, A., Lu, G., Pitha-Rowe, I., and Pitha, P.M. (2006). Innate antiviral response targets HIV-1 release by the induction of ubiquitin-like protein ISG15. Proc. Natl. Acad. Sci. USA *103*, 1440–1445.

Ratia, K., Saikatendu, K.S., Santarsiero, B.D., Barretto, N., Baker, S.C., Stevens, R.C., and Mesecar, A.D. (2006). Severe acute respiratory syndrome coronavirus papain-like protease: Structure of a viral deubiquitinating enzyme. Proc. Natl. Acad. Sci. USA *103*, 5717–5722.

Shin, J.S., Ebersold, M., Pypaert, M., Delamarre, L., Hartley, A., and Mellman, I. (2006). Surface expression of MHC class II in dendritic cells is controlled by regulated ubiquitination. Nature *444*, 115–118.

Snijder, E.J., Wassenaar, A.L., and Spaan, W.J. (1994). Proteolytic processing of the replicase ORF1a protein of equine arteritis virus. J. Virol. *68*, 5755–5764.

Snijder, E.J., Wassenaar, A.L., Spaan, W.J., and Gorbalenya, A.E. (1995). The arterivirus Nsp2 protease. An unusual cysteine protease with primary structure similarities to both papain-like and chymotrypsin-like proteases. J. Biol. Chem. *270*, 16671–16676.

Snijder, E.J., Wassenaar, A.L., van Dinten, L.C., Spaan, W.J., and Gorbalenya, A.E. (1996). The arterivirus nsp4 protease is the prototype of a novel group of chymotrypsin-like enzymes, the 3C-like serine proteases. J. Biol. Chem. *271*, 4864–4871.

Sudo, K., Yamaji, K., Kawamura, K., Nishijima, T., Kojima, N., Aibe, K., Shimotohno, K., and Shimizu, Y. (2005). High-throughput screening of low molecular weight NS3-NS4A protease inhibitors using a fluorescence resonance energy transfer substrate. Antivir. Chem. Chemother. *16*, 385–392.

Tergaonkar, V. (2006). NFκB pathway: A good signaling paradigm and therapeutic target. Int. J. Biochem. Cell Biol. *38*, 1647–1653.

Treier, M., Staszewski, L.M., and Bohmann, D. (1994). Ubiquitin-dependent c-Jun degradation in vivo is mediated by the delta domain. Cell *78*, 787–798.

Wang, X., Li, M., Zheng, H., Muster, T., Palese, P., Beg, A.A., and Garcia-Sastre, A. (2000). Influenza A virus NS1 protein prevents activation of NF-κB and induction of alpha/beta interferon. J. Virol. *74*, 11566–11573.

Wang, Y., Satoh, A., Warren, G., and Meyer, H.H. (2004). VCIP135 acts as a deubiquitinating enzyme during p97-p47-mediated reassembly of mitotic Golgi fragments. J. Cell Biol. *164*, 973–978.

Weck, K.E., Kim, S.S., Virgin, H.I., and Speck, S.H. (1999). B cells regulate murine gammaherpesvirus 68 latency. J. Virol. *73*, 4651–4661.

Wertz, I.E., O'Rourke, K.M., Zhou, H., Eby, M., Aravind, L., Seshagiri, S., Wu, P., Wiesmann, C., Baker, R., Boone, D.L., et al. (2004). De-ubiquitination and ubiquitin ligase domains of A20 downregulate NF-κB signalling. Nature *430*, 694–699.

Whitehouse, C.A. (2004). Crimean-Congo hemorrhagic fever. Antiviral Res. *64*, 145–160.

Yuan, W., and Krug, R.M. (2001). Influenza B virus NS1 protein inhibits conjugation of the interferon (IFN)-induced ubiquitin-like ISG15 protein. EMBO J. *20*, 362–371.

Yuan, W., Aramini, J.M., Montelione, G.T., and Krug, R.M. (2002). Structural basis for ubiquitin-like ISG 15 protein binding to the NS1 protein of influenza B virus: A protein-protein interaction function that is not shared by the corresponding N-terminal domain of the NS1 protein of influenza A virus. Virology *304*, 291–301.

Zhao, C., Beaudenon, S.L., Kelley, M.L., Waddell, M.B., Yuan, W., Schulman, B.A., Huibregtse, J.M., and Krug, R.M. (2004). The UbcH8 ubiquitin E2 enzyme is also the E2 enzyme for ISG15, an IFN-alpha/beta-induced ubiquitin-like protein. Proc. Natl. Acad. Sci. USA *101*, 7578–7582.

Ziebuhr, J., Snijder, E.J., and Gorbalenya, A.E. (2000). Virus-encoded proteinases and proteolytic processing in the Nidovirales. J. Gen. Virol. *81*, 853–879.

Structural basis for the removal of ubiquitin and interferon-stimulated gene 15 by a viral ovarian tumor domain-containing protease

Terrence W. James[a,1], Natalia Frias-Staheli[b,1,3], John-Paul Bacik[a], Jesica M. Levingston Macleod[b], Mazdak Khajehpour[c], Adolfo García-Sastre[b,d,e], and Brian L. Mark[a,2]

[a]Department of Microbiology, and [c]Department of Chemistry, University of Manitoba, Winnipeg, MB, R3T 2N2 Canada; and [b]Department of Microbiology, [d]Department of Medicine, Division of Infectious Diseases, and [e]Global Health and Emerging Pathogens Institute, Mount Sinai School of Medicine, New York, NY 10029

Edited by J. Wade Harper, Harvard, Boston, MA, and accepted by the Editorial Board December 7, 2010 (received for review September 7, 2010)

The attachment of ubiquitin (Ub) and the Ub-like (Ubl) molecule interferon-stimulated gene 15 (ISG15) to cellular proteins mediates important innate antiviral responses. Ovarian tumor (OTU) domain proteases from nairoviruses and arteriviruses were recently found to remove these molecules from host proteins, which inhibits Ub and ISG15-dependent antiviral pathways. This contrasts with the Ub-specific activity of known eukaryotic OTU-domain proteases. Here we describe crystal structures of a viral OTU domain from the highly pathogenic Crimean–Congo haemorrhagic fever virus (CCHFV) bound to Ub and to ISG15 at 2.5-Å and 2.3-Å resolution, respectively. The complexes provide a unique structural example of ISG15 bound to another protein and reveal the molecular mechanism of an ISG15 cross-reactive deubiquitinase. To accommodate structural differences between Ub and ISG15, the viral protease binds the β-grasp folds of Ub and C-terminal Ub-like domain of ISG15 in an orientation that is rotated nearly 75° with respect to that observed for Ub bound to a representative eukaryotic OTU domain from yeast. Distinct structural determinants necessary for binding either substrate were identified and allowed the reengineering of the viral OTU protease into enzymes with increased substrate specificity, either for Ub or for ISG15. Our findings now provide the basis to determine in vivo the relative contributions of deubiquitination and deISGylation to viral immune evasion tactics, and a structural template of a promiscuous deubiquitinase from a haemorrhagic fever virus that can be targeted for inhibition using small-molecule-based strategies.

innate immunity | viral deubiquitinase | bunyavirus | Crimean–Congo haemorrhagic fever virus | viral immune evasion

The posttranslational modification of proteins by Ub and Ub-like (Ubl) molecules is a regulatory process that controls numerous biological events (1, 2). Ub is conjugated to a lysine residue of target proteins through an isopeptide bond between the terminal carboxyl group of Ub and ε-amino group of the target lysine (3). Additional Ub molecules can be conjugated to lysines within Ub itself to form polyubiquitin chains. Lys 48-linked polyubiquitination is the canonical signal that targets proteins for proteasomal degradation, whereas Lys 63-linked polyubiquitination can initiate proteasome-independent events (4). Both Lys 48- and Lys 63-linked polyubiquitination have been established as key signaling events that activate innate and adaptive immune responses (5).

A critical innate immune response to viral infection is the rapid production of type I interferon (IFN) and tumor necrosis factor alpha (TNFα). The induction and activity of these antiviral cytokines is controlled by, among other factors, Ub and Ubl conjugation (4). A hallmark of type I IFN stimulation is the rapid production of the Ubl molecule ISG15 (6). ISG15 is composed of two tandem Ub-like folds (7) and is known to exhibit potent antiviral activity against several important viruses (8). It conjugates to ε-amino groups of target lysine residues on the surface of cellular target proteins similarly to Ub (9). Although conjugation is essential (8), several possible antiviral mechanisms have recently been proposed for ISG15 (10).

Ub and ISG15 conjugation can be reversed by deubiquitinating enzymes (DUBs). Ovarian tumor (OTU) domain proteases are papain-like cysteine DUBs that have been identified in eukaryotes, bacteria, and viruses (11). We have assayed a number of eukaryotic OTU-domain-containing proteins for deubiquitinating and deISGylating activity, including human A20, Cezanne, otubain1, and otubain2 (12) and the *Saccharomyces cerevisiae* OTU-domain-containing protein Otu1 (see *Results and Discussion*). While these eukaryotic proteins exhibit deubiquitinating activity as expected, none have been found to exhibit deISGylating activity, suggesting that eukaryotic OTU domains are Ub-specific. Importantly, the deubiquitinating activities of human A20, and the OTU-domain-containing protein DUBA, have been found to down-regulate TNFα and type I IFN production, respectively, by removing Ub from signaling proteins (13, 14).

In contrast to the Ub-specific activity of known eukaryotic OTU domains, we recently found that OTU-domain-containing proteins from nairoviruses and arteriviruses, two unrelated groups of RNA viruses, act as ISG15 cross-reactive deubiquitinases, removing both Ub and ISG15 from host proteins (12). CCHFV is a nairovirus that causes severe haemorrhagic fever in humans, with a mortality rate approaching 30% (15). As for other members in the genus, its genome consists of three negative-sense RNA segments, the largest of which encodes a 448 kDa viral RNA polymerase (L) that contains an amino terminal OTU domain of approximately 18 kDa (16, 17). Arteriviruses, such as equine arteritis virus (EAV) and porcine respiratory and reproductive syndrome virus (PRRSV), are nonsegmented, positive-sense RNA viruses that contain an OTU domain within their nonstructural protein 2 (nsp2) (18). The catalytic activity of these viral OTU domains not only inhibits NF-κB-dependent signaling (12, 19), we found that expression of the OTU domain from CCHFV antagonizes the antiviral effects of ISG15, suggesting

Author contributions: A.G.-S. and B.L.M. designed research; T.W.J., N.F.-S., J.-P.B., J.M.L.M., and B.L.M. performed research; T.W.J., N.F.-S., J.-P.B., M.K., A.G.-S., and B.L.M. analyzed data; and T.W.J. and B.L.M. wrote the paper.

The authors declare no conflict of interest.

This article is a PNAS Direct Submission. J.H. is a guest editor invited by the Editorial Board.

Freely available online through the PNAS open access option.

Data deposition: The coordinates and structure factors for the CCHFV–OTU–Ub and CCHFV–OTU–ISG15 protein complexes have been deposited in the Protein Data Bank, www.pdb.org (PDB ID codes 3PT2 and 3PSE, respectively).

[1]T.W.J. and N.F.-S. contributed equally to this work.

[2]To whom correspondence should be addressed. E-mail: brian_mark@umanitoba.ca.

[3]Present address: Laboratory of Virology and Infectious Disease, The Rockefeller University, 1230 York Avenue, Box 64, New York, NY 10065.

This article contains supporting information online at www.pnas.org/lookup/suppl/doi:10.1073/pnas.1013388108/-/DCSupplemental.

that viral OTU domains act as virulence factors to suppress host inflammatory and antiviral responses (12).

A number of eukaryotic OTU-domain structures have been determined (20–23), including a covalent complex between the OTU domain from the *Saccharomyces cerevisiae* protein Otu1 and Ub (24). The structure of a viral OTU domain has not been reported, however, and the mechanism of ISG15 cross-reactivity has remained unknown. Here we report crystal structures of the viral OTU-domain protease domain from CCHFV covalently bound to Ub and to ISG15 at 2.5-Å and 2.3-Å resolution, respectively. The complexes provide a unique structural example of ISG15 bound to another protein and together reveal the molecular mechanism of an ISG15 cross-reactive deubiquitinase. The expanded substrate-specificity arises from a unique topological feature of the viral OTU-domain fold, which causes the protein to bind Ub and C-terminal Ub-like domain of ISG15 in an orientation that is rotated nearly 75° with respect to that observed for Ub bound to a representative eukaryotic OTU domain from yeast. This permits the viral OTU domain to accommodate additional bulk within the C-terminal domain of ISG15 that is not present in Ub. Individual residues within the substrate-binding site of viral protease were identified as key interactions sites for Ub or ISG15, which allowed the reengineering of the protease into enzymes with increased substrate specificity, either for Ub or for ISG15. By identifying the unique structural determinants that underlie ISG15 cross-reactivity, our findings now provide the basis to determine in vivo the relative contributions of deubiquitination and deISGylation to viral immune evasion tactics and the potential to develop small-molecule based strategies that specifically inhibit viral OTU-domain proteases.

Results and Discussion

Structure of CCHFV-OTU Bound to Ub or ISG15. Crystal structures of the CCHFV–OTU domain were obtained using recombinantly expressed CCHFV L protein residues 1–185 for the Ub complex and L residues 1–169 for the ISG15 complex. For both complexes, residues 1–162 were clearly observed in the electron density and comprise the complete viral OTU domain. It consists of two lobes that clamp around a central substrate-binding groove, which narrows into a channel to direct the conserved C-terminal LRLRGG motif of Ub or ISG15 toward the enzyme active site (Figs. 1*A* and 2*A*). The larger of the two lobes (amino acids 1–34 and 114–162) is referred to as the β-sheet lobe because it is composed predominantly of a seven-stranded β-sheet (β1↑ β2↓ β3↑ β4↓ β5↓ β6↑ β7↓) that is sandwiched between helices α1, α2, α3, and α7. The smaller lobe (residues 35–113) is exclusively α-helical (composed of helices α3, α4, α5, α6, and α7) and referred to as the α-helical lobe.

Superposing the CCHFV–OTU structure onto the crystal structure of the Ub-bound eukaryotic OTU domain from yeast Otu1 (24) (Fig. 3*A*) reveals the presence of a unique N-terminal β1↑-β2↓ hairpin atop the β-sheet lobe of CCHFV–OTU, a feature not present in Otu1 (Fig. 3*A*) or any of the other OTU-domain structures that have been reported (Fig. S1*A*). Relative to the OTU domains from Otu1 and human A20, Otubain1 and Otubain2, the entire N terminus of CCHFV–OTU, which includes strands β1 and β2, is relocated to the opposite side of the core β-sheet structure of the OTU-domain fold (Fig. 3 *B* and *C*). Yeast Otu1 is the only additional OTU-domain-containing protein to be determined in complex with Ub. Residues comprising the substrate-binding groove of the OTU domain of Otu1 are highly conserved in other eukaryotic OTU domains, suggesting the Otu1–Ub complex is representative of Ub complexes that are formed by other eukaryotic OTU domains (24).

The β1↑–β2↓ hairpin comprises a significant part of the CCHFV–OTU substrate-binding groove and causes the viral protein to bind the β-grasp fold of Ub in a strikingly different manner than yeast Otu1 (Fig. 3 *D* and *E*). When bound to CCHFV–OTU, Ub is rotated about an axis defined by its extended C-terminal

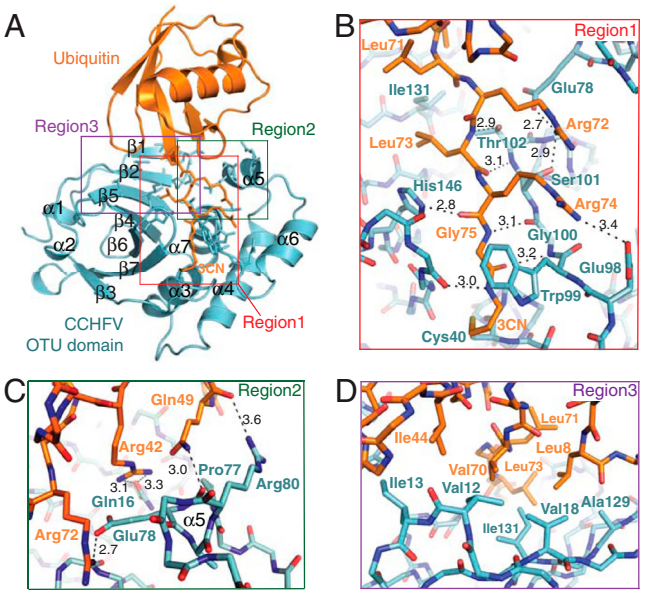

Fig. 1. Crystal structure of CCHFV–OTU (cyan) bound to Ub (orange). (*A*) Ribbon diagram of the complex highlighting the three major regions of interaction between Ub and the protease. Ub is bound within a substrate-binding groove that is flanked on either side by the β-sheet lobe (left) and α-helical lobe (right) of the protease. The groove narrows into a channel that directs the C terminus of Ub toward the enzyme active site. Gly 76 of Ub is replaced with a propylamine linker (3CN) that covalently attaches Ub to the enzyme nucleophile (Cys 40) located on helix α3. Residue side chains involved in protein–protein contacts in regions 1 (*B*), 2 (*C*), and 3 (*D*) are shown with hydrogen bonds in black. All other side chains have been omitted for clarity. Figures were drawn using PyMol (42).

LRLRG-3CN motif by nearly 75° with respect to its position when bound to yeast Otu1. The C-terminal Ub-like domain of

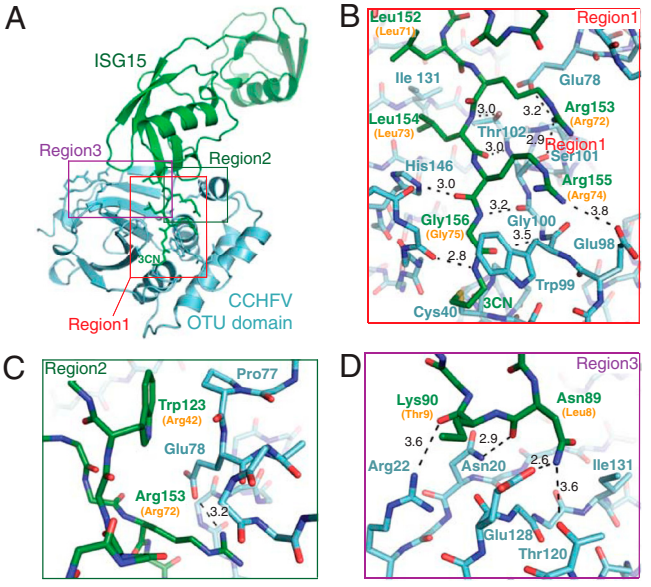

Fig. 2. Crystal structure of the CCHFV–OTU (cyan) domain bound to ISG15 (green). (*A*) Ribbon diagram of the complex highlighting the three major regions of interaction between ISG15 and the protease. The C-terminal Ub-like domain of ISG15 binds the substrate-binding groove of the proteases in an analogous manner to Ub. Gly 157 of ISG15 is replaced with a propylamine linker (3CN) that is covalently attached to the enzyme nucleophile (Cys 40) on helix α3. Side chains of residues involved in protein–protein contacts in regions 1 (*B*), 2 (*C*), and 3 (*D*) are shown with hydrogen bonds in black. Equivalent residues of Ub are in parentheses. All other side chains have been omitted for clarity. Atoms Cε and Nζ of Lys 90 of ISG15 are disordered and not shown in *D*.

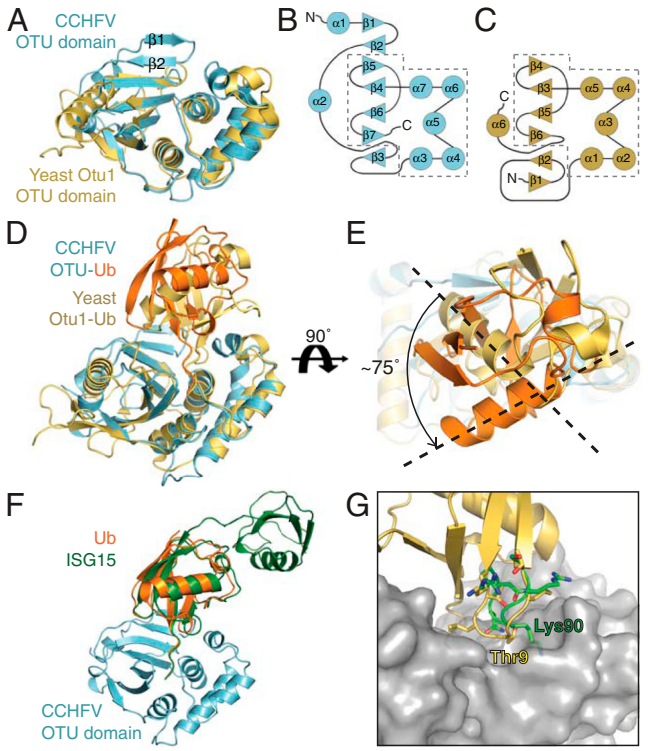

Fig. 3. Comparison of the CCHFV–OTU–Ub and yeast Otu1–Ub crystal structures. (*A*) Superposition of CCHFV–OTU (cyan) and the OTU domain from yeast Otu1 (yellow) (Ub omitted for clarity). Strands β1 and β2 of CCHFV–OTU are labeled. Secondary structure topologies of CCHFV–OTU (*B*) and yeast Otu1 (*C*) are shown (dashed boxes enclose the core topology that is conserved in all known OTU domain structures). (*D*) Superposition shown in *A* including Ub. (*E*) Superposition in *D* rotated 90° showing the difference in binding orientation of Ub bound to the CCHFV–OTU versus yeast Otu1. (*F*) Superposition of the CCHFV–OTU–Ub and CCHFV–OTU–ISG15 complexes. (*G*) Location of Ub Thr 9 (yellow) bound to yeast Otu1 (gray). Superposing ISG15 (green residues) onto Ub predicts that Lys90 would clash with the Otu1 binding groove. Atoms Cε and Nζ of Lys 90 have been modeled for clarity.

ISG15 (residues 82–157) binds CCHFV–OTU in the same position and orientation as Ub (rmsd of 0.9 Å for 75 Cα carbons) (Fig. 3*F*). Importantly, this permits CCHFV–OTU to accommodate bulky and polar residues on loop Arg 87–Ser 93 in the C-terminal domain of ISG15 that are not present in the analogous loop of Ub (Lys 6–Thr 12). The bulk arises primarily from Lys 90, which corresponds to Thr 9 in Ub (Fig. 3*G*). In the CCHFV–OTU–ISG15 complex, the Arg 87–Ser 93 loop is solvent accessible, held near the edge of the binding groove where it participates in key interactions with the viral protease (Fig. 2 *A* and *D*). In the yeast Otu1–Ub complex, the analogous loop of Ub is buried within the substrate-binding groove. Lys 90 within the Arg 87–Ser 93 loop of ISG15 would likely be too large to fit the binding groove of yeast Otu1 (which we found to be Ub-specific) (Fig. S2), or other Ub-specific eukaryotic OTU domains that bind Ub similarly to Otu1 (Fig. 3*G*).

Molecular Interactions of CCHFV–OTU with Ub and ISG15. Analysis of protein interface interactions using PISA (25), revealed the binding of Ub or ISG15 buries approximately 900 Å^2 of solvent accessible surface area of the CCHFV–OTU substrate-binding groove, which in turn buries roughly 20% (approximately 1,000 Å^2) of the total surface area of Ub or C-terminal Ubl domain of ISG15 (Fig. 4*A*). Both Ub and ISG15 were found to interact with three distinct regions within this buried surface area of the enzyme (Figs. 1 and 2). Region 1 comprises the channel that guides the C-terminal LRLRGG motifs of Ub (amino acids 71–76) or ISG15 (amino acids 152–157) toward the enzyme active site (Figs. 1*B* and 2*B*). Regions 2 (Figs. 1*C* and 2*C*) and 3 (Figs. 1*D* and 2*D*) are located on the α-helical and β-sheet lobe, respectively, and form the interface that binds the β-grasp folds of Ub or C-terminal Ub-like domain of ISG15.

In region 1 (Figs. 1*B* and 2*B*), both lobes of CCHFV–OTU participate in forming the channel that guides the terminal carboxyl group of the LRLRGG motif of Ub and ISG15 toward the enzyme nucleophile (Cys 40) of the active site (Fig. 4 *B* and *C*). The C-terminal motifs of Ub and ISG15 adopt nearly identical conformations within this channel (Fig. 3*F*). It is worth noting that although the bound orientation of the β-grasp fold of Ub (and C-terminal domain ISG15) is significantly different from that observed in the yeast Otu1–Ub complex, the C-terminal tail of Ub in Otu1–Ub complex superposes with the analogous residues of Ub (or ISG15) bound to CCHFV–OTU (Fig. 3*D*). The carboxy termini of Ub or ISG15 enter the active site of CCHFV–OTU that contains a cataylic diad (Cys 40 and His 151), which is spatially conserved with cysteine/histidine catalytic diad found in the archetype cysteine protease papain (26) (Fig. 4*D*). The catalytic mechanism of cysteine proteases requires the cysteine thiol to be deprotonated by the histidine residue. This promotes a nucleophilic attack by the cysteine on the carbonyl carbon of the scissile peptide bond of the substrate and formation of a covalent acyl-enzyme intermediate, which is subsequently resolved by a water molecule (27, 28). Cys 40 of CCHFV–OTU is conserved in other OTU-domain proteases (11). Mutation of this residue to alanine was found to eliminate catalytic activity (12), and the covalent adducts we observed between Cys 40 and Ub or ISG15 confirms this cysteine as the catalytic nucleophile CCHFV–OTU (Fig. 4 *B* and *C*).

In addition to the Cys 40/His 151 catalytic dyad, the carboxyl group of Asp 153 in CCHFV–OTU likely enhances catalysis of the viral protease by hydrogen-bonding with the imidazole group of His 151 (Fig. 4 *B* and *C*). This interaction is analogous to the interaction between Asn 175 and His 159 in papain (26) and is believed to correctly orient the imidazolium ring of the histidine residue during catalysis (28). For most cysteine proteases, the main chain amide of the cysteine nucleophile and a glutamine side chain from an oxianion hole, which stabilizes the oxianion that develops along the reaction coordinate (28). While the amide of the cysteine nucleophile is present, an equivalent glutamine is not present in CCHFV–OTU and is substituted by the main chain amide of Asp 37, which appears well positioned to help stabilize the oxianion. Similar oxianion hole architectures are observed in the OTU domains of yeast Otu1 (24) and human Otubain1 (23), Otubain2 (22), and A20 (20, 21) (Fig. S1*B*).

Region 2 centers on helix α5 of the α-helical lobe of CCHFV–OTU. Relatively few distinct contacts are made between this region and Ub or C-terminal Ub-like domain of ISG15 with the exception of a hydrogen bond between Arg 42 of Ub and Gln 16 of strand β2 of CCHFV–OTU. The region appears to act primarily as a buttress to support the substrates against region 3 and help guide the C-terminal motifs of each substrate toward the active site (Figs. 1*C* and 2*C*).

Region 3 centers on the distinctive β1↑–β2↓ hairpin of the viral protease, where hydrophobic interactions with Ub (Fig. 1*D*) or electrostatic interactions with ISG15 are mediated (Fig. 2*D*). When bound to Ub, Val 12 and Ile 13 of strand β1, Val 18 of strand β2, and Ala 129 and Ile 131 from strand β5, comprise a hydrophobic patch that interacts with Leu 8, Ile 44, Val 70, and Leu 73 of Ub. This hydrophobic patch on Ub, in particular Ile 44, is a critical interaction site that is recognized by DUB enzymes (29), and CCHFV–OTU uses it to orient Ub within the binding groove. Interestingly, due to the difference in binding orientation of Ub to CCHFV–OTU versus yeast Otu1, a cluster of hydrophobic residues analogous to those in region 3 of CCHFV–OTU exist on the α-helical lobe of Otu1, where they serve to bind the Ile 44 patch of Ub (24). This patch of residues on Otu1 is conserved in

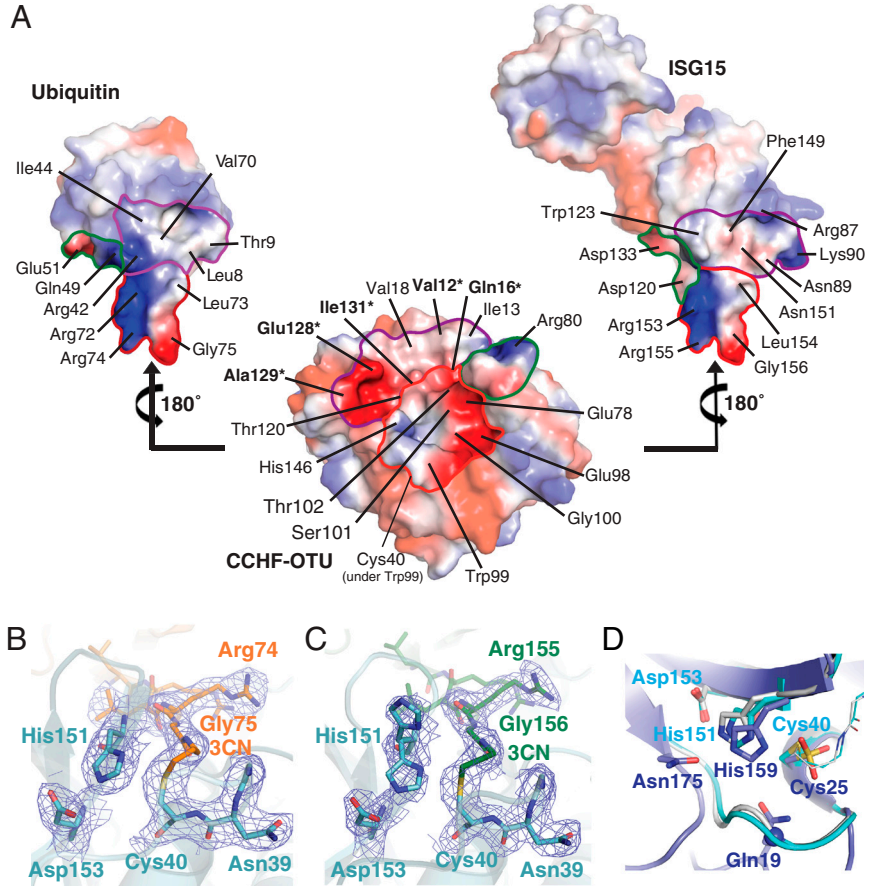

Fig. 4. Regions of interaction of Ub and ISG15 with the substrate-binding groove and active site of CCHFV–OTU. (*A*) The Ub and ISG15 structures are separated from CCHFV–OTU and rotated 180° to expose the areas of interaction between these substrates and the binding groove of the protease. Resides marked with an asterisk were functionally characterized by mutagenesis (Table 1). Electrostatic surface potentials are drawn at −60 kT/*e* [red (–), blue (+)] as implemented in PyMol (42). Three distinct regions within the CCHFV–OTU binding groove [region 1 (outlined in red), region 2 (outlined in green), and region 3 (outlined in purple)] interact with patches on Ub or ISG15 that are outlined by the same color. Region 3 on CCHFV–OTU contains a notable patch of negative charge around Glu128, which plays a key role in binding the Arg 87–Ser 93 loop of ISG15. Although atoms Cϵ and Nζ of Lys 90 of ISG15 are disordered in the ISG15:CCHFV–OTU complex, they have been modeled onto the ISG15 structure shown here to reveal their position on the ISG15 structure. *B* and *C* show the CCHFV–OTU active site and propylamine linker (3CN) that covalently joins the enzyme nucleophile (Cys 40) to Ub or ISG15, respectively. Electron densities are maximum-likelihood weighted $2F_{obs} - F_{calc}$ syntheses contoured at 1σ. His151 adopts two conformations in the ISG15 complex. Only one of these conformations is observed in the Ub complex and is presumed to be the catalytically competent conformation. (*D*) Superposition of CCHFV–OTU–Ub (cyan) and CCHFV–OTU–ISG15 (gray) with papain (PDB ID code 9PAP) (purple). The papain nucleophile (Cys 25) is oxidized. The Gln19 side chain and main chain amide of Cys 25 form the oxianion hole of papain. Gln19 is substituted by the main chain amide of Asp 37 (blue sphere) in CCHFV–OTU.

other eukaryotic OTU domains and supports the conjecture that they bind Ub in the same orientation as Otu1.

The C-terminal Ub-like domain of ISG15 does not possess a patch of hydrophobic residues analogous to Leu 8, Ile 44, Val 70, and Leu 73 of Ub with the exception of Leu 154 (Leu 73 of Ub). Instead, this region of ISG15 is composed primarily of polar residues (equivalent Ub residues in parentheses): Asn 89 (Leu 8), Thr 125 (Ile 44), Asn 151 (Val 70). To compensate for this difference in substrate structure, region 3 contains residues Asn 20, Arg 22, Thr 120, and Glu 128, which form a network of hydrogen bonds with the Arg 87–Ser 93 loop of ISG15 (Fig. 2*D*). In particular, Lys 90 of the loop is fully solvent exposed and the side chain of Asn 89 appears to form critical hydrogen-bonding interactions with Glu 128 and Thr 120 of the viral protease. With the exception of region 1, this hydrogen-bonding network is the major site of interaction between CCHFV–OTU and ISG15. Thus, the Arg 87–Ser 93 loop of the C-terminal β-grasp fold of ISG15 appears to be an important site of interaction for proteins that recognize ISG15.

Functional Analysis of the CCHFV–OTU Substrate-Binding Interface. Structural analysis revealed that Ub and ISG15 interact with discrete patches of residues within the substrate-binding groove of CCHFV–OTU (Fig. 4*A*). Site-directed mutagenesis was used to verify the importance of individual enzyme residues in forming the enzyme–substrate reactive complex and to determine if it was possible to selectively attenuate DUB or deISGylating activity. With this objective in mind, we produced the following mutants of CCHFV–OTU: (*i*) Mutations Val12Thr, Ile131Asn, and Ala129Ser of region 3 were created to disrupt the binding of region 3 of the protease to the Ile 44 patch of Ub (Figs. 1*D* and 4*A*); (*ii*) residue Gln16 of region 2 was mutated to serine to disrupt an apparent Ub-specific electrostatic interaction between Gln 16 in region 2 of the *CCHFV–OTU* and Arg 42 of Ub (Figs. 1*C* and 4*A*); and (*iii*) the mutation Glu128Ala was created to perturb the hydrogen-bonding network existing between region 3 of CCHFV–OTU and the Arg 87–Ser 93 loop of ISG15 (an interaction that does not occur between Ub and CCHFV–OTU) (Figs. 2*D* and 4*A*).

The Michaelis constant K_M can be used as a measure of the amount of enzyme that is bound in any form to the substrate (30). However, because the commercially available Ub–AMC substrate stock was dissolved in dimethylsulfoxide (DMSO), a limit (dictated by enzyme denaturation and substrate solubility) existed on the maximum substrate concentration that could be used, making it difficult to obtain reliable K_m values directly. Our kinetic analysis of protease activity toward Ub–AMC was thus limited to the linear portion of the Michaelis–Menten curve (Fig. S3), which still allowed us to quantitatively determine the specificity constant $\frac{k_{cat}}{K_M}$ of the enzyme relative to the substrate. In order to compare the effect of each mutation, we determined the specificity constants for all mutant CCHFV–OTU enzymes toward Ub–AMC, ISG15–AMC, and the peptide RLRGG–AMC using the linear portion of the relevant Michaelis–Menten plots. These values are shown in Table 1.

In comparing the various specificity constant values in Table 1, the following points must be considered. We designed our mutations expecting that they would not strongly perturb the catalytic site of the CCHFV–OTU enzymes because they were located in regions 2 and 3 of the enzyme, which are far from the active site. We verified this expectation by using a traditional Michaelis–Menten analysis using the substrate ISG15–AMC (which could be used at concentrations that approached kinetic saturation of the enzyme) (Fig. S4). We indeed observed that the various mutations have limited effect on the k_{cat} values: The maximum change in k_{cat} observed between mutant enzymes and the wild type is a reduction by a factor less than 2 (Table S1). It should be noted that the value of the wild-type enzyme specificity con-

stant reported in Table S1 is within 10% of the value reported in Table 1, and the specificity constants of the mutant enzymes reported in the Table 1 and Table S1 agree with one another within the uncertainty limits. Therefore, it is reasonable to assume that if the specificity constant of a mutant enzyme toward a given substrate is more than five times less than that of the wild type, this change is likely due to an increase in K_M and thus reflects a change in the binding of substrate to enzyme rather than any drastic deformation of the catalytic site that would lead to a change in the catalytic mechanism.

Of all the mutated CCHFV–OTU residues within region 3 that form van der Waals packing interactions with the hydrophobic Ile 44 patch of Ub (Fig. 1*D*), Ile 131 appeared to be the most important for Ub binding. Mutating Ile 131 to an asparagine caused the specificity constant of enzyme toward Ub–AMC to drop by a factor of 30. Other residues analyzed by mutagenesis were found to contribute significantly less, with Val 12 perhaps being the next most important contributor to Ub–AMC binding and Ala129Ser having the least effect (Table 1). Residue Ile 131 also appears to significantly contribute to the binding of the peptide substrate RLRGG–AMC, because the Ile131Asn mutation caused the specificity constant of the enzyme toward the peptide to drop by two orders of magnitude. This change is consistent with our structural data, which demonstrates that the peptide extends some distance from the enzyme active site such that the Leu residue of the peptide interacts directly with Ile 131 of the enzyme (Figs. 1 *B* and *D* and 2*B*). The Ile131Asn mutation had less of an effect on the specificity constant of enzyme toward ISG15–AMC, dropping it by a factor of three. Interestingly, unlike Ub or the RLRGG peptide substrate, ISG15 contains polar residues within the vicinity of the Ile131Asn mutation as observed in the CCHFV–OTU: ISG15 crystal structure. In particular, the side chain of ISG15 residue Asn 89 (Ub: Leu 8) lies within 4.0 Å of Ile 131 (Fig. 2*D*) and may assist in stabilizing the interaction between ISG15 and the Ile131Asn mutant by hydrogen-bonding directly to the introduced Asn side chain. This interaction could not occur with Ub or the RLRGG peptide.

Based on our structural analysis, the hydrogen-bonding interaction between Gln 16 in region 2 and Arg 42 of Ub (Fig. 1*C*) appeared to be selective for Ub, because the corresponding residue in ISG15 is a tryptophan (Trp 123) that does not participate in an analogous interaction with the enzyme (Fig. 2*C*). Surprisingly, we found that this mutation had an equal effect on the specificity constants for Ub–AMC and ISG15–AMC. As expected, however, because this mutation is far from region 1, it did not have any measurable effect on the specificity constant for the RLRGG–AMC peptide.

In contrast to the above findings using Ub–AMC, our functional assessment of CCHFV–OTU residues Val12, Ile131, and Ala129 showed that they have a less important role in the binding of ISG15–AMC, with the probable exception of Ile 131 (Table 1). Instead, our structural data revealed that a hydrogen-bonding network exists between the Arg 87–Ser 93 loop of ISG15 and region 3 of CCHFV–OTU, which appeared critical for interacting with ISG15. The shortest hydrogen bond within the network occurred between Glu 128 of CCHFV–OTU and Asn 89 of ISG15 (Fig. 2*D*) and was thus predicted to contribute strongly to the binding of ISG15 to the enzyme. Indeed, mutating this residue reduced the specificity constant of CCHFV–OTU toward ISG15 by a factor of five, while the specificity constants of the enzyme toward Ub–AMC or the RLRGG–AMC peptide substrates were unimpaired by this mutation. Significantly decreasing the binding of ISG15 by perturbing the hydrogen-bonding network between the Arg 87–Ser 93 loop of ISG15 and region 3 of CCHFV–OTU is consistent with the conjecture that this loop is a protein interaction "hot spot" and supports a previous prediction suggesting that the loop is involved in binding the ISG15 activating enzyme UbE1L (7) and perhaps additional proteins that interact with ISG15.

OTU-Domain Proteases as Virulence Factors for Viral Immune Evasion. The discovery of viruses that have acquired the ability to remove Ub and ISG15 from cellular targets underscores the importance of Ub and ISG15 conjugation to innate immunity. Moreover, alternative immune evasion tactics such as NS1 of influenza B virus, a protein that prevents ISGylation of proteins by binding ISG15 (31), further highlights the importance of ISG15 to host defense. The small and compact genomes of nairoviruses and arteriviruses likely selected for a unique deconjugating OTU protease with the ability to target both Ub and ISG15 at the same time, a property that appears not to be shared by eukaryotic OTU enzymes. We show here that a rearrangement in the β-sheet topology of the CCHFV OTU-domain fold yields an ISG15 cross-reactive viral DUB capable of binding Ub or ISG15, yet it retains an active site architecture that is conserved with eukaryotic OTU-domain proteases. Importantly, the ISG15 cross-reactive deubiquitinating activity of CCHFV–OTU is retained when the domain is expressed as part of the intact CCHFV RNA polymerase L protein (12). However, it remains to be determined if other structural components of the viral L protein can modulate the DUB and deISGylating activities of the CCHFV–OTU domain during viral replication. Given the low sequence conservation of ISG15 in higher eukaryotes, there is the intriguing possibility of species-specific deISGylating activity by viral OTU domains, which may correlate with host tropism. Having demonstrated that Ub and ISG15 hydrolysis can be selectively attenuated by site directed mutagenesis, it may be possible to study the relative contributions these deconjugating activities have to the immune evasion tactics of nairoviruses and arteriviruses.

In addition to viral OTU domains, the papain-like protease from severe acute respiratory syndrome (SARS) coronavirus (32, 33) and the adenoviral protease adenain (34) are also ISG15 cross-reactive DUBs, which suggests that ISG15 cross-reactive DUBs may be a widely used viral mechanism to simultaneously suppress inflammatory and IFN responses of the host.

Table 1. Effect of substrate binding site mutations on CCHFV–OTU activity*

Enzyme	Substrate					
	Ub–AMC		ISG15–AMC		RLRGG–AMC	
	k_{cat}/K_M (×10^{-5})	Ratio of specificity constants (mutant/wild type)	k_{cat}/K_M (×10^{-5})	Ratio of specificity constants (mutant/wild type)	k_{cat}/K_M (×10^{-5})	Ratio of specificity constants (mutant/wild type)
Wild type	**3.41 ± 0.07**	**1**	**3.6 ± 0.1**	**1**	**0.60 ± 0.02**	**1**
Val12Thr	0.81 ± 0.02	0.24 ± 0.01	1.40 ± 0.06	0.39 ± 0.02	0.26 ± 0.01	0.43 ± 0.01
Ile131Asn	0.111 ± 0.001	0.0326 ± 0.0006	1.20 ± 0.03	0.33 ± 0.01	0.008 ± 0.001	0.01 ± 0.001
Ala129Ser	2.47 ± 0.03	0.72 ± 0.01	2.07 ± 0.07	0.58 ± 0.09	0.22 ± 0.02	0.37 ± 0.04
Gln16Ser	1.81 ± 0.02	0.53 ± 0.01	1.80 ± 0.06	0.50 ± 0.02	0.63 ± 0.02	1.1 ± 0.03
Glu128Ala	3.8 ± 0.2	1.11 ± 0.06	0.82 ± 0.02	0.23 ± 0.03	0.65 ± 0.05	1.10 ± 0.09

*For wild-type and mutant enzymes the specificity constants were obtained from the slopes of the lines shown in Fig. S3.

Targeting DUB viral proteases with small-molecule inhibitors might then represent an effective therapeutic approach. The CCHFV–OTU crystal structure revealed that ISG15 cross-reactivity requires a significantly altered substrate-binding groove architecture compared to Ub-specific eukaryotic OTU proteases. These structural differences may now be exploited to facilitate the development of inhibitors that are selective for viral OTU-domain-containing DUBs.

Materials and Methods

Preparation and Crystallization of CCHFV–OTU Bound to Ub or ISG15. Residues 1–185 (CCHFV-OTU$_{(1–185)}$) or 1–169 (CCHFV-OTU$_{(1–169)}$) of the CCHFV L protein were expressed as GST fusion proteins in *Escherichia coli* and purified. GST tags were removed using HRV 3c protease. Ub$_{(1–75)}$-3-bromopropylamine (Ub-3Br) and ISG15(Cys78Ser)$_{(1–156)}$-3-bromopropylamine (ISG15-3Br) were prepared according to Messick et al. (24) and Borodovsky et al. (35). The ISG15 mutation Cys78Ser was required to reduce aggregation (7). Selenomethionyl CCHFV-OTU$_{(1–185)}$ (produced according to Van Duyne et al.) (36) and native CCHFV-OTU$_{(1–169)}$ were complexed with Ub–Br3 and ISG15–Br3, respectively, then purified and dialyzed into 20 mM Tris-Cl, pH 8.0, 50 mM NaCl. Crystals were grown by hanging-drop vapor diffusion. Selenomethionyl OTU$_{(1–185)}$–Ub crystallized at 10 mg/ml in 27% PEG 4000-6000, 100 mM NaOAc, pH 5.4-5.6, 210 mM $(NH_4)_2SO_4$. OTU$_{(1–169)}$-ISG15 crystallized at 7 mg/ml in 100 mM MES, pH 6.3-6.5, 22–25% PEG 6000 or 8000. Crystals were flash-cooled in liquid nitrogen after the addition of 20% glycerol.

Data Collection and Structure Determination. X-ray data were collected at the Canadian Light Source (beam line 08ID-1) and processed using MOSFLM and SCALA (37). Diffraction data from a selenomethionyl OTU$_{(1–185)}$–Ub crystal was phased by single wavelength anomalous dispersion (SAD) phasing using PHENIX AutoSol (38). Initial phases (overall FOM of 0.326) were improved by density modification using RESOLVE (final FOM of 0.66). A model was built using PHENIX autobuild and manually completed and refined using COOT (39) and phenix.refine. The structure of OTU$_{(1–169)}$–ISG15 was determined by molecular replacement using PHASER (40) and the crystal structures of CCHFV–OTU and ISG15 (7) (PDB ID code 1Z2M) as search models. Model building and refinement, which included the use of TLS partitions, was performed using COOT and phenix.refine (38, 39, 41). Crystallographic statistics are summarized in Table S2.

Enzymatic Assays. Enzymatic assays were carried out in 50 mM Tris-HCl, pH 8.0, 2 mM DTT buffer at 25 °C in 25 ul final volume. Ub–AMC and ISG15–AMC (Boston Biochem) hydrolysis were initiated by adding enzyme to the reaction mixture having varying concentrations of substrates; the resulting final concentration of enzyme in the reaction mixture for each case was 3 nM. For RLRGG–AMC (Enzo Life Sciences) hydrolysis, identical assay conditions were used as above; however, the final concentration of enzyme in the reactive mixture was 100 nM of enzyme. The enzyme concentration for initial rate determinations was chosen so that less than 10% of the substrate was hydrolyzed. Hydrolysis at each given substrate concentration was monitored continuously by recording the fluorescence of the released AMC product as a function of time. Initial rates were calculated from the slopes of the linear portion of the time-dependent fluorescence profiles. The rate of fluorescence increase was converted to changes in concentration (nM) of product (free AMC) produced per second using the fluorescence standardization curves of the AMC standard (Boston Biochem) that were also used for calibration. All assays were performed in triplicate at minimum. The kinetic results were analyzed with Sigmaplot software.

ACKNOWLEDGMENTS. We thank V. Larmour and R. Cadagan for technical assistance, and J. Wilkins for providing cDNA clones of human Ub and ISG15. X-ray diffraction data were collected at the Canadian Light Source (CLS) beamline 08ID-1. The CLS is supported by the Natural Sciences and Engineering Research Council of Canada (NSERC), National Research Council, the Canadian Institutes of Health Research, and the University of Saskatchewan. The research was partly funded by NSERC and Manitoba Health Research Council (MHRC) grants to B.L.M. and by National Institute of Allergy and Infectious Disease (NIAID) Grant U54AI057158 to A.G.S. T.W.J. was supported by a studentship from the MHRC.

1. Welchman RL, Gordon C, Mayer RJ (2005) Ubiquitin and ubiquitin-like proteins as multifunctional signals. *Nat Rev Mol Cell Biol* 6:599–609.
2. Hochstrasser M (2009) Origin and function of ubiquitin-like proteins. *Nature* 458:422–429.
3. Hicke L (2001) Protein regulation by monoubiquitin. *Nat Rev Mol Cell Biol* 2:195–201.
4. Kirkin V, Dikic I (2007) Role of ubiquitin- and Ubl-binding proteins in cell signaling. *Curr Opin Cell Biol* 19:199–205.
5. Bhoj VG, Chen ZJ (2009) Ubiquitylation in innate and adaptive immunity. *Nature* 458:430–437.
6. Farrell PJ, Broeze RJ, Lengyel P (1979) Accumulation of an mRNA and protein in interferon-treated Ehrlich ascites tumour cells. *Nature* 279:523–525.
7. Narasimhan J, et al. (2005) Crystal structure of the interferon-induced ubiquitin-like protein ISG15. *J Biol Chem* 280:27356–27365.
8. Lenschow DJ, et al. (2007) IFN-stimulated gene 15 functions as a critical antiviral molecule against influenza, herpes, and Sindbis viruses. *Proc Natl Acad Sci USA* 104:1371–1376.
9. Loeb KR, Haas AL (1992) The interferon-inducible 15-kDa ubiquitin homolog conjugates to intracellular proteins. *J Biol Chem* 267:7806–7813.
10. Skaug B, Chen ZJ (2010) Emerging role of ISG15 in antiviral immunity. *Cell* 143:187–190.
11. Makarova KS, Aravind L, Koonin EV (2000) A novel superfamily of predicted cysteine proteases from eukaryotes, viruses and Chlamydia pneumoniae. *Trends Biochem Sci* 25:50–52.
12. Frias-Staheli N, et al. (2007) Ovarian tumor domain-containing viral proteases evade ubiquitin- and ISG15-dependent innate immune responses. *Cell Host Microbe* 2:404–416.
13. Wertz IE, et al. (2004) De-ubiquitination and ubiquitin ligase domains of A20 downregulate NF-[kappa]B signalling. *Nature* 430:694–699.
14. Kayagaki N, et al. (2007) DUBA: A Deubiquitinase that regulates Type I interferon production. *Science* 318:1628–1632.
15. Whitehouse CA (2004) Crimean–Congo hemorrhagic fever. *Antiviral Res* 64:145–160.
16. Honig JE, Osborne JC, Nichol ST (2004) Crimean–Congo hemorrhagic fever virus genome L RNA segment and encoded protein. *Virology* 321:29–35.
17. Kinsella E, et al. (2004) Sequence determination of the Crimean–Congo hemorrhagic fever virus L segment. *Virology* 321:23–28.
18. Snijder EJ, Wassenaar AL, Spaan WJ, Gorbalenya AE (1995) The arterivirus Nsp2 protease. An unusual cysteine protease with primary structure similarities to both papain-like and chymotrypsin-like proteases. *J Biol Chem* 270:16671–16676.
19. Sun Z, Chen Z, Lawson SR, Fang Y (2010) The cysteine protease domain of porcine reproductive and respiratory syndrome virus nonstructural protein 2 possesses deubiquitinating and interferon antagonism functions. *J Virol* 84:7832–7846.
20. Komander D, Barford D (2008) Structure of the A20 OTU domain and mechanistic insights into deubiquitination. *Biochem J* 409:77–85.
21. Lin SC, et al. (2008) Molecular basis for the unique deubiquitinating activity of the NF-kappaB inhibitor A20. *J Mol Biol* 376:526–540.
22. Nanao MH, et al. (2004) Crystal structure of human otubain 2. *EMBO Rep* 5:783–788.
23. Edelmann MJ, et al. (2009) Structural basis and specificity of human otubain 1-mediated deubiquitination. *Biochem J* 418:379–390.
24. Messick TE, et al. (2008) Structural basis for ubiquitin recognition by the Otu1 ovarian tumor domain protein. *J Biol Chem* 283:11038–11049.
25. Krissinel E, Henrick K (2007) Inference of macromolecular assemblies from crystalline state. *J Mol Biol* 372:774–797.
26. Kamphuis IG, Kalk KH, Swarte MBA, Drenth J (1984) Structure of papain refined at 1.65 ≈ resolution. *J Mol Biol* 179:233–256.
27. Drenth j, Kalk KH, Swen HM (1976) Binding of chloromethyl ketone substrate analogues to crystalline papain. *Biochemistry* 15:3731–3738.
28. Rawlings ND, Barrett AJ, Bateman A (2010) MEROPS: The peptidase database. *Nucleic Acids Res* 38(Suppl 1):D227–233.
29. Komander D, Clague MJ, Urbe S (2009) Breaking the chains: Structure and function of the deubiquitinases. *Nat Rev Mol Cell Biol* 10:550–563.
30. Fersht A (1998) *Structure and Mechanism in Protein Science: A Guide to Enzyme Catalysis and Protein Folding* (WH. Freeman and Co., New York).
31. Yuan W, Krug RM (2001) Influenza B virus NS1 protein inhibits conjugation of the interferon (IFN)-induced ubiquitin-like ISG15 protein. *EMBO J* 20:362–371.
32. Lindner HA, et al. (2005) The papain-like protease from the severe acute respiratory syndrome coronavirus is a deubiquitinating enzyme. *J Virol* 79:15199–15208.
33. Clementz MA, et al. (2010) Deubiquitinating and interferon antagonism activities of coronavirus papain-like proteases. *J Virol* 84:4619–4629.
34. Balakirev MY, Jaquinod M, Haas AL, Chroboczek J (2002) Deubiquitinating function of adenovirus proteinase. *J Virol* 76:6323–6331.
35. Borodovsky A, et al. (2002) Chemistry-based functional proteomics reveals novel members of the deubiquitinating enzyme family. *Chem Biol* 9:1149–1159.
36. Van Duyne GD, Standaert RF, Karplus PA, Schreiber SL, Clardy J (1993) Atomic structures of the human immunophilin FKBP-12 complexes with FK506 and rapamycin. *J Mol Biol* 229:105–124.
37. Collaborative Computational Project Number 4 (1994) The CCP4 suite: Programs for protein crystallography. *Acta Crystallogr D* 50:760–763.
38. Adams PD, et al. (2002) PHENIX: Building new software for automated crystallographic structure determination. *Acta Crystallogr D* 58:1948–1954.
39. Emsley P, Cowtan K (2004) Coot: Model-building tools for molecular graphics. *Acta Crystallogr D* 60:2126–2132.
40. McCoy AJ, Grosse-Kunstleve RW, Storoni LC, Read RJ (2005) Likelihood-enhanced fast translation functions. *Acta Crystallogr D* 61:458–464.
41. Painter J, Merritt EA (2006) Optimal description of a protein structure in terms of multiple groups undergoing TLS motion. *Acta Crystallogr D* 62:439–450.
42. DeLano WL (2002) *The PyMOL Molecular Graphics System* (DeLano Scientific, PaloAlto, CA).